

Enzymology of the C8-Oxylipin Biosynthesis
in *Cyclocybe aegerita*.

Cumulative Dissertation

submitted to the Faculty of Biology and Chemistry
of the Justus-Liebig-University Giessen

in fulfilment of the requirements for the degree of
doctor rerum naturalium

Dr. rer. nat.

presented by
M.Sc. Dominik Karrer

Giessen 2022

Members of the thesis committee:

Prof. Dr. Martin Rühl

Prof. Dr. Till Schäberle

Prof. Dr. Hermann Wegner

Prof. Dr. Katja Sträßer

1. Referee: Prof. Dr. Martin Rühl

2. Referee: Prof. Dr. Till Schäberle

Declaration

I declare that I have completed this dissertation single-handedly without the unauthorized help of a second party and only with the assistance acknowledged therein. I have appropriately acknowledged and cited all text passages that are derived verbatim from or are based on the content of published work of others, and all information relating to verbal communications. I consent to the use of an anti-plagiarism software to check my thesis. I have abided by the principles of good scientific conduct laid down in the charter of the Justus-Liebig-University Giessen „Satzung der Justus-Liebig-Universität Gießen zur Sicherung guter wissenschaftlicher Praxis“ in carrying out the investigations described in the dissertation.

Date, Place

Signature

List of publications

Karrer D, Rühl M. A new lipoxygenase from the agaric fungus *Agrocybe aegerita*: Biochemical characterization and kinetic properties. PLOS ONE 14, 6 (2019): e0218625

Karrer D, Gand M, Rühl M. Expanding the biocatalytic toolbox with a new type of ene/yne-reductase from *Cyclocybe aegerita*. ChemCatChem 13, 9 (2021): 1-10

Karrer D, Gand M, Rühl M. Engineering a lipoxygenase from *Cyclocybe aegerita* towards long chain polyunsaturated fatty acids. AMB Express 11, 1 (2021): 1-7

Karrer D, Weigel V, Hoberg N, Atamasov A, Rühl M. Biotransformation of [U-¹³C]linoleic acid suggests two independent ketonic- and aldehydic cycles within C8-oxylin biosynthesis in *Cyclocybe aegerita* (V. Brig.) Vizzini. Mycological Progress 20, 8 (2021): 929-940

Conference contributions

Presentation

Cyclocybe aegerita - A model organism for biosynthetic pathways of volatile substances in edible fungi. 13th Symposium of the VAAM Special Group Biology and Biotechnology of Fungi in Göttingen, 19. - 21. September 2019.

Short presentation with poster

Novel reductions with an ene/yne-reductase from *Cyclocybe aegerita*: a new tool in biocatalysis. Biotrans in Graz, 19. - 22. Juli 2021.

Acknowledgements

First of all, thanks a lot to the whole Institut für Lebensmittelchemie und Lebensmittelbiotechnologie. The relaxed and familial atmosphere was very nice and made the working place feel like home. At every time i felt supported in my every day work, so much thanks to Dr. Marco Fraatz, Bianka Daubertshäuser and Peter Seum. Whenever something was wrong with a device or something was missing, you were there to help!

I highly appreciate the agreement of Prof. Dr. Till Schäberle to be the second referee. I am also thankful for the contribution in the thesis committee of Prof. Dr. Hermann Wegner and Prof. Dr. Katja Sträßer.

I would also like to thank Prof. Dr. Holger Zorn and Prof. Dr. Gerd Hamscher for the scientific exchange and tips during my thesis. This is also true for the other members of the institute helping me with a lot of problems in the last years. Besides that, you were always fun to hang out with. So thanks to Fabio Brescia, Andreas Hammer, Bernhard Hellmann, Dr. Tetiana Zhuk, Dr. Alejandra Omarini, Friederike Hahne, Friederike Bürger, Victoria Klis, Wendell Albuquerque, Garima Maheshwari, Julia Büttner, Suzan Yalman, Nadine Sella, Patrick Klüber, Philipp Honold, Dr. Judith Delius, Dr. Miriam Sowa, Dr. Daniel Bakonyi as well as Darleen and Weronika.

A very special thanks to Dr. Martin Rühl for the opportunity to work in his group and his trust in my work. At every time i felt supported in every aspects of science. The given freedom in my research is not self-evident and therefore thank you very much! Also thank you for the discussions and encouragement over the last years. Thanks to Dr. Martin Gand for the nice collaboration and exchange. Furthermore, thanks to Axel Orban and Nadine Sella for providing me valuable preliminary volatilome and transcriptome data. That helped a lot!

Thanks to Druid-Austernpilze for providing a never ending supply of *Cyclocybe aegerita* for scientific as well as culinary purposes.

A special tanks to the W1-Gang. Some of the most beautiful, funny and rememberable moments were with you. Marcus Schulze, Axel Orban, Carolin Mewe, Svenja Sommer, Florian

Birk, Janin Pfeiffer and Christopher Back you always made my day!

I would also like to thank my Masterstudents Alexander Atamasov, Vanessa Weigl, Nikolas Hoberg, Erika Wedler and Annika Wagner for your work and dedication which helped me a lot.

Last but not least, thanks to the Einhörner Kai Krämer, Thomas Klaus and Nikolai Huwa as well as Maria for the advices over the last years. All of your input was very welcome and helpful!

Abstract

Based on transcriptomic, volatilomic and metabolomic data of the model organism *Cylocybe aegerita*, the endogenous and enzymatic production of the C8-oxylipins oct-2-en-1-ol, octan-1-ol, oct-2-enal, octanal, octan-3-ol, oct-1-en-3-ol, oct-1-en-3-one and octan-3-one via biotransformations with [U-¹³C]linoleic acid was compared to the developmental state depending gene expression patterns of putative oxylipin-associated enzyme classes like lipoxygenases, dioxygenases, ene-reductases and alcohol dehydrogenases. On closer consideration of these data sets, the C8-oxylipin production seemed to occur cluster-like. While one cluster (ketonic-cycle) consisted of octan-3-ol, oct-1-en-3-one, octan-3-one and oct-1-en-3-ol, which were detected through out all developmental stages, a second cluster (aldehydic-cycle) primarily active at early developmental stages involved oct-2-enal, octanal, oct-2-en-1-ol and octan-1-ol. Studying these clusters revealed that all C8-oxylipins of the aldehydic-cycle and ketonic-cycle can be derived from oct-2-enal and oct-1-en-3-one, respectively. A detailed consideration of the gene expression patterns revealed several enzyme classes putatively involved in the C8-oxylipin biosynthesis. Especially the two genes AAE3_04864 and AAE3_13549 encoding the *lox4*- and *enr1*-gene showed great similarities between their strongly increasing transcript counts with maturation. Subsequent recombinant production of CaeLOX4 and CaeEnR1 revealed that CaeLOX4 showed a preference for C18-fatty acids with the highest affinity towards linoleic acid. Analysis of the reaction product revealed that this LOX selectively oxygenated linoleic acid at position 13 to 13-hydroperoxyoctadecadienoic acid (13-HPOD). CaeEnR1 showed high affinities towards the reduction of oct-1-en-3-one and oct-2-enal to their saturated counterparts octan-3-one and octanal, respectively. Due to the strong similarities between the expression patterns of CaeLOX4 and CaeEnR1 a coherence between their main reaction products 13-HPOD and the precursor of the ketonic-cycle oct-1-en-3-one seems very likely. This suggests a biosynthetic route from linoleic acid to 13-HPOD, followed by a subsequent cleavage step to oct-1-en-3-one and therefore to C8-oxylipins of the ketonic-cycle.

Contents

1	Introduction	1
1.1	Oxylipins and their Physiological Importance in Different Biological Domains	1
1.2	Fungal Oxylipins	2
1.3	Enzymology of the Oxylipin-Biosynthesis	4
1.3.1	Lipoxygenases	4
1.3.2	Dioxygenase-Cytochrome P450 Fusion Proteins	6
1.3.3	Hydroperoxide Lyases/Isomerases	8
1.3.4	Oxidoreductases	11
1.4	Objectives	13
1.5	Literature	14
2	Publications	23
2.1	Publication 1: A new lipoxygenase from the agaric fungus <i>Agrocybe aegerita</i> : biochemical characterization and kinetic properties	23
2.2	Publication 2: Expanding the biocatalytic toolbox with a new type of ene/yne- reductase from <i>Cyclocybe aegerita</i>	36
2.3	Publication 3: Engineering a lipoxygenase from <i>Cyclocybe aegerita</i> towards long chain polyunsaturated fatty acids	74
2.4	Publication 4: Biotransformation of [U- ¹³ C]linoleic acid suggests two inde- pendent ketonic- and aldehydic cycles within C8-oxylipin biosynthesis in <i>Cy- clocybe aegerita</i> (V. Brig.) Vizzini	82

1 Introduction

1.1 Oxylipins and their Physiological Importance in Different Biological Domains

Lipid metabolism fulfills various biological functions ranging from energy generation, energy conservation, structural functions in cell membranes or hormonal signal transduction naming only a few of the primary metabolism. Besides that, a secondary metabolism producing a variety of fatty acid derived compounds exists in all living cells. Oxylipins are part of these secondary metabolites. The most important precursors of oxylipins are polyunsaturated fatty acids (PUFAs) which are fed into various biosynthetic pathways with different enzymatic conversions, leading to plenty different structures. These metabolites were detected in almost all biological domains, particularly in plants, mammals, bacteria and fungi (Brodhun & Feussner 2011, de Leon et al. 2015, Holighaus & Rohlf 2019, Wasternack & Feussner 2018).

In mammals, prostanoids and leukotrienes are the most prominent oxylipins which are mainly derived from C20-fatty acids like arachidonic- and eicosapentaenoic acid. Their importance is displayed by their broad impact in various physiological processes such as different allergic- and inflammatory reactions, they act as local tissue hormones, strong bronchoconstrictors or are involved in hair growth (Brodhun & Feussner 2011, Funk 2001, Jagusch et al. 2019).

In plants, the known oxylipins are derived from C18- and C20-fatty acids. Hydroperoxidation and following conversions lead to various metabolites with epoxy-, keto- or oxo groups with unknown biological purpose. Besides, short chain plant oxylipins such as the comprehensively investigated jasmonic acid and its derivatives, particularly glycosyl- and amino acid conjugates are known for their versatile physiological role. These compounds act mainly

as signal molecules and are involved in stress response like abiotic stress like drought-, salt-, temperature-, UV-tolerance, plant development like germination, tuber formation or blossom or in defence against plant pathogens (Andreou et al. 2009, Goosens et al. 2017, Kohlmann et al. 1999, Major et al. 2017, Wasternack & Song 2017, Wasternack & Feussner 2018). In algae, oxylipins with various functionalities were identified but a biological role was not hypothesized yet (Andreou et al. 2009).

1.2 Fungal Oxylipins

In fungi as well as other organisms, oxylipin production depends highly on the developmental stage. A typical life cycle of fungi of the phyla Basidiomycota starts with the germination of basidiospores, leading to the formation of monokaryotic hyphal cells, which branch out to so called hyphae. The joint network of such hyphae to a higher order are called mycelium (Kües 2000). Subsequently, one of the most complicated developmental processes, the formation of fruiting bodies initiates. First, hyphae aggregate to mycelial cords that further develop into hyphal knots and initial fruiting bodies. Progressing development leads to primordia, mature fruiting bodies and finally to the formation of basidiospores, which are released during sporulation completing the life cycle (Kües 2000). However, the formation of fruiting bodies is mostly limited to dikaryotic mycelium, which is formed by hyphal fusion between two monokaryotic mycelia with compatible mating types, leading to a dikaryotic state with distinct haploid nuclei per cell (Kües 2000). Occasionally, monokaryotic *C. aegerita* as well as other monokaryotic strains are also able to develop fruiting bodies which differ greatly from fruiting bodies of a dikaryon (Herzog et al. 2016)

A comprehensive investigation of the volatilome and, therefore, C8-oxylipins in the head space of *C. aegerita* throughout one life cycle was carried out by Orban et al. (2020), detecting a preliminary production of oct-1-en-3-ol in mycelium after 10 days, peaking with the development of young fruiting bodies and decreased with ongoing maturation. A contrary progression was described for octan-3-one, which was detected in very low levels at young developmental stages, that increased strongly in mature fruiting bodies and sporulation. Other studies focusing on developmental stage dependent oxylipin production are

scarce and always limited to the comparison of different fruiting body stages, mycelium and mature fruiting bodies. Although presenting an incomplete and limited picture of volatile C8-oxylipins, the studies confirmed that oct-1-en-3-ol and octan-3-one are the predominant C8-oxylipins in fungi, mainly present in fruiting bodies (Cho et al. 2006, Combet et al. 2009, Cruz et al. 1997, Li et al. 2016, Matsui et al. 2003, Mau et al. 1997, Rapior et al. 1998, Tasaki et al. 2019). Biological explanations deduced from these results are also restricted. Nevertheless, volatile oxylipins with biological activities, such as the participation in the sexual and asexual life cycle or the interaction with invertebrates or microbes are known for Ascomycota and Basidiomycota (Chitarra et al. 2004, Holighaus & Rohlf 2019, Schulz-Bohm et al. 2017).

It was shown that high oct-1-en-3-ol concentrations of up to 4 mM inhibited germination of conidia from the Ascomycota *Penicillium paneum* (Chitarra et al. 2004). However, it was detected that octan-3-one and octan-3-ol (100 - 500 μ M) stimulated the asexual reproduction in *Trichoderma* spp. (Nemcovic et al. 2008). Another biological aspect of oct-1-en-3-ol, octan-3-one and octan-3-ol (Fig. 1.1) is the interspecies communication in which these compounds act as attractant or repellent (Holighaus et al. 2014). On the one hand, fruiting bodies are valuable nutrient sources for invertebrates as well as a place for oviposition displaying the attractant character of these oxylipins produced by mature fruiting bodies leading to a survival advantage. On the other hand, these oxylipins can also prevent the settlement of fungivore organisms illustrating a repellent effect (Holighaus et al. 2014, Holighaus & Rohlf 2019, Schulz-Bohm et al. 2017, Tsitsigiannis & Keller 2007). Furthermore, the volatile C8-oxylipins are also the main odor contributors of the characteristic mushroom aroma (Fig. 1.1).

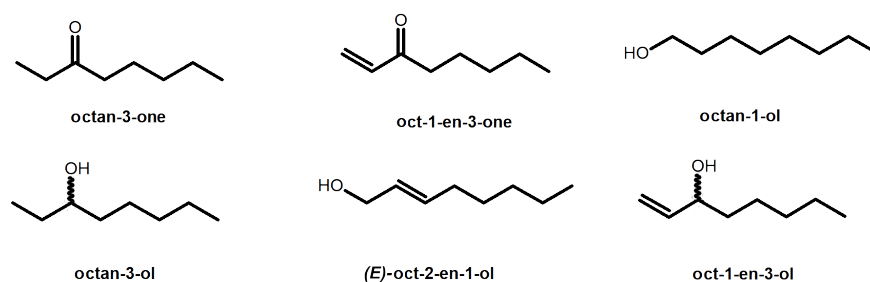


Figure 1.1: Structures of the most important volatile C8-oxylipins

1.3 Enzymology of the Oxylipin-Biosynthesis

In fungi of the phyla Basidiomycota and Ascomycota the main fatty acid is linoleic acid and therefore considered as the main precursor in C8-oxylipin biosynthesis. Comprehensive studies by Wurzenberger and Grosch (1982, 1984) showed, that cell lysates from fruiting bodies of *Agaricus bisporus* convert linoleic acid mainly to oct-1-en-3-ol. Furthermore, incubation with [U¹⁴-C]-linoleic acid lead to [U¹⁴-C]-oct-1-en-3-ol and [U¹⁴-C]-10-Oxo-trans-8-decenoic acid. These results were confirmed by Matsui et al. (2003) and Akakabe et al. (2005). Both studies showed that addition of linoleic acid to cell homogenates of *Tricholoma matsutake* and *Lentinula edodes*, led to a significant increase of oct-1-en-3-ol and octan-3-one was detectable.

The enzymological description of the oxylipin-pathway in Basidiomycota is scarce due to the very limited genetic editing approaches, which complicates the identification of putative oxylipin-associated genes. Recent studies primarily identified and characterized lipoxygenases (LOX) via genome mining. These LOX oxygenate PUFAs to hydroperoxy fatty acids (Brodhun et al. 2013, Kuribayashi et al. 2003, Plagemann et al. 2013, Oliw et al. 2011). Enzymes involved in following modification steps of intermediates are completely unknown. Nevertheless, biotransformations of hydroperoxy fatty acids and other putative intermediates suggested various enzyme classes such as ene-reductases (ERs), alcohol dehydrogenases (ADHs) or hydroperoxide lyases (HPLs). An experimental confirmation is still missing.

1.3.1 Lipoxygenases

LOX (E.C. 1.13.11.-) catalyze the stereo- and regioselective oxidation of PUFAs with one or more (1*Z*,4*Z*)- pentadiene motifs to the corresponding hydroperoxy species via the insertion of molecular oxygen classifying them into the group of dioxygenases (Fig. 1.2) (Andreou et al. 2009).

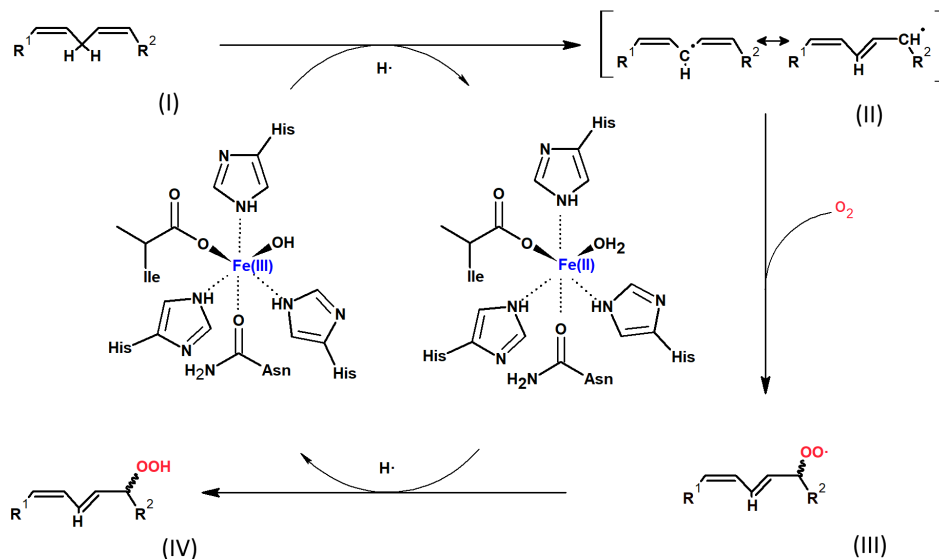


Figure 1.2: Catalytic cycle of the oxidation of an (1*Z*,4*Z*)-pentadiene motif to a hydroperoxy species. (I) Hydrogen abstraction. (II) Radical rearrangement of the substrate. (III) Insertion of molecular oxygen. (IV) Reduction of the peroxy radical to the hydroperoxide. Figure adjusted from Andreou et al. (2009)

One catalytic cycle consists of four consecutive steps. Abstraction of the hydrogen atom and the uptake of an electron by Fe(III) leading to Fe(II) (Fig. 1.2, I). The resulting (1*Z*,4*Z*)-pentadiene radical undergoes a [+2] or [-2] rearrangement (Fig. 1.2, II) followed by the addition of molecular oxygen to the carbon radical resulting in peroxy radical intermediate (Fig. 1.2, III). Hydrogen and electron release of the Fe(II)-species to the peroxy radical leads to the stable hydroperoxide with a conjugated double bond and a recovered Fe(III)-species is ready for the next cycle (Fig. 1.2, IV). This catalytic cycle is also applicable for the manganese-dependent LOX (Andreou et al. 2009). Biochemical characterizations of LOX from Basidiomycota are very limited. Yet, only two Fe-dependent basidiomycetous LOX from *P. ostreatus* and *P. sapidus* and two LOX from the Ascomycota *Gaeumannomyces graminis* and *Fusarium oxysporum* have been comprehensively characterized (Brodhun et al. 2013, Kuribayashi et al. 2003, Plagemann et al. 2013, Su & Oliw 1996 and 1997). The main substrates of the so far characterized Fe-dependent LOX were linoleic acid, linolenic acid and arachidonic acid from which linoleic acid was converted with the highest affinity whereas Mn-dependent LOX showed a higher preference towards linolenic acid (Brodhun et al. 2013, Kuribayashi et al. 2003, Plagemann et al. 2013, Su & Oliw 1996 and 1998). Although multiple regiospecific products are conceivable, the main product from basidiomycetous LOX and linoleic acid is 13-hydroperoxyoctadecadienoic acid (13-HPOD) whereas only low amounts

of 9-hydroperoxydecadienoic acid (9-HPOD) have been detected (Kuribayashi et al. 2003, Plagemann et al. 2013).

1.3.2 Dioxygenase-Cytochrome P450 Fusion Proteins

Besides LOX, dioxygenase-cytochrome P450 fusion proteins (DOX-P450) may play an important role in oxylipin biosynthesis. The domain structure of these proteins consists of an N-terminal DOX-domain that is part of the heme-peroxidase superfamily (E.C. 1.11.-.-) capable of introducing molecular oxygen to PUFAs and the C-terminal P450-domain part of the CYP74 family (E.C. 1.14.-.-). This subgroup of cytochrome P450 proteins does not need an external oxygen source or an electron-donor (e.g. NADH, NADPH, FAD or FMN) which is why these P450-domains are considered isomerases and not monooxygenases (Brodhun & Feussner 2011).

The pairings of such DOX- and P450-domains result in fusion proteins like dioxygenase-linoleat diol synthases (DOX-LDS), dioxygenase-allene oxide synthases (DOX-AOS) or dioxygenase-epoxy alcohol synthases (DOX-EAS) leading to a variety of different catalyzed reactions and metabolites (Fig. 1.3).

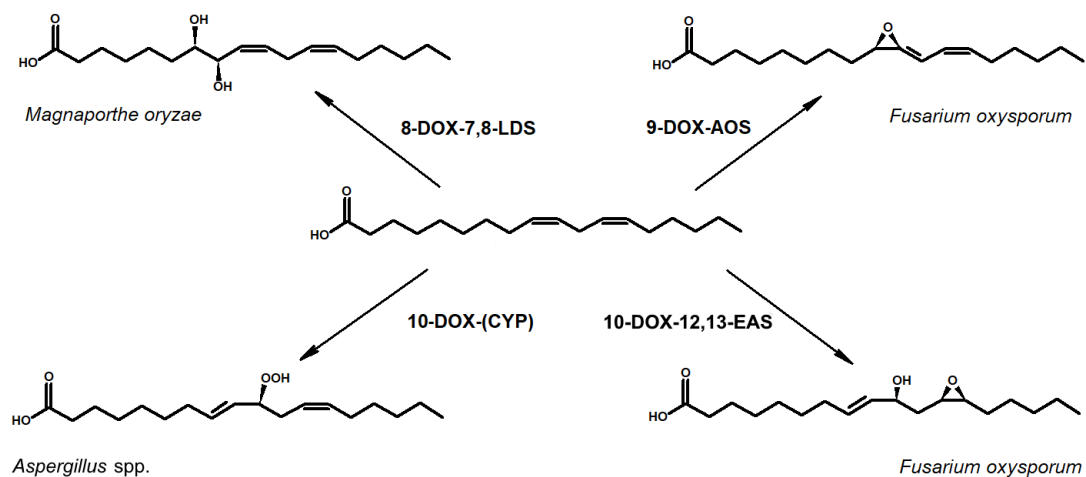


Figure 1.3: Summary of DOX-P450 catalyzed reactions with linoleic acid as substrate. The DOX-domain oxygenates PUFAs to hydroperoxy species, followed by an epoxidation, linoleat diol or epoxy alcohol formation by the P450-domain. Figure adjusted from Brodhun & Feussner 2011.

The hypothetical reaction mechanism of DOX-P450 fusion proteins starts with a hydroperoxy formation of the DOX-domain and proceeds with an isomerization to an epoxy, diol or epoxy

alcohol species by the P450-domain (Fig. 1.4) (Brodhun & Feussner 2011, Jernereren et al. 2010, Oliw et al. 2011, Oliw et al. 2016, Oliw 2018, Song et al. 1992).

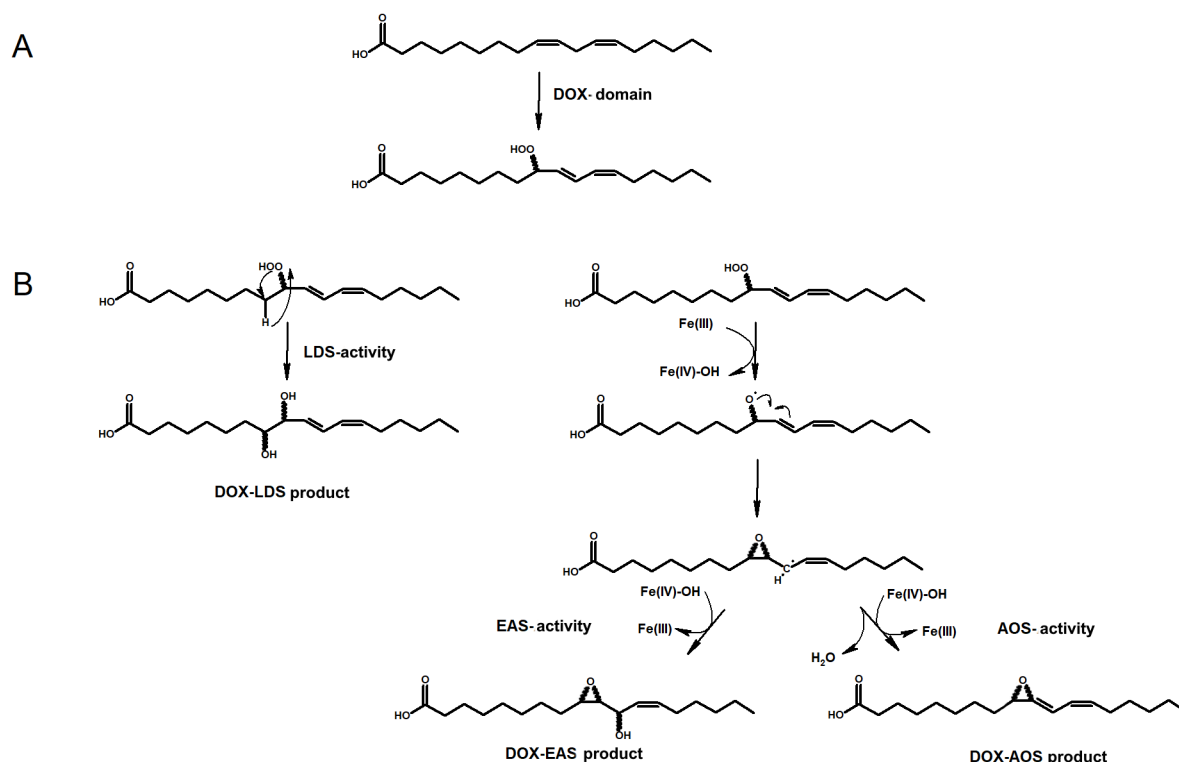


Figure 1.4: Suggested reaction mechanism of DOX-P450 proteins with linoleic acid as substrate. (A) Formation of the HPOD by the DOX-domain. (B) Modification of the HPOD by the P450-domain. P450-domains with an LDS-activity insert intramolecular oxygen from the hydroperoxide which leads to diols. Domains with EAS- or AOS-activity convert the hydroperoxide to an epoxy allyl radical intermediate which reacts to an allene oxide or epoxy alcohol by a hydrogen abstraction or the insertion of a hydroxy group via a Fe(IV)-OH species, respectively. Figure adjusted from Brodhun & Feussner 2011.

In this enzyme group only ascomycetous proteins from *Magnaporthe grisea*, *Coccidioides immitis*, *Colletotrichum graminicola*, *Lasiodiplodia theobromae*, *F. oxysporum*, *G. graminis* and various *Aspergillus*-Species have been characterized so far (Brodhun et al. 2009, Brodhun et al. 2010, Cristea et al. 2003, Hoffmann et al. 2013, Kataoka et al. 2020, Jernereren et al. 2010, Oliw et al. 2016, Sooman & Oliw 2015, Su & Oliw 1996). However, biotransformations with mycelia from the Basidiomycota *Rhizoctonia solani* revealed metabolites that assume the existence of these enzymes also in the phylum of Basidiomycota (Oliw 2018). However, a biochemical characterization of a single basidiomycetous DOX-P450 is missing.

DOX-P450 enzymes with a missing cysteine in the CXG-motif of the P450-domain exist which leads to inactivity. The reaction of these proteins is confined to the hydroperoxide formation with a lacking isomerization step. Investigations of such proteins from *F. oxysporum*, *A. terreus*, *A. fumigatus* or PpoC from *A. nidulans* revealed that the products are mainly oxygenated at the n-10 position from the methyl end of the fatty acid (Brodhun et al. 2009, 2010). Although PpoC was able to oxygenate linoleic acid to 10-hydroperoxyoctadecadienoic acid (10-HPOD) with 10-oxooctadecadienoic acid (10-KOD) and 10-hydroxyoctadecadienoic acid (10-HOD) as byproducts, it is not clear if these byproducts were enzymatically formed or by spontaneous redox processes. Furthermore, a separate conversion of 8-HPOD or 10-HPOD by PpoC lead to an epoxidation at position 12 and 13 resulting in 12,13-epoxy-10-hydroxyoctadecadienoic acid and 12,13-epoxy-8-hydroxyoctadecadienoic acid (Brodhun et al. 2009, 2010). Interestingly, neither Δppo nor Δlox strains of *A. flavus* showed differences in oct-1-en-3-ol production compared to the wild type, suggesting that none of these fatty acid oxygenases are involved in short chain oxylipins (Miyamoto et al. 2014). Taken together, a direct link between these enzymes, their reaction products (long chain oxylipins) and short chain volatiles is not confirmed yet.

1.3.3 Hydroperoxide Lyases/Isomerases

The cleavage of hydroperoxy fatty acids by hydroperoxide lyases (E.C. 4.2.99.-) to short chain oxylipins is known and well described in plants (Grechkin & Hamberg 2004, Hatanaka et al. 1988, Matsui et al. 1991, Suurmeijer et al. 2000, Teder et al. 2017, Wan et al. 2013). Specific HPL or hydroperoxy isomerases (HPI) are used to cleave 13-HPOD and 9-HPOD to the corresponding short chain C6- or C9-oxylipins (Grechkin & Hamberg 2004, Stolterfoht et al. 2019). The mechanism proceeds via a radical rearrangement of the hydroperoxide to an epoxid intermediate, which instantly reacts to a hemiacetal (Fig. 1.5). Following decomposition of the hemiacetal to aldehydes is hypothesized to be a spontaneous step and not enzymatically catalyzed (Grechkin & Hamberg 2004).

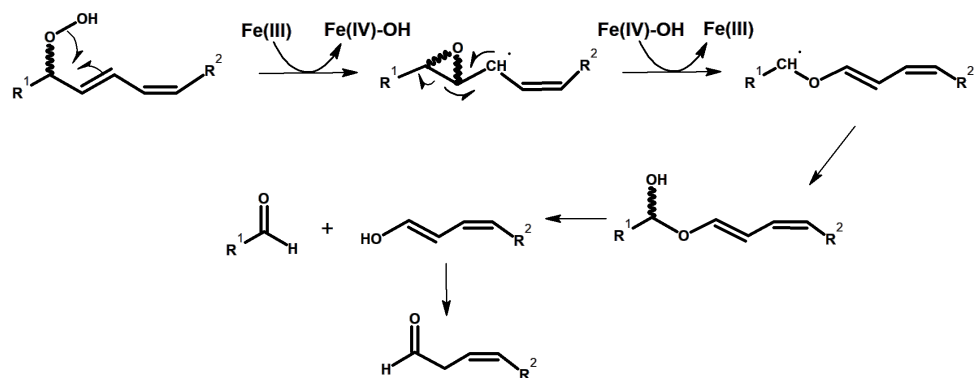


Figure 1.5: Cleavage mechanism of hydroperoxy fatty acids to short chain oxylipins by HPLs according to Grechkin & Hamberg (2004).

Although HPLs from plants are well characterized, homologous proteins in fungi are not identified yet. Nevertheless, biotransformation experiments with the 9-, 10-, 12- and 13-hydroperoxy isomers of linoleic acid in cell lysates from *Agaricus bisporus* suggested the existence of such enzymes despite the interesting finding that only 10-HPOD was converted to the C8-oxylipin oct-1-en-3-ol, proposing 10-HPOD as the precursor of this omnipresent C8-oxylipin (Akakabe et al. 2005, Matsui et al. 2003, Wurzenberger & Grosch 1984). This was partly confirmed by Assaf et al. (1995, 1997) for *Pleurotus pulmonaris* showing that 13-HPOD was not converted to oct-1-en-3-ol, which was later confirmed by Matsui et al. 2003 where fruiting body lysates of *Lentinus decadetes* did not convert 13-HPOD to C8-oxylipins. Instead an increase of *n*-hexanal was detected in *L. decadetes* (Matsui et al. 2003). Investigations of the oxylipin biosynthesis in *Penicillium*-species revealed that with the addition of 10-HPOD, an increasing amount of oct-1-en-3-ol, oct-2-en-1-ol, oct-1-en-3-one, oct-2-enal and *n*-hexanal was detected (Kermasha et al. 2002). Joh et al. (2012) was able to show that cell homogenates of *Pleurotus ostreatus* converted 13-HPOD as well as 10-HPOD to oct-1-en-3-ol. Summarizing these studies suggest that the main oxygenation products of LOX, 13-HPOD and 9-HPOD might be partly involved in C8-oxylipin biosynthesis.

However, Tressl et al. (1981, 1982) showed that hydroperoxy fatty acids were cleaved to short chain oxylipins via thermal oxidation, autoxidation or light-induced oxidation. Typical fragments of 13-HPOD were *n*-hexanal and 12-oxo-10-dodecanoic acid as well as C8-oxylipins like oct-1-en-3-one or octan-3-one while 9-HPOD showed various decadienals, oxooctanoic acid derivatives and octadiens. The mechanistic explanation for that observation was the epoxidation of the conjugated double bond of hydroperoxides to γ -ketol species, which were

than cleaved via an unknown mechanism to short chain oxylipins (Figure 1.6).

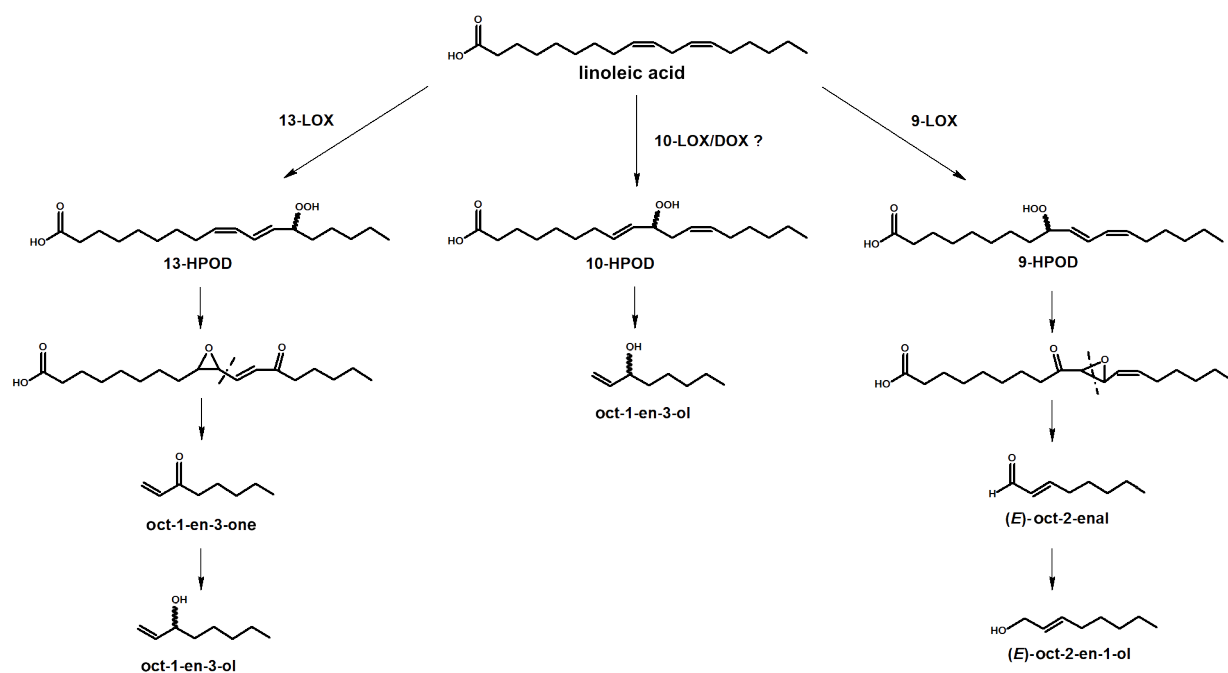


Figure 1.6: Postulated biosynthetic pathway of C8-oxylipins in *A. bisporus* according to Tressl et al. (1981) and Wurzenberger & Grosch (1984).

The formation of γ -ketol species was also described in the jasmonic acid pathway in plants and in *Aspergillus*-species (Jerneren et al. 2010, Schaller et al. 2019). However, a direct connection between C8-oxylipins and these intermediates is not confirmed. An alternative route to short chain volatiles was shown by a LOX-HPL/AOS fusion protein of the algae *Pyropia haitensis*, for which enzyme assays with different C18-22 PUFAs revealed the formation of different oxylipins (Fig. 1.7) (Zhu et al. 2018).

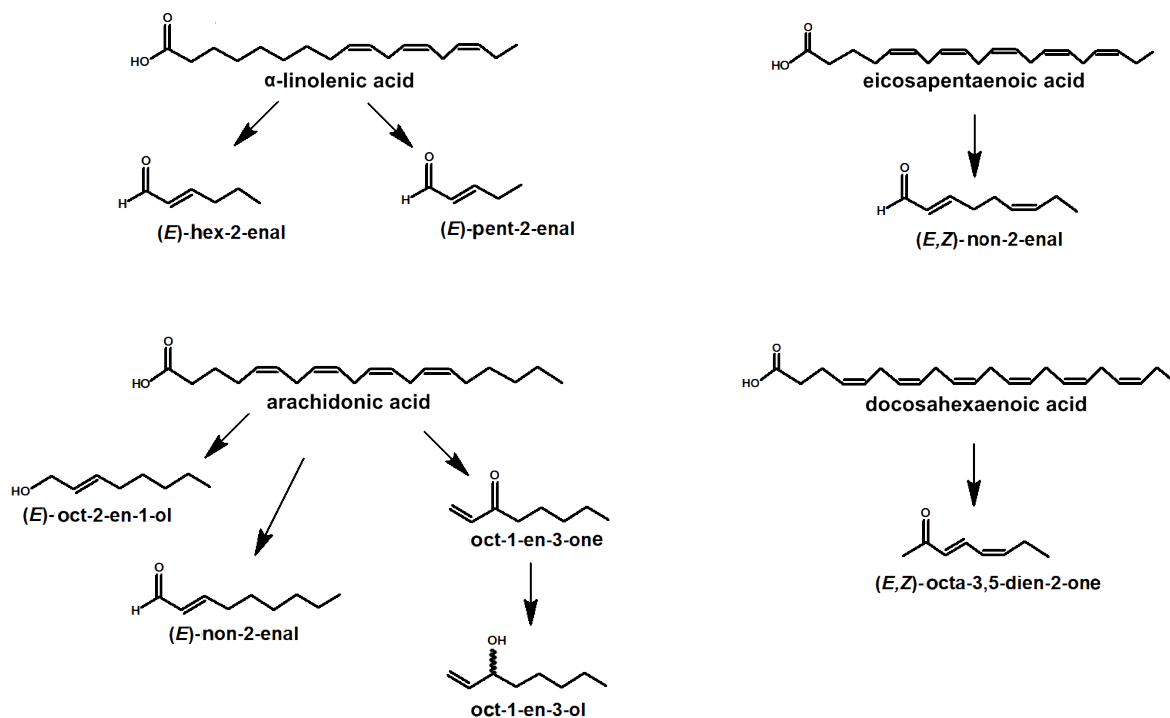


Figure 1.7: Oxylipin formation from different PUFAs by a LOX-HPL/AOS fusion protein of *P. haitensis*.

1.3.4 Oxidoreductases

The oxidation or reduction of short chain C8-oxylipins was observed in various cell lysates (Fig. 1.8). Chen & Wu (1984) showed that *A. bisporus* reduced oct-1-en-3-one to octan-3-one and oct-1-en-3-ol implicating the existence of ene-reductases (E.C. 1.3.-.-) and alcohol dehydrogenases (E.C. 1.1.-.-). Similar results were published by Darriet et al. (2002) with an successful reduction of oct-1-en-3-one and (*Z*)-octa-1,5-dien-3-one to octan-3-one and (*Z*)-oct-5-en-3-one in *S. cerevisiae*.

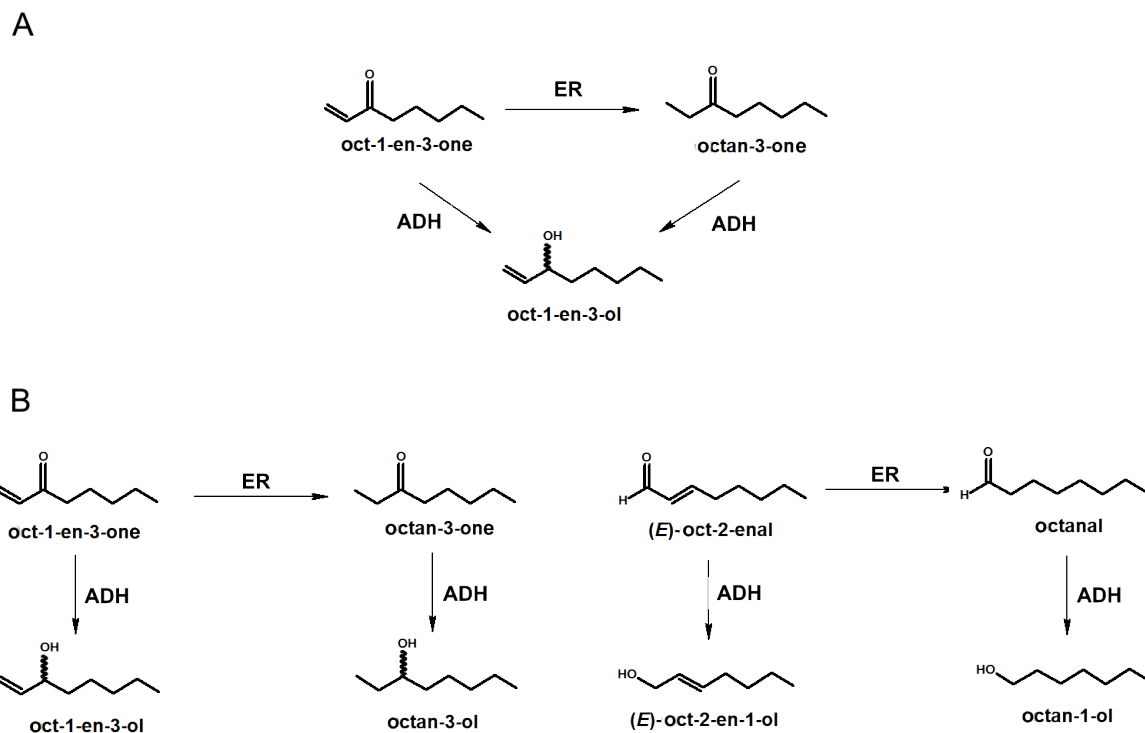


Figure 1.8: Observed reductions of short chain oxylipins in protein extracts of *A. bisporus* (A) and *S. cerevisiae* (B).

Wanner & Tressl (1998) purified and characterized two ERs from *S. cerevisiae* which showed a high affinity towards oct-1-en-3-one. Additionally, various α, β -unsaturated enones and enals which might be precursors of relevant C8-oxylipins like (*E*)-oct-2-enal were successfully reduced. Furthermore, enzyme extracts of *S. cerevisiae* reduced (*E*)-oct-2-enal to (*E*)-oct-2-en-1-ol, octanal to octan-1-ol, oct-1-en-3-one to oct-1-en-3-ol and octan-3-on to octan-3-ol indicating the expression of various ERs and ADHs (Fig. 1.8) (Wanner & Tressl 1998). More evidence for a broad variety of ERs in Basidiomycota was shown by analysing the reduction products of different α, β -unsaturated enones and enals by fungal cultures (Romagnolo et al. 2015). Though, a biochemical characterization of basidiomycetous ERs or ADHs are not described yet.

1.4 Objectives

The enzymology of the C8-oxylin biosynthesis in Basidiomycota is very unclear. Genome mining approaches revealed only two LOX and putative enzyme classes for the following metabolization of linoleic acid derived oxylin. An experimental evaluation of enzymes like ERs oder ADHs is completely missing. This displays the scarcely explored enzymology of the C8-oxylin biosynthesis.

Studying biosynthetic pathways in Basidiomycota harbours various difficulties. First, gene editing methods are in the early stages of development and limited to proof of concept studies. Second, the landscape of sequenced genomes is increasing but partially annotated data sets with various hypothesized genes complicate the identification of relevant enzymes. However, Basidiomycota provide a variety of novel secondary metabolites with diverse biological activities. This also implies a large library of undiscovered potential biocatalysts.

To overcome these issues, the group of Dr. Martin Rühl (Institute of Food Chemistry and Food Biotechnology, University of Giessen) pursues a completely new approach to identify biosynthetic pathways. The combination and comparison of volatilomic and transcriptomic data at different developmental stages is believed to reveal up- or downregulated genes which then can be assigned to a certain metabolite occurrence at various developmental stages. Based on these data, the following steps shall be applied to acquire new insights in the C8-oxylin biosynthesis:

- Highlighting correlations between transcription rates and metabolite occurrence at certain developmental stages
- Identification of putatively C8-oxylin associated genes and function prediction via sequence alignments and phylogenetic analysis
- Cloning and heterologous expression of C8-oxylin associated genes in *E. coli* and biochemical characterization

1.5 Literature

Akakabe Y, Matsui K and Kajiwara T. „Stereochemical Correlation between 10-Hydroperoxyoctadecadienoic acid and 1-octen-3-ol in *Lentinula edodes* and *Tricholoma matsutake* Mushrooms“. *Bioscience, Biotechnology and Biochemistry* 69, 8 (2005): 1539–44.

Andreou A, Brodhun F and Feussner I. „Biosynthesis of Oxylipins in Non-Mammals“. *Progress in Lipid Research* 48, 3–4 (2009): 148–70.

Andreou A and Feussner I. „Lipoxygenases – Structure and Reaction Mechanism“. *Phytochemistry* 70, 13–15 (2009): 1504–10.

Assaf S, Hadar Y and Dosoretz CG. „Biosynthesis of 13-hydroperoxylinoleate, 10-oxo-8-decenoic acid and 1-octen-3-ol from Linoleic Acid by a Mycelial-Pellet Homogenate of *Pleurotus pulmonarius*“. *Journal of Agricultural and Food Chemistry* 43, 8 (1995): 2173–78.

Assaf S, Hadar Y and Dosoretz CG. „1-octen-3-ol and 13-hydroperoxylinoleate Are Products of Distinct Pathways in the Oxidative Breakdown of Linoleic Acid By“. *Enzyme and Microbial Technology* 21, 7 (1997): 484-490.

Brodhun F, Cristobal-Sarramian A, Zabel S, Newie J, Hamberg M and Feussner I. „An Iron 13S-Lipoxygenase with an α -Linolenic Acid Specific Hydroperoxidase Activity from *Fusarium oxysporum*“. *PLOS ONE* 8, 5 (2013): e64919.

Brodhun F, Göbel C, Hornung E and Feussner I. „Identification of PpoA from *Aspergillus nidulans* as a Fusion Protein of a Fatty Acid Heme Dioxygenase/Peroxidase and a Cytochrome P450“. *Journal of Biological Chemistry* 284, 18 (2009): 11792–805.

Brodhun F, Schneider S, Göbel C, Hornung E and Feussner I. „PpoC from *Aspergillus nidulans* Is a Fusion Protein with Only One Active Haem“. *Biochemical Journal* 425, 3 (2010): 553–65.

- Brodhun F and Feussner I. „Oxylipins in Fungi“. FEBS Journal 278, 7 (2011): 1047–63.
- Chen CC and May Wu C. „Studies on the Enzymic Reduction of 1-octen-3-one in Mushroom (*Agaricus bisporus*)“. Journal of Agricultural and Food Chemistry 32, 6 (1984): 1342–44.
- Chitarra GS, Abee T, Rombouts FM, Maarten A. Posthumus and Jan Dijksterhuis. „Germination of *Penicillium paneum* Conidia Is Regulated by 1-octen-3-ol, a Volatile Self-Inhibitor“. Applied and Environmental Microbiology 70, 5 (2004): 2823–29.
- Cho IH, Choi H-K and Kim Y-S. „Difference in the Volatile Composition of Pine-Mushrooms (*Tricholoma matsutake* Sing.) According to Their Grades“. Journal of Agricultural and Food Chemistry 54, 13 (2006): 4820–25.
- Combet E, Henderson J, Eastwood DC and Burton KS. „Influence of Sporophore Development, Damage, Storage and Tissue Specificity on the Enzymic Formation of Volatiles in Mushrooms (*Agaricus bisporus*)“. Journal of Agricultural and Food Chemistry 57, 9 (2009): 3709–17.
- Cristea M, Osbourn AE and Oliw EH. „Linoleate Diol Synthase of the Rice Blast Fungus *Magnaporthe grisea*“. Lipids 38, 12 (2003): 1275–80.
- Cruz C, Noël-Suberville C and Montury M. „Fatty Acid Content and Some Flavor Compound Release in Two Strains of *Agaricus bisporus* , According to Three Stages of Development“. Journal of Agricultural and Food Chemistry 45, 1 (1997): 64–67.
- Darriet P, Pons M, Henry R, Dumont O, Findeling V, Cartolaro P, Calon nec A and Dubourdieu D. „Impact Odorants Contributing to the Fungus Type Aroma from Grape Berries Contaminated by Powdery Mildew (*Uncinula necator*); Incidence of Enzymatic Activities of the Yeast *Saccharomyces cerevisiae*“. Journal of Agricultural and Food Chemistry 50, 11 (2002): 3277–82.

Funk CD. „Prostaglandins and Leukotrienes: Advances in Eicosanoid Biology“. *Science* 294, 5548 (2001): 1871–75.

Grechkin NA and Hamberg M. „The “Heterolytic Hydroperoxide Lyase” Is an Isomerase Producing a Short-Lived Fatty Acid Hemiacetal“. *Biochimica et Biophysica Acta (BBA) - Molecular and Cell Biology of Lipids* 1636, 1 (2004): 47–58.

Goossens J, Mertens J and Goossens A. „Role and functioning of bHLH transcription factors in jasmonate signalling“. *Journal of Experimental Botany* 68, 6 (2017):1333–47.

Hatanaka A, Kajiwara T and Matsui K. „Concentration of Hydroperoxide Lyase Activities in Root of Cucumber Seedlings“. *Zeitschrift Für Naturforschung C* 43, 3–4 (1988): 308–10.

Herzog R, Solovyeva I, Rühl M, Thines M and Henricke F. „Dikaryotic Fruiting Body Development in a Single Dikaryon of *Agrocybe aegerita* and the Spectrum of Monokaryotic Fruiting Types in Its Monokaryotic Progeny“. *Mycological Progress* 15, 9 (2016): 947–57.

Hoffmann I, Jernerén F and Oliw EH. „Expression of Fusion Proteins of *Aspergillus terreus* Reveals a Novel Allene Oxide Synthase“. *Journal of Biological Chemistry* 288, 16 (2013): 11459–69.

Holighaus G, Weissbecker B, von Fragstein M and Schütz S. „Ubiquitous Eight-Carbon Volatiles of Fungi Are Infochemicals for a Specialist Fungivore“. *Chemoecology* 24, 2 (2014): 57–66.

Holighaus G and Rohlf M. „Volatile and Non-Volatile Fungal Oxylipins in Fungus-Invertebrate Interactions“. *Fungal Ecology* 38 (2019): 28–36.

Jagus H, Werner M, Okuno T, Yokomizo T, Werz O and Pohnert G. „An Alternative Pathway to Leukotriene B4 Enantiomers Involving a 1,8-Diol-Forming Reaction of an Algal Oxylipin“. *Organic Letters* 21, 12 (2019): 4667–70.

Jernerén F, Hoffmann I and Oliw EH. „Linoleate 9R-Dioxygenase and Allene Oxide Synthase Activities of *Aspergillus terreus*“. Archives of Biochemistry and Biophysics 495, 1 (2010): 67–73.

Jernerén F, Garscha I, Hoffmann I, Hamberg M and Oliw EH. „Reaction Mechanism of 5,8-Linoleate Diol Synthase, 10R-Dioxygenase and 8,11-Hydroperoxide Isomerase of *Aspergillus clavatus*“. Biochimica et Biophysica Acta (BBA) - Molecular and Cell Biology of Lipids 1801, 4 (2010): 503–7.

Joh T, Kudo T, Tasaki Y and Hara T. „Mushroom Flavor Compounds and the Biosynthesis Mechanism.“ Aroma Research 13, 1 (2012): 26–30.

Kataoka R, Watanabe T, Yano S, Mizutani O, Yamada O, Kasumi T and Ogihara J. „*Aspergillus luchuensis* Fatty Acid Oxygenase PpoC Is Necessary for 1-octen-3-ol Biosynthesis in Rice Koji“. Journal of Bioscience and Bioengineering 129, 2 (2020): 192–98.

Kermasha S, Perraud X, Bisakowski B and Husson F. „Production of Flavor Compounds by Hydroperoxide Lyase from Enzymatic Extracts of *Penicillium* Sp.“ Journal of Molecular Catalysis B: Enzymatic 19–20 (2002): 479–87.

Kohlmann M, Bachmann A, Weichert H, Kolbe A, Balkenhohl T, Wasternack C and Feussner I. „Formation of Lipoyxygenase-Pathway-Derived Aldehydes in Barley Leaves upon Methyl Jasmonate Treatment“. European Journal of Biochemistry 260, 3 (1999): 885–95.

Kües U. „Life History and Developmental Processes in the Basidiomycete *Coprinus cinereus*“. Microbiology and Molecular Biology Reviews 64, 2 (2000): 316–53.

Kuribayashi T, Kaise H, Uno C, Hara T, Hayakawa T and Joh T. „Purification and Characterization of Lipoyxygenase from *Pleurotus ostreatus*“. Journal of Agricultural and Food Chemistry 50, 5 (2002): 1247–53.

León IP de, Hamberg M and Castresana C. „Oxylipins in Moss Development and Defense“. *Frontiers in Plant Science* 6, (2015): 483.

Li QLZ, Li W, Li X, Huang W, Yang H and Zheng L. „Chemical Compositions and Volatile Compounds of *Tricholoma matsutake* from Different Geographical Areas at Different Stages of Maturity“. *Food Science and Biotechnology* 25, 1 (2016): 71–77.

Major IT, Yoshida Y, Campos ML, Kapali G, Xin XF, Sugimoto K, de Oliveira Ferraira D, He, SY and Hose GA. „Regulation of growth–defense balance by the JASMONATE ZIM-DOMAIN (JAZ)-MYC transcriptional module“. *New Phytologist* 4, 215 (2017): 1533–47.

Matsui K, Toyota H, Kajiwara T, Kakuno T and Hatanaka A. „Fatty Acid Hydroperoxide Cleaving Enzyme, Hydroperoxide Lyase, from Tea Leaves“. *Phytochemistry* 30, 7 (1991): 2109–13.

Matsui K, Sasahara S, Akakabe Y and Kajiwara T. „Linoleic Acid 10-hydroperoxide as an Intermediate during Formation of 1-octen-3-ol from Linoleic Acid in *Lentinus Decadetes*“. *Bioscience, Biotechnology and Biochemistry* 67, 10 (2003): 2280–82.

Mau, JL, Chyau CC, Li JY and Tseng YH. „Flavor compounds in straw mushrooms *Volvariella volvacea* harvested at different stages of maturity.“ *Journal of Agricultural and Food Chemistry* 45, 12 (1997): 4726–4729.

Miyamoto K, Murakami T, Kakumyan P, Keller NP, and Matsui K. „Formation of 1-octen-3-ol from *Aspergillus flavus* conidia is accelerated after disruption of cells independently of Ppo oxygenases, and is not a main cause of inhibition of germination.“ *PeerJ* 2, e395 (2014).
Nemčovič M, Jakubíková L, Víden I and Farkaš V. „Induction of conidiation by endogenous volatile compounds in *Trichoderma* spp.“ *FEMS Microbiology Letters* 284, 2 (2008): 231–36.

Oliw EH „Product Specificity of Fungal 8R - and 9S-Dioxygenases of the Peroxidase-Cyclooxygenase Superfamily with Amino Acid Derivatized Polyenoic Fatty Acids“. *Archives of Biochemistry and Biophysics* 640 (2018): 93–101.

Oliw EH, Jernerén F, Hoffmann I, Sahlin M and Garscha U. „Manganese Lipoygenase Oxidizes Bis-Allylic Hydroperoxides and Octadecenoic Acids by Different Mechanisms“. *Biochimica et Biophysica Acta (BBA) - Molecular and Cell Biology of Lipids* 1811, 3 (2011): 138–47.

Oliw EH, Aragó M, Chen Y and Jernerén F. „A New Class of Fatty Acid Allene Oxide Formed by the DOX-P450 Fusion Proteins of Human and Plant Pathogenic Fungi, *C. immitis* and *Z. tritici*“. *Journal of Lipid Research* 57, 8 (2016): 1518–28.

Orban A, Hennicke F and Rühl M. „Volatilomes of *Cyclocybe aegerita* during Different Stages of Monokaryotic and Dikaryotic Fruiting“. *Biological Chemistry* 401, 8 (2020): 995-1004.

Plagemann I, Zelena K, Arendt P, Ringel PD, Krings U and Berger RG. „LOXPsa1, the First Recombinant Lipoygenase from a Basidiomycete Fungus“. *Journal of Molecular Catalysis B: Enzymatic* 87 (2013): 99–104.

Rapier S, Breheret S, Talou T, Pelissier Y, Milhau M and Bessiere JM. „Volatile components of fresh *Agrocybe aegerita* and *Tricholoma sulfureum*“. *Cryptogramie Mycologie* 19, 1–2 (1998): 15–23.

Romagnolo A, Spina F, Brenna E, Crotti M, Parmeggiani F and Varese GC. „Identification of Fungal Ene-Reductase Activity by Means of a Functional Screening“. *Fungal Biology* 119, 6 (2015): 487–93.

Schaller A and Stintzi A. „Enzymes in jasmonate biosynthesis - structure, function, regulation“. *Phytochemistry* 70, 13-14 (2009): 1532-1538.

Schulz-Bohm K, Martin-Sanchez L and Garbeva P. „Microbial Volatiles: Small Molecules with an Important Role in Intra- and Inter-Kingdom Interactions“. *Frontiers in Microbiology* 8 (2017) :2484.

Song W-C, Baertschi WS, Boeglin EW, Harris T and Brash A. „Formation of Epoxyalcohols by a purified Allene Oxide Synthase“. *The Journal of Biological Chemistry* 268, 9 (1993): 6293-6298.

Sooman L and Oliw EH. „Discovery of a Novel Linoleate Dioxygenase of *Fusarium oxysporum* and Linoleate Diol Synthase of *Colletotrichum Graminicola*“. *Lipids* 50, 12 (2015): 1243–52.

Stolterfoht H, Rinnofner C, Winkler M and Pichler . „Recombinant Lipoxygenases and Hydroperoxide Lyases for the Synthesis of Green Leaf Volatiles“. *Journal of Agricultural and Food Chemistry* 67, 49 (2019): 13367–92.

Su C and Oliw EH. „Manganese Lipoxygenase: Purification and characterization“. *Journal of Biological Chemistry* 273, 21 (1998): 13072–79.

Su C and Oliw EH. „Purification and Characterization of Linoleate 8-Dioxygenase from the Fungus *Gaeumannomyces graminis* as a Novel Hemoprotein“. *Journal of Biological Chemistry* 271, 24 (1996): 14112–18.

Suurmeijer CNSP, Pérez-Gilabert M, van Unen D-J, van der Hijden HTWM, Veldink GA and Vliegthart JFG. „Purification, Stabilization and Characterization of Tomato Fatty Acid Hydroperoxide Lyase“. *Phytochemistry* 53, 2 (2000): 177–85.

Tasaki Y, Kobayashi D, Sato R, Hayashi S and Joh T. „Variations in 1-octen-3-ol and lipoxygenase gene expression in the oyster mushroom *Pleurotus ostreatus* according to fruiting bodydevelopmental, tissue specificity, maturity, and postharvest storage“. *Mycoscience* 60, 3 (2019): 170-176.

Teder T, Löhelaid H and Samel N. „Structural and Functional Insights into the Reaction Specificity of Catalase-Related Hydroperoxide Lyase: A Shift from Lyase Activity to Allene Oxide Synthase by Site-Directed Mutagenesis“. PLOS ONE 12, 9 (2017): e0185291.

Tressl R, Bahri D and Engel KH. „Formation of Eight-Carbon and Ten-Carbon Components in Mushrooms (*Agaricus campestris*)“. Journal of Agricultural and Food Chemistry 30, 1 (1982): 89-93.

Tressl R, Bahri D and Engel KH. „Lipid Oxidation in Fruits and Vegetables“. Quality of Selected Fruits and Vegetables of North America. ACS Symposium Series 170, 16 (1981): 213-232.

Tsitsigiannis DI and Keller NP. „Oxylipins as Developmental and Host–Fungal Communication Signals“. Trends in Microbiology 15, 3 (2007): 109–18.

Wan X-H, Chen S-X, Wang C-Y, Zhang R-R, Cheng S-Q, Meng H-W and Shen X-Q. „Isolation, Expression and Characterization of a Hydroperoxide Lyase Gene from Cucumber“. International Journal of Molecular Sciences 14, 11 (2013): 22082–101.

Wanner P and Tressl R. „Purification and Characterization of Two Enone Reductases from *Saccharomyces cerevisiae*“. European Journal of Biochemistry 255, 1 (1998): 271–78.

Wasternack C and Song S. „Jasmonates: biosynthesis, metabolism, and signaling by proteins activating and repressing transcription“. Journal of Experimental Botany 68, 6 (2017): 1303-1321.

Wasternack C and Feussner I. „The Oxylipin Pathways: Biochemistry and Function“. Annual Review of Plant Biology 69, 1 (2018): 363–86.

Wurzenberger M and Grosch W. „The Enzymic Oxidative Breakdown of Linoleic Acid in Mushrooms (*Psalliota bispora*)“. Zeitschrift Für Lebensmittel-Untersuchung and -Forschung 175, 3 (1982): 186–90.

Wurzenberger M and Grosch W. „Stereochemistry of the Cleavage of the 10-hydroperoxide Isomer of Linoleic acid to 1-octen-3-ol by a Hydroperoxide Lyase from Mushrooms (*Psalliota bispora*)“. *Biochimica et Biophysica Acta* 795, (1984): 163-165.

Zhu Z-J, Chen H-M, Chen J-J, Yang R and Yan X-J. „One-Step Bioconversion of Fatty Acids into C8–C9 Volatile Aroma Compounds by a Multifunctional Lipoxygenase Cloned from *Pyropia Haitanensis*“. *Journal of Agricultural and Food Chemistry* 66, 5 (2018): 1233–41.

2 Publications

2.1 Publication 1: A new lipoxygenase from the agaric fungus *Agrocybe aegerita*: biochemical characterization and kinetic properties

Dominik Karrer, Dr. Martin Rühl

PLOS ONE (2019), e0218625.

DOI: [10.1371/journal.pone.0218625](https://doi.org/10.1371/journal.pone.0218625)

RESEARCH ARTICLE

A new lipoxygenase from the agaric fungus *Agrocybe aegerita*: Biochemical characterization and kinetic properties

Dominik Karrer¹, Martin Rühl^{1,2*}

1 Institute of Food Chemistry and Food Biotechnology, Justus Liebig University Giessen, Giessen, Hesse, Germany, **2** Fraunhofer Institute for Molecular Biology and Applied Ecology IME Business Area Bioresources, Giessen, Hesse, Germany

* martin.ruehl@uni-giessen.de



Abstract

Oxylipins are metabolites with a variety of biological functions. However, the biosynthetic pathway is widely unknown. It is considered that the first step is the oxygenation of polyunsaturated fatty acids like linoleic acid. Therefore, a lipoxygenase (LOX) from the edible basidiomycete *Agrocybe aegerita* was investigated. The AaeLOX4 was heterologously expressed in *E. coli* and purified via affinity chromatography and gel filtration. Biochemical properties and kinetic parameters of the purified AaeLOX4 were determined with linoleic acid and linolenic acid as substrates. The obtained K_m , v_{max} and k_{cat} values for linoleic acid were 295.5 μM , 16.5 $\mu\text{M} \cdot \text{min}^{-1} \cdot \text{mg}^{-1}$ and 103.9 s^{-1} , respectively. For linolenic acid K_m , v_{max} and k_{cat} values of 634.2 μM , 19.5 $\mu\text{M} \cdot \text{min}^{-1} \cdot \text{mg}^{-1}$ and 18.3 s^{-1} were calculated. Maximum activities were observed at pH 7.5 and 25 °C. The main product of linoleic acid conversion was identified with normal-phase HPLC. This analysis revealed an explicit production of 13-hydroperoxy-9,11-octadecadienoic acid (13-HPOD). The experimental regio specificity is underpinned by the amino acid residues W384, F450, R594 and V635 considered relevant for regio specificity in LOX. In conclusion, HPLC-analysis and alignments revealed that AaeLOX4 is a 13-LOX.

OPEN ACCESS

Citation: Karrer D, Rühl M (2019) A new lipoxygenase from the agaric fungus *Agrocybe aegerita*: Biochemical characterization and kinetic properties. PLoS ONE 14(6): e0218625. <https://doi.org/10.1371/journal.pone.0218625>

Editor: Daotai Nie, Southern Illinois University School of Medicine, UNITED STATES

Received: February 11, 2019

Accepted: June 5, 2019

Published: June 19, 2019

Copyright: © 2019 Karrer, Rühl. This is an open access article distributed under the terms of the [Creative Commons Attribution License](https://creativecommons.org/licenses/by/4.0/), which permits unrestricted use, distribution, and reproduction in any medium, provided the original author and source are credited.

Data Availability Statement: Gene sequence for AaeLOX4 is available from the GenBank database under the accession number MK451709.

Funding: The grant RU 2137/1 from the Deutsche Forschungsgemeinschaft (<http://www.dfg.de/en/>) was awarded to MR. DK and MR used facilities of the LOEWE Center for Insect Biotechnology & Bioresources financed by the Hessen State Ministry of Higher Education, Research and the Arts (<http://www.proloewe.de/en/>). The funders had no role in study design, data collection and

Introduction

Oxylipins are lipoxygenase-derived metabolites with a variety of different structures and biological functions. These metabolites can be found in plants, mammals, bacteria, algae, mosses and fungi [1]. In mammals, they are involved in the regulation of immune response. In recent years, human lipid mediators like e.g. hepxilins and trioxilins, which play an important role in tissue healing, organ protection, pain reduction and host defense received a lot of attention [2, 3].

In plants, they serve as signaling molecules, are involved in mediate stress response or in defense against pathogens, whereas in fungi they are associated with sporulation and the sexual as well as asexual life cycle [4, 5]. Lipoxygenases (LOX) are non-heme iron dependent dioxygenases which catalyze the insertion of molecular oxygen at a (1Z,4Z)-pentadiene motif, which

analysis, decision to publish, or preparation of the manuscript.

Competing interests: The authors have declared that no competing interests exist.

occurs e.g. in polyunsaturated fatty acids (PUFAs), in a regio- and stereospecific manner [2, 3, 6, 7]. Additionally, fungal LOX with manganese instead of iron in the active site were also described [8, 9]. The oxidation of PUFAs leads to a reactive hydroperoxide and is considered to be the first step in the oxylipin-pathway. In higher fungi of the phyla Basidiomycota and Ascomycota, C₁₈-PUFAs are predominantly present, whereas C₂₀-PUFAs can be found only in very minor amounts [1]. This indicates that the oxygenation of linoleic-, linolenic- or arachidonic acid is the initial step in oxylipin-biosynthesis. Subsequent steps lead to a variety of oxylipins such as C8 volatile compounds which contribute to the significant flavor of mushroom. Among them, the most important and well known is oct-1-en-3-ol derived from linoleic acid [10]. The pathways, leading to oct-1-en-3-ol and other C8 volatile compounds are unknown. Several studies showed that fungi can convert linoleic acid into different oxylipins. It was found that the button mushroom *Agaricus bisporus* is able to produce oct-1-en-3-ol in several steps from linoleic acid. These steps include amongst others an oxygenation of linoleic acid to 10-hydroperoxyoctadecadienoic acid (10-HPOD). It was proposed that LOX generate the needed 10-HPOD, but up to now the corresponding enzyme yet has to be found [11, 12, 13]. Another study with *A. bisporus* revealed the conversion of linoleic acid into 8(*R*)-hydroxy-9*Z*,12*Z*-octadecadienoic acid and 8(*R*)-11(*S*)dihydroxy-9*Z*,12*Z*-octadecadienoic acid [14]. It also has been reported, that a mycelial pellet homogenate of an oyster mushroom *Pleurotus pulmonaris* produced oct-1-en-3-ol and the 10-oxo-acid from linoleic acid [15]. In general, studies on basidiomycetous LOX are scarce with only two LOX described so far [6, 10]. This shortcoming is addressed in this paper and a new LOX from the black poplar mushroom *Agrocybe aegerita*, also known to produce C8 volatile compounds [16, 17], is expressed, purified and characterized.

Materials and methods

Cloning and protein expression of *AaeLOX4*

The codon optimized *AaeLOX4* gene (*Aaelox4*), whose original cDNA was deposited under the accession number MK451709, was commercially purchased and cloned into the plasmid pET28a (BioCat GmbH, Heidelberg, Germany). For protein expression, pET28a/*AaeLOX4* plasmid was transformed into *E. coli* BL21(DE3) Gold. Recombinant *E. coli* cells were cultivated in Terrific Broth medium (TB) containing 12 g tryptone, 24 g yeast extract and 5 g glycerol, supplemented with 50 mg·L⁻¹ kanamycin as selection marker, at 37 °C until an OD₆₀₀ of 0.5 was reached. Expression was induced by adding isopropyl-β-D-thiogalactopyranoside to a final concentration of 0.5 mM. Expression temperature was reduced to 24 °C and cultivated for another 24 h. Cells were harvested by centrifugation (4,000 g, 30 min, 4 °C) and stored at -20 °C until further use.

Protein purification

The cell pellet was thawed on ice and resuspended in lysis-buffer (50 mM phosphate, 300 mM NaCl, pH 7.5). Disruption of cells was carried out by sonification (3 cycles for 60 s on, 60 s rest) on ice using a sonifier (Bandelin Sonopuls, Berlin, Germany). After complete disruption, cell debris was removed by centrifugation (14,000 g, 30 min, 4 °C). The resulting supernatant was loaded twice on a 5 mL HisTrap column (GE-Healthcare), washed with 5 column volumes lysis-buffer containing 25 mM imidazole and eluted with 5 column volumes with the same buffer containing 500 mM imidazole. Gel filtration was performed on a Superdex 200 16/60 (GE Healthcare) using a buffer containing 50 mM Tris(hydroxymethyl)amino-methane (Tris/HCl), 300 mM NaCl, 10% (v/v) glycerol, pH 7.5 and a flow rate of 0.2 mL·min⁻¹. Elution was

collected in 2 mL fractions and analyzed via SDS-PAGE. Fractions with purified *Aae*-LOX4 were used for further analysis.

Lipoxygenase assay

The substrate solution for the LOX assay was prepared as follows. 10 μ L linoleic acid or linolenic acid was added to 915 μ L ddH₂O containing 15 μ L Tween 20 and 60 μ L 1M NaOH. Aliquots were stored at -20 °C and thawed before use. LOX activity was determined by recording the formation of the conjugated double bond at 234 nm ($\epsilon = 25,000 \text{ M}^{-1} \cdot \text{cm}^{-1}$) on a Nanophotometer (Implen, Munich, Germany). Typical reaction mixture contained 0.5 mM linoleic acid, 20 μ L enzyme solution and 50 mM phosphate buffer, pH 7.5 to a final volume of 1 mL.

Determination of pH- and temperature-optimum

For the determination of the pH-optimum, three different buffers were used: 50 mM acetate buffer, pH 4.5–6; 50 mM phosphate buffer, pH 6.5–8 and 50 mM borate buffer, pH 8.5–10. Effects of the temperature were determined by incubating the reaction mixture at different temperatures, ranging from 15 °C– 65 °C.

Kinetic parameters

Michaelis-Menten kinetics were calculated by incubating purified *Aae*LOX4 with different linoleic acid or linolenic acid concentrations ranging from 0.025 mM– 2 mM. All measurements were carried out in 50 mM phosphate buffer at pH 7.5 and 25 °C. Initial formation rates of the conjugated double bond were recorded at 234 nm in triplicates and consulted for calculating K_m , v_{max} and k_{cat} .

Product analysis

Product specificity of *Aae*LOX4 was determined by incubating 1 mM linoleic acid, 20 μ L *Aae*-LOX4 and 50 mM phosphate buffer, pH 7.5 in a final volume of 1 mL. Reaction progress was followed by recording the formation of the conjugated double bond at 234 nm. Incubations were stopped when no further increase in extinction was detectable. The resulting hydroperoxy linoleic acids were extracted by adding 1 mL n-hexane. For HPLC-analysis, the extracts were dried under a continuous N₂ stream and dissolved in n-hexane/2-propanol/acetic acid (100/5/1, v/v/v). Normal-phase-HPLC was carried out on a Nucleodur SiOH 100–5 column (Macherey-Nagel; 4.6x250 mm, 5 μ m particle size) with an isocratic eluent system of n-hexane/2-propanol/acetic acid (100/5/1, v/v/v) at a flow rate of 1 mL \cdot min⁻¹. Elution was followed at 234 nm for hydroperoxy fatty acids and 210 nm for unsaturated fatty acids. Product specificity was evaluated by comparison with 13-HPOD and 9-HPOD standards prepared with commercial soybean LOX-1 [10]. Control experiments were carried out like described above without adding enzyme to the reaction mixture.

Results

Lipoxygenases of the black poplar mushroom *Agrocybe aegerita*

In the recently sequenced genome of *Agrocybe aegerita* (also known as *Cyclocybe aegerita* and *Pholiota aegerita*), five genes coding for putative LOX have been annotated and labelled as LOX1 (AAE3_00896), LOX2 (AAE3_01552), LOX3 (AAE3_09652), LOX4 (AAE3_04864) and LOX5 (AAE3_07753) ([18], www.thines-lab.senckenberg.de/agrocybe_genome). Deduced amino acid sequences of *A. aegerita* LOX genes and already characterized fungal LOX from Ascomycota (*Fusarium oxysporum* and *Gaeumannomyces graminis*) and Basidiomycota

(*Pleurotus sapidus* and *Pleurotus ostreatus*) were used for phylogenetic analysis (<http://www.phylogeny.fr/> using default parameters). LOX separated into two distinct sections with the characterized LOX from *G. graminis* [19] on one side and all basidiomycetous LOX as well as the characterized LOX from *F. oxysporum* [20] on the other side (S1 Fig). The latter group split into three parts: i) a large cluster containing both characterized LOXs from the *Pleurotus* species and four putative LOXs from *A. aegerita* (LOX1, LOX2, LOX4, LOX5), ii) LOX3 from *A. aegerita* and iii) the LOX from *F. oxysporum*.

Heterologous expression and purification

Active and soluble *AaeLOX4* was obtained from cultures of *E. coli* BL21(DE3) Gold carrying the pET28a/*AaeLOX4* plasmid. SDS-PAGE analysis of cell lysate indicated that *AaeLOX4* is present in the soluble lysate fraction (Fig 1). Thus, the cell lysate was directly applied onto an

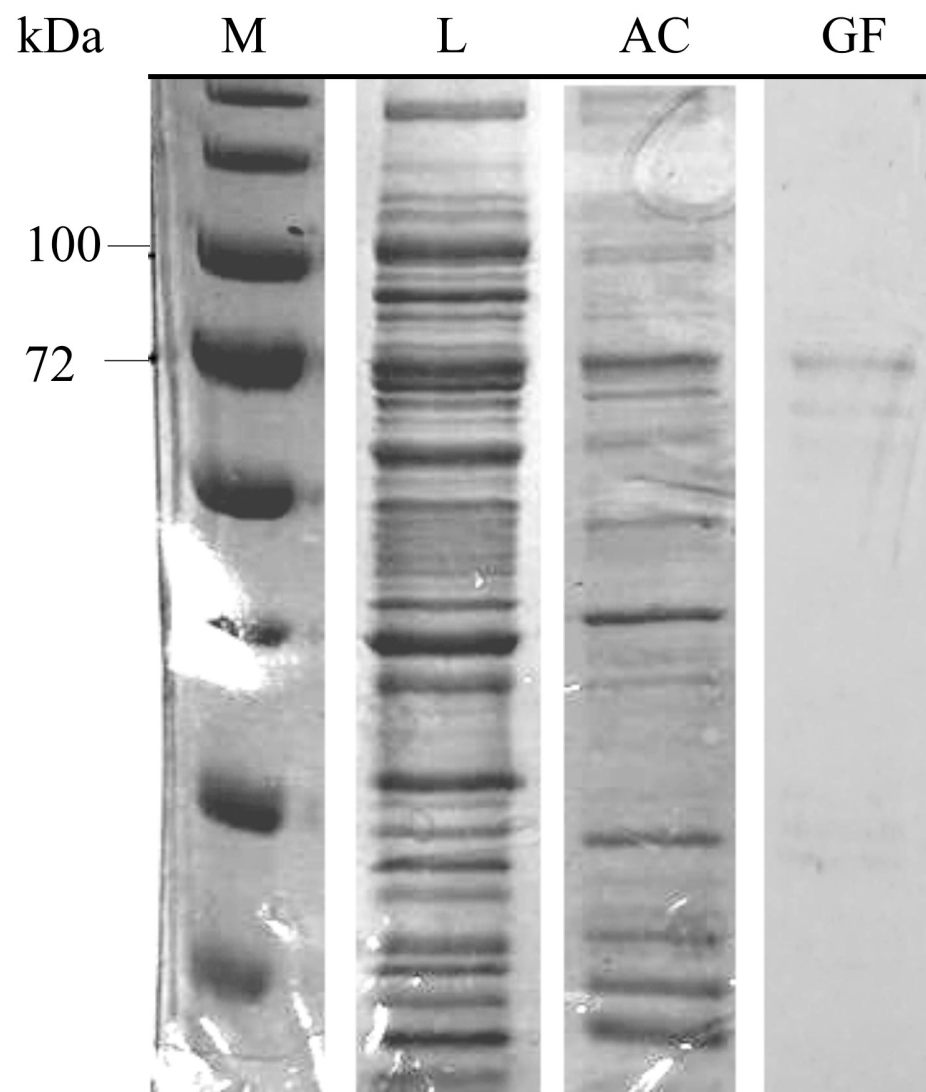


Fig 1. SDS-PAGE analysis of *AaeLOX4* expression and purification. M = marker, L = cleared lysate, AC = Purification after affinity chromatography, GF = Purified enzyme after gel filtration.

<https://doi.org/10.1371/journal.pone.0218625.g001>

Table 1. Summary of the purification steps of *AaeLOX4* in *E. coli*.

Step	Total protein (mg)	Specific activity (U · mg ⁻¹)	Purification (fold)
Crude extract	146.97	0.038	1.0
Affinity chromatography	37.16	0.329	8.6
Gel filtration	0.09	51.34	1351.1

<https://doi.org/10.1371/journal.pone.0218625.t001>

affinity chromatographic column, which resulted in the removal of crude impurities. Subsequent gel filtration led to pure *AaeLOX4* (Fig 1). The main band had an estimated molecular weight of around 80 kDa confirming the predicted molecular weight of the amino acid sequence of 79 kDa. Overall, a 1,351-fold purification yield was obtained (Table 1).

LOX biochemical properties and characteristics

The activity of *AaeLOX4* was determined in a temperature range between 15 °C and 65 °C. While the relative activity from 25 °C to 45 °C resulted in a steady loss of about one-fifth of activity, a further temperature increase to 55 °C caused a dramatic loss in activity and no activity could be detected at 65 °C. At the lowest analyzed temperature of 15 °C, one-third of the maximal LOX activity remained (Fig 2).

With increasing pH of the buffer system used for LOX activity assays, a steady activity enhancement is obtained reaching its maximum at pH 7.5. Further increase of the pH showed a drastic activity loss with no detectable activity from pH 9 and above. In the acidic environment, *AaeLOX4* showed more tolerable activity properties. Decreasing the pH from 7.5 to 6,

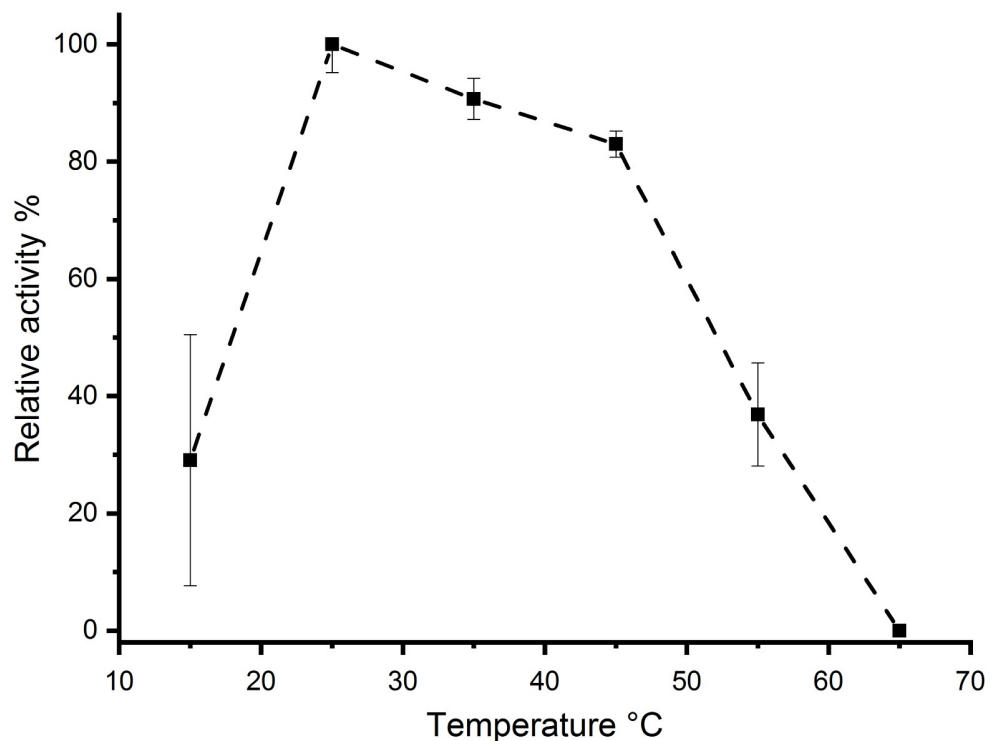


Fig 2. Effects of the temperature on *AaeLOX4* activity.

<https://doi.org/10.1371/journal.pone.0218625.g002>

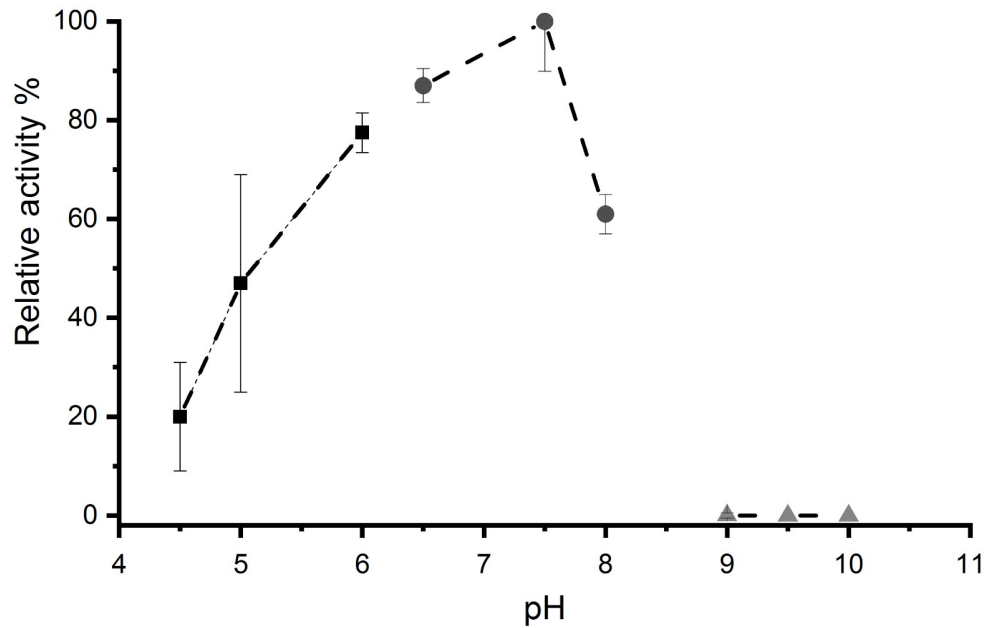


Fig 3. Effects of pH on *AaeLOX4* activity. 50 mM acetate buffer (squares), 50 mM phosphate buffer (circles), 50 mM borate buffer (triangles).

<https://doi.org/10.1371/journal.pone.0218625.g003>

resulted in a loss of about 20% activity. Nevertheless, at pH 5.0 the relative activity decreased to 50%, while 20% relative activity was left at pH 4.5 (Fig 3).

Michaelis-Menten parameters were deduced on basis of the Lineweaver-Burk plot depicting *AaeLOX4* activity with linoleic acid or linolenic acid concentrations between 0.025–2 mM (Fig 4). The obtained K_m , v_{max} and k_{cat} values for linoleic acid were 295.5 μM , 16.5 $\mu\text{M} \cdot \text{min}^{-1} \cdot \text{mg}^{-1}$ and 103.9 s^{-1} , respectively. For linolenic acid as substrate K_m , v_{max} and k_{cat} values of 634.2 μM , 19.5 $\mu\text{M} \cdot \text{min}^{-1} \cdot \text{mg}^{-1}$ and 18.3 s^{-1} were calculated (Table 2). Substrate specificity of *AaeLOX4*

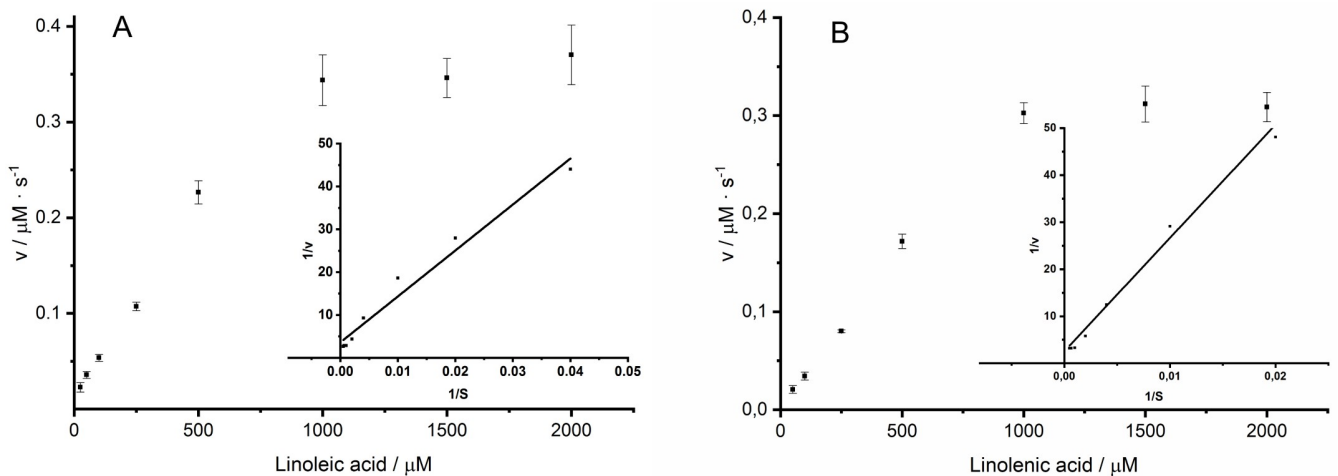


Fig 4. Velocity of *AaeLOX4* dependent on linoleic acid (A) and linolenic acid (B) concentrations. Values represent the means of triplicates and their standard deviation. Inset represents Lineweaver-Burk plot.

<https://doi.org/10.1371/journal.pone.0218625.g004>

Table 2. Kinetic parameters of *AaeLOX4*.

Substrate	$K_m / \mu\text{M}$	$v_{\text{max}} / \mu\text{M} \cdot \text{min}^{-1} \cdot \text{mg}^{-1}$	$k_{\text{cat}} / \text{s}^{-1}$
linoleic acid	295.5	16.5	103.9
linolenic acid	634.2	19.5	18.3

<https://doi.org/10.1371/journal.pone.0218625.t002>

Table 3. Substrate specificity of *AaeLOX4*.

Substrate	Relative activity / %
linoleic acid	100
linolenic acid	88.8
arachidonic acid	7.3

<https://doi.org/10.1371/journal.pone.0218625.t003>

was estimated by comparing the relative activities towards different PUFAs (Table 3). The enzyme showed the highest specificity for linoleic acid and a high relative activity for linolenic acid (88.8%). However, arachidonic acid showed the lowest relative activity with 7.3%.

HPLC-analysis of products

Specificity of *AaeLOX4* was analyzed by normal-phase HPLC. The elution profile of *AaeLOX4* shows two major products which elute at 3.12 min and 3.81 min (Fig 5). 13-*Z,E*-HPOD and 13-*E,E*-HPOD as well as 9-*Z,E*-HPOD and 9-*E,E*-HPOD have been prepared with soybean LOX-1 according to Kuribayashi et al. [10]. 13-*Z,E*-HPOD and 13-*E,E*-HPOD elute at 3.33 min and 3.79 min, respectively, whereas the isomeric 9-HPOD mixture elute as one peak at 5.79 min. The negative control showed no peaks at these retention times. The comparison between *AaeLOX4* products and soybean LOX-1 products revealed that *AaeLOX4* produces highly specific 13-HPOD. A production of 9-HPOD by *AaeLOX4* was not detectable and ruled out by comparing the UV-spectra of 9-HPOD eluting at 5.79 min from soybean LOX-1 with peaks in this range in the elution profile of *AaeLOX4* products.

Discussion

In this study, we were able to express a soluble and active *AaeLOX4* from *A. aegerita* in *E. coli*. As far as we know, this is the second basidiomycetous LOX recombinantly expressed in *E. coli*. While Plagemann et al. [5] used an approach with co-expression of chaperones to accomplish a soluble LOX expression from cDNA of *P. sapidus*, we reached the soluble expression with a codon optimized gene. Affinity chromatography with following gel filtration led to a highly purified protein in sufficient concentrations for further characterization experiments. The observed influence of temperature and pH on *AaeLOX4* with its maximum activity at 25 °C and pH 7.5 is in accordance with LOXs from other fungi, such as a wildtype LOX from *P. ostreatus*, having its maximum activity at 25 °C and pH values between 7.5 and 8.0 [10]. However, the recombinant LOX from *P. sapidus* showed a temperature range with highest activities ranging from 25 °C to 35 °C. The optimal pH value of *P. sapidus* LOX was 7.0 and in contrast to *AaeLOX4* showed activity up to a pH of 9.5 [5]. Interestingly, *AaeLOX4* showed differences in the kinetic parameters for linoleic acid compared to other LOXs from Basidiomycota. The K_m values for the LOXs from *P. sapidus* and from *P. ostreatus* are 40.3 μM and 130 μM , which are both lower than our calculated K_m of 295.5 μM . On the other hand, the obtained v_{max} of 16.5 $\mu\text{M} \text{min}^{-1} \text{mg}^{-1}$ is comparable with the LOX from *P. ostreatus* (23.4 $\mu\text{M} \text{min}^{-1} \text{mg}^{-1}$) and the k_{cat} value of 103.9 s^{-1} is comparable with the LOX from *P. sapidus* (157 s^{-1}) [5, 10].

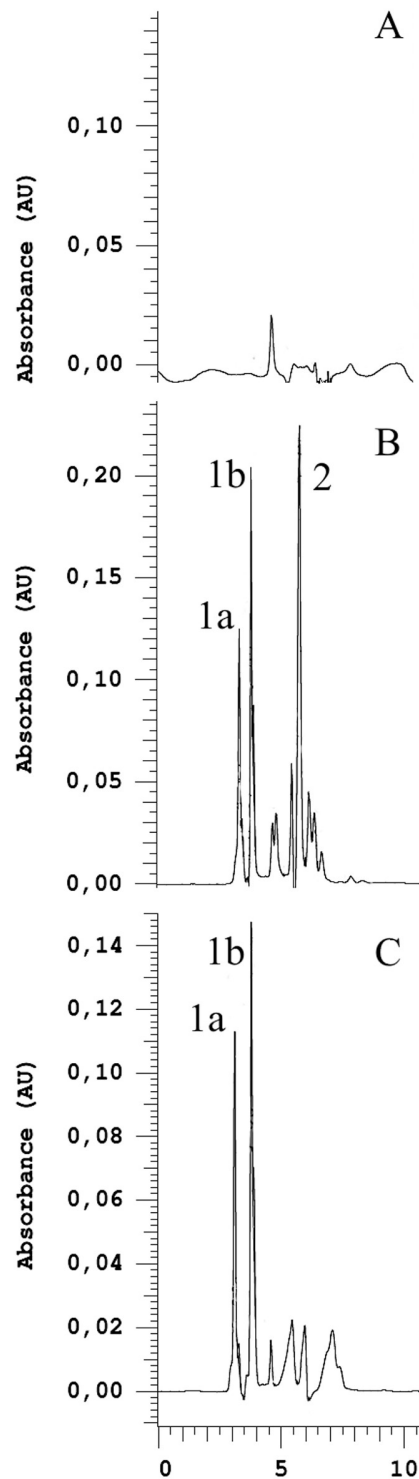


Fig 5. NP-HPLC analysis of the oxygenated products of linoleic acid. Chromatogram was recorded at 234 nm. (A) negative control. Extract of the reaction mixture lacking enzyme. (B) Extract of the reaction products from soybean LOX-1. (C) Extract of the reaction products from *Aae*LOX4. (1a) 13-*Z,E*-HPOD, (1b) 13-*E,E*-HPOD, (2) 9-*Z,E*-HPOD + 9-*E,E*-HPOD.

<https://doi.org/10.1371/journal.pone.0218625.g005>

Analogous K_m and v_{max} values were also found for a LOX in oriental melon (230.3 μM and 15.25 $\mu\text{M min}^{-1} \text{mg}^{-1}$) [21]. Interestingly, a LOX originating from the bacteria *Myxococcus xanthus* shows comparable K_m values for linoleic acid (380 μM) but drastically lower K_m with linolenic acid and other C_{20} -PUFAs like arachidonic acid or eicosapentaenoic acid [6]. Soybean LOX-1 shows a lower K_m of 150 μM but shares a comparable v_{max} of 13.5 $\mu\text{M min}^{-1} \text{mg}^{-1}$ [22]. The catalytic efficiency of *AaeLOX4* was higher with linoleic acid than with linolenic acid. This finding reflects the estimated relative activities towards different PUFAs which revealed a preference for linoleic acid. High activity was also found for linolenic acid, whereas arachidonic acid showed poor activity. These results are comparable with the LOXs from *P. ostreatus* and *F. oxysporum* [10, 20]. The analysis of product specificity revealed that 13-HPOD (13-*Z,E*-HPOD and 13-*E,E*-HPOD) was the only detectable product and thus, *AaeLOX4* can be considered as a 13-LOX. Equally, LOXs from *P. sapidus*, *P. ostreatus*, *F. oxysporum* and *G. graminis* showed a specific conversion of linoleic acid to 13-HPOD [5, 10, 19, 20]. Nevertheless in contrast to *AaeLOX4*, LOXs from *P. sapidus*, *P. ostreatus* and *F. oxysporum* produced minor amounts of 9-HPOD. Whereas the LOX from *G. graminis* showed no significant synthesis of 9-HPOD [19]. This finding was confirmed with amino acid sequence alignments which showed that various determinants responsible for the regio- and stereo-specificity can also be found in *AaeLOX4* (S2 Fig). Three positions, which are responsible for the depth of substrate penetration and thus are responsible for regio-specificity, have been described for mammalian LOX [23, 24]. While space-filling amino acids at these positions lead to oxygenation near the methyl end, enlargement of the active site favors oxygenations towards the carboxy end [24]. Applying this concept on *AaeLOX4*, the bulky amino acids at the crucial positions (W384, F450 and V635) are present in the amino acid sequence of *AaeLOX4* and result in the transformation of linoleic acid to 13-HPOD (Fig 5). Also the LOXs from *P. ostreatus*, *P. sapidus* and *F. oxysporum* led to a specific production of 13-HPOD [5, 10, 20]. Consistently, all these LOXs share the same bulky amino acids at the crucial positions [23, 24]. According to Andreou et al. [25, 26] and Hornung et al. [27], regio-specificity is mainly determined by the orientation of the substrate. Based on their model, substrate orientation with the methyl end first leads to an oxygenation at C-13. The inverse orientation of the substrate therefore is proposed to oxygenate C-9. Additionally, reduced space in the active site is also considered to favor a substrate orientation with its methyl end towards the active site. This model involves the importance of a positive charged amino acid at the end of the active site with no interference from another amino acid masking the positive charge to stabilize the carboxy end of the substrate. On the one hand the LOXs from *P. ostreatus*, *P. sapidus* and *F. oxysporum* share a lysine, considered to stabilize the negative charged carboxy end of the substrate and therefore differ in their amino acid sequence compared to *AaeLOX4* where this lysine is replaced by an arginine which could of course fulfil the same purpose. On the other hand, the alignment shows that the LOXs from *P. ostreatus*, *P. sapidus*, *F. oxysporum* and *AaeLOX4* share a phenylalanine near the positive charged amino acids lysine or arginine which masks the charge and therefore leads to a substrate orientation with the methyl end penetrating the active site leading to a region-specific oxygenation at C-13 [25, 26, 27]. Phylogenetic analysis shows that the fungal LOXs cluster in different groups. Whether LOXs of the same group harbor similar enzymatic properties is an important question, which can help to depict distinct enzyme function. This assumption is reasonable by comparing the K_m values for linoleic acid LOXs in the phylogenetic tree. *FoxLOX* and *GgrLOX*, show low K_m values of 4.4 and 6.9 μM while the subgroup of *PosLOX* and *PsaLOX* show distinctly higher K_m values of 130 and 40.3 μM , respectively. The characterized *AaeLOX4*, which does not cluster with other subgroups of characterized LOX showed an even higher K_m value of 295.5.

Supporting information

S1 Fig. Phylogenetic analysis of different fungal LOX. *Aae*—*Agrocybe aegerita*, *Fox*—*Fusarium oxysporum*, *Ggr*—*Gaeumannomyces graminis*, *Pos*—*Pleurotus ostreatus*, *Psa*—*Pleurotus sapidus*; *AaeLOX1*, *AaeLOX2*, *AaeLOX3*, *AaeLOX4* (MK451709), *AaeLOX5*, *FoxLOX* (KNB01601), *GgrLOX* (AAK81882), *PsaLOX* (CCV01580), *PosLOX* (CCV01578). (TIF)

S2 Fig. Partial amino acid sequence alignment of different LOX. *Agrocybe aegerita* *AaeLOX1*, *AaeLOX2*, *AaeLOX3*, *AaeLOX4*, *AaeLOX5*, *Pleurotus sapidus* *PsaLOX*, *Pleurotus ostreatus* *PosLOX*, *Fusarium oxysporum* *FoxLOX*, *Gaeumannomyces graminis* *GgrLOX*. Alignment was carried out by using Clustal Omega with default parameters. The highlighted amino acid residues involved in ligand binding are indicated as “L”. Stereo specificity related amino acids are indicated as “B” [24], “H” [27] and “S” [23]. (TIF)

Acknowledgments

We would like to thank the anonymous reviewer for providing valuable feedback that helped to improve the paper.

Author Contributions

Conceptualization: Dominik Karrer, Martin Rühl.

Data curation: Dominik Karrer, Martin Rühl.

Funding acquisition: Martin Rühl.

Investigation: Dominik Karrer.

Project administration: Martin Rühl.

Supervision: Martin Rühl.

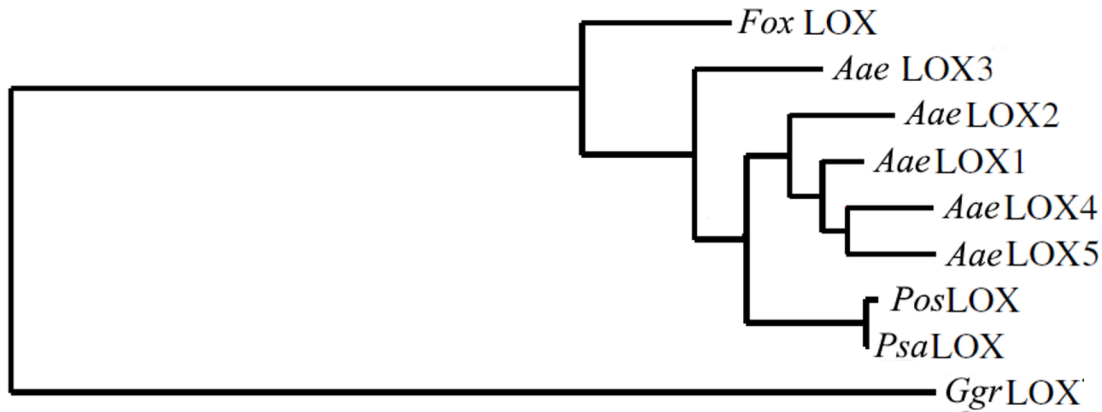
Writing – original draft: Dominik Karrer, Martin Rühl.

References

1. Brodhun F, Feussner I. Oxylipins in fungi. *FEBS J.* 2011; 278(7):1047–1063. <https://doi.org/10.1111/j.1742-4658.2011.08027.x> PMID: 21281447
2. An JU, Song YS, Kim KR, Ki YJ, Yoon DY, Oh DK. Biotransformation of polyunsaturated fatty acids to bioactive hepoxilins and trioxilins by microbial enzymes. *Nat Commun.* 2018; 9(1):128. <https://doi.org/10.1038/s41467-017-02543-8> PMID: 29317615
3. Lee IG, An JU, Ko YJ, Park JB, Oh DK. Enzymatic synthesis of new hepoxilins and trioxilins from polyunsaturated fatty acids. *Green Chem.* 2019. <https://doi.org/10.1039/c9gc01031a>
4. Kock JLF, Venter P, Linke D, Schewe T, Nigam S. Biological dynamics and distribution of 3-hydroxy fatty acids in the yeast *Dipodascopsis uninucleata* as investigated by immunofluorescence microscopy. Evidence for a putative regulatory role in the sexual reproductive cycle 1. *FEBS Lett.* 1998; 427(3):345–348. PMID: 9637254
5. Plagemann I, Zelena K, Arendt P, Ringel PD, Krings U, Berger R. LOXPsa1, the first recombinant lipoxygenase from a basidiomycete fungus. *J Mol Catal B: Enzym.* 2013; 87(1):99–104.
6. An JU, Hong SH, Oh DK. Regiospecificity of a novel bacterial lipoxygenase from *Myxococcus xanthus* for polyunsaturated fatty acids. *Biochim Biophys Acta, Mol Cell Biol Lipids.* 2018; 8(8):823–833.
7. Liavonchanka A, Feussner I. Lipoxygenases: occurrence, functions and catalysis. *J Plant Physiol.* 2006; 163(3):348–357. <https://doi.org/10.1016/j.jplph.2005.11.006> PMID: 16386332

8. Hamberg M, Su C, Oliw E. Manganese Lipoxygenase. Discovery of a bis-allylic hydroperoxide as product and intermediate in a lipoxygenase reaction. *J Biol Chem*. 1998; 273(21):13080–13088. <https://doi.org/10.1074/jbc.273.21.13080> PMID: 9582346
9. Oliw EH, Jernerén F, Hoffmann I, Sahlin M, Garscha U. Manganese lipoxygenase oxidizes bis-allylic hydroperoxides and octadecenoic acids by different mechanisms. *Biochim Biophys Acta*. 2011; 1811(3):138–147. <https://doi.org/10.1016/j.bbailip.2010.12.002> PMID: 21167311
10. Kuribayashi T, Kaise H, Uno C, Hara T, Hayakawa T, Joh T. Purification and Characterization of Lipoxygenase from *Pleurotus ostreatus*. *J Agric Food Chem*. 2002; 50(5):1247–1253. PMID: 11853512
11. Wurzenberger M, Grosch W. The enzymic oxidative breakdown of linoleic acid in mushrooms (*Psalliota bispora*). *Z Lebensm Unters Forsch*. 1982; 175(3):186–190.
12. Wurzenberger M, Grosch W. Origin of the oxygen in the products of the enzymatic cleavage reaction of linoleic acid to 1-octen-3-ol and 10-oxo-trans-8-decenoic acid in mushrooms (*Psalliota bispora*). *Biochim Biophys Acta*. 1984; 794(1):18–24.
13. Wurzenberger M, Grosch W. Stereochemistry of the cleavage of the 10-hydroperoxide isomer of linoleic acid to 1-octen-3-ol by a hydroperoxide lyase from mushrooms (*Psalliota bispora*). *Biochim Biophys Acta*. 1984; 795(1):163–165.
14. Wadman M, van Zadelhoff G, Hamberg M, Visser T, Veldink G, Vliegthart JG. Conversion of linoleic acid into novel oxylipins by the mushroom *Agaricus bisporus*. *Lipids*. 2005; 40(11):1163–1170. PMID: 16459929
15. Assaf S, Hadar Y, Dosoretz C. Biosynthesis of 13-hydroperoxylinoleate, 10-oxo-8-decenoic acid and 1-octen-3-ol from linoleic acid by a mycelial-pellet homogenate of *Pleurotus pulmonarius*. *J Agric Food Chem*. 1995; 43(8):2173–2178.
16. Rapior S, Breheret S, Talou T, Pélissier Y, Milhau M, Bessière JM. Volatile Components of Fresh *Agrocybe aegerita* and *Tricholoma sulfureum*. *Cryptogam Mycol*. 1998; 19(1):15–23.
17. Kleofas V, Sommer L, Fraatz MA, Zorn H, Rühl M. Fruiting body production and aroma profile analysis of *Agrocybe aegerita* cultivated on different substrates. *Nat Resour*. 2014; 5(6):233–240.
18. Gupta DK, Rühl M, Mishra B, Kleofas V, Hofrichter M, Herzog R, et al. The genome sequence of the commercially cultivated mushroom *Agrocybe aegerita* reveals a conserved repertoire of fruiting-related genes and a versatile suite of biopolymer-degrading enzymes. *BMC Genomics*. 2018; 19(1):48. <https://doi.org/10.1186/s12864-017-4430-y> PMID: 29334897
19. Su C, Oliw E. Manganese Lipoxygenase. Purification and Characterization. *J Biol Chem*. 1998; 273(21):13072–13079. <https://doi.org/10.1074/jbc.273.21.13072> PMID: 9582345
20. Brodhun F, Cristobal-Sarramian A, Zabel S, Newie J, Hamberg M, Feussner I. An 13S-Lipoxygenase with an α -Linolenic Acid Specific Hydroperoxidase Activity from *Fusarium oxysporum*. *PLoS ONE*. 2013; 8(5):5.
21. Cao S, Chen H, Zhang C, Tang Y, Liu J, Qi H. Heterologous Expression and Biochemical Characterization of Two Lipoxygenases in Oriental Melon, *Cucumis melo var. makuwa Makino*. *PLoS ONE*. 2016; 11(4):4.
22. Pinto M, García-Barrado J, Macías P. Oxidation of resveratrol catalyzed by soybean lipoxygenase. *J Agric Food Chem*. 2003; 51(6):1653–1657. <https://doi.org/10.1021/jf025818d> PMID: 12617600
23. Sloane D, Leung R, Craik C, Sigal E. A primary determinant for lipoxygenase positional specificity. *Nature*. 1991; 354(6349):149–152. <https://doi.org/10.1038/354149a0> PMID: 1944593
24. Borngräber S, Browner M, Gillmor S, Gerth C, Anton M, Fletterick R, et al. Shape and Specificity in Mammalian 15-Lipoxygenase Active Site. *J Biol Chem*. 1999; 274(52):37345–37350. <https://doi.org/10.1074/jbc.274.52.37345> PMID: 10601303
25. Andreou A, Feussner I. Lipoxygenases—Structure and reaction mechanism. *Phytochemistry*. 2009; 70(13–14):1504–1510. <https://doi.org/10.1016/j.phytochem.2009.05.008>
26. Andreou A, Hornung E, Kunze S, Rosahl S, Feussner I. On the substrate binding of linoleate 9-lipoxygenases. *Lipids*. 2009; 44(3):207–215. <https://doi.org/10.1007/s11745-008-3264-4> PMID: 19037675
27. Hornung E, Kunze S, Liavonchanka A, Zimmermann G, Kühn D, Fritsche K. Identification of an amino acid determinant of pH regiospecificity in a seed lipoxygenase from *Momordica charantia*. *Phytochemistry*. 2008; 69(16):2774–2780. <https://doi.org/10.1016/j.phytochem.2008.09.006> PMID: 18945457

Supporting Information



1.

Figure 2.1: S1. Phylogenetic analysis of different fungal LOX.

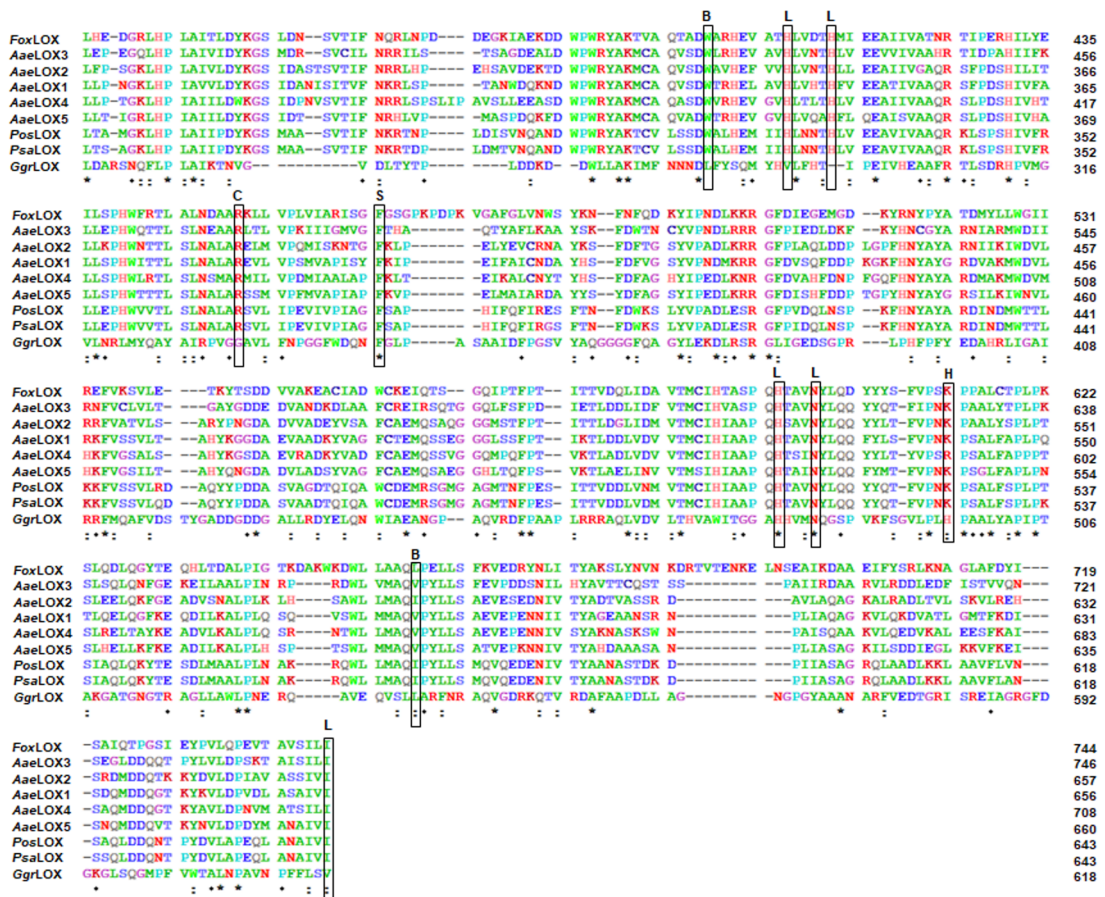


Figure 2.2: S2. Partial amino acid sequence alignment of different LOX.

2.2 Publication 2: Expanding the biocatalytic toolbox with a new type of ene/yne-reductase from *Cyclocybe aegerita*

Dominik Karrer, Dr. Martin Gand, Dr. Martin Rühl

ChemCatChem (2021), 13, 1-10.

DOI: 10.1002/cctc.202002011

Expanding the Biocatalytic Toolbox with a New Type of ene/yne-Reductase from *Cyclocybe aegerita*

Dominik Karrer,^[a] Martin Gand,^[a] and Martin Rühl^{*[a, b]}

This study introduces a new type of ene/yne-reductase from *Cyclocybe aegerita* with a broad substrate scope including aliphatic and aromatic alkenes/alkynes from which aliphatic C8-alkenones, C8-alkenals and aromatic nitroalkenes were the preferred substrates. By comparing alkenes and alkynes, a ~2-fold lower conversion towards alkynes was observed. Furthermore, it could be shown that the alkyne reduction proceeds via a slow reduction of the alkyne to the alkene followed by a rapid reduction to the corresponding alkane. An accumulation of the

alkene was not observed. Moreover, a regioselective reduction of the double bond in α,β -position of $\alpha,\beta,\gamma,\delta$ -unsaturated alkenals took place. This as well as the first biocatalytic reduction of different aliphatic and aromatic alkynes to alkanes underlines the novelty of this biocatalyst. Thus with this study on the new ene-reductase CaeEnR1, a promising substrate scope is disclosed that describes conceivably a broad occurrence of such reactions within the chemical landscape.

Introduction

Regarding the principles and metrics of green chemistry, waste prevention, atom efficiency, reduction of hazardous materials, harmless solvents and auxiliaries, energy efficiency, use of renewable raw materials, shorter synthesis routes (avoiding derivatization), use of catalytic rather than stoichiometric reagents, analytics for pollution prevention and inherently safer processes are core points.^[1] Biocatalytic approaches can fulfill these principles. Therefore, interdisciplinary collaborations in the field of biotechnology, molecular biology and biochemistry achieved major advances in this field in the recent decades. Recently, the ACS Green Chemistry Institute's Pharmaceutical Round Table (GCIPR) defined ten key research areas including among others the asymmetric hydrogenation of olefins/enamines and imines, displaying the importance of novel biocatalysts reducing multiple carbon-carbon bonds.^[2] Enzymes capable to reduce such carbon bonds, collectively known as ene-reductases (ERs) have been studied intensely throughout the last decades. The physiological importance of ERs is broadly defined, which includes among others, detoxification of compounds derived from lipid peroxides in plants, quinone

accumulation in yeast or the putative involvement in various biosynthetic pathways such as the modification of lipoxigenase-derived C8-oxylinols displaying a vast variability in their biological importance.^[3,4,5,6,7] This variability agitated a lot of attention concerning biocatalytic approaches like the production of bioactive compounds, pharmaceuticals, agricultural chemicals or chiral building blocks.^[4] The most prominent family of ERs are the flavin mononucleotide (FMN) depending Old Yellow Enzymes (OYEs) which reduce multiple α,β -unsaturated aldehydes, ketones, esters or nitro compounds.^[8–10] Due to significant advances in protein engineering strategies, OYEs have been successfully employed to improve their catalytic activities, invert stereoselectivities, broaden the substrate scope or even catalyze a variety of unusual reductions with a high value for industrial approaches (Figure 1).^[11] Furthermore, the application of ERs with novel reduction capabilities due to site-directed mutagenesis or by implementing ERs in biocatalytic

[a] D. Karrer, Dr. M. Gand, Dr. M. Rühl
Department of Biology and Chemistry
Justus-Liebig University Giessen
Institute of Food Chemistry and Food Biotechnology
35392 Giessen (Germany)
E-mail: martin.ruehl@uni-giessen.de

[b] Dr. M. Rühl
Fraunhofer Institute for Molecular Biology and Applied Ecology IME Business
Area Bioresources
35392 Giessen (Germany)

Supporting information for this article is available on the WWW under <https://doi.org/10.1002/cctc.202002011>

© 2021 The Authors. ChemCatChem published by Wiley-VCH GmbH. This is an open access article under the terms of the Creative Commons Attribution Non-Commercial NoDerivs License, which permits use and distribution in any medium, provided the original work is properly cited, the use is non-commercial and no modifications or adaptations are made.

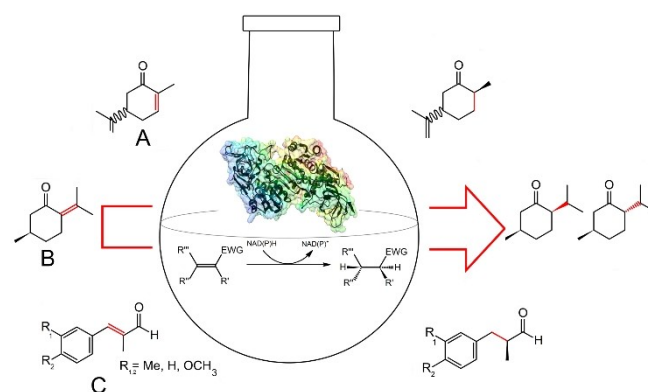


Figure 1. Reactions catalyzed by various ERs (A) OYE from *Synechococcus* sp. PCC 7942 reducing carvone to a key intermediate in striatenic and pechuloic acid production. (B) MDR from *Mentha piperita* reducing (+)-pulegone to (-)-menthone and (+)-isomenthone. (C) OYE1-3 from *Lycopersicon esculentum* reducing cinnamaldehyde-like substrates to fragrances.

cascades to replace traditional synthetic steps is obviously popular and constantly increasing.^[3,4] Although ERs are studied extensively, their interest in sustainable and green chemistry is still rising and exemplifies the need of an increasing biocatalytic landscape filled with a broad range of biocatalysts for more and more tailored and “new-to-nature” C=C or C≡C containing compounds.^[11]

On closer consideration of currently known ERs, several structures with C=C bonds can be reduced but a variable biocatalyst that is also able to perform a “new-to-nature”-like reduction of C≡C bonds has only been shown once for solely one compound. Due to the prevalence of activated alkynes, organic chemists extensively investigated efficient methods for their reduction. The most common strategies include the use of transition metal catalysts to produce saturated products. It has been reported that aromatic and aliphatic alkynes were successfully reduced by using Pd/C or Pd-dibenzylideneacetone catalysts.^[12,13] More recently, quantitative hydrogenations towards two aliphatic alkynes were accomplished with a methyl-substituted phosphetane oxide catalyst in the presence of organosilanes as the terminal reductant.^[14] An alternative method to reduce aliphatic alkynes was shown with an iridium (III)-complex as catalyst.^[15] In general, these methods do not meet all of the mentioned green and sustainable chemistry standards, due to their inevitable use of costly transition-metal catalysts.^[1] Furthermore, the synthesis of such catalysts often require various additional synthetic steps.^[16,17] To our knowledge, these reductions are mostly limited to alkynoates, meaning that reports of the reduction of alkynals and alkynones are scarce. Taken together, the biocatalytic landscape lacks a reductase targeting C≡C bonds that opens up an uncovered field of biocatalysis. To overcome this issue, focusing on other types of ERs or targeting other organisms than bacteria, plants or baker's yeast could be productive. Regarding other types of ERs, the flavin adenine dinucleotide (FAD)- and [4Fe-4S]-depending ERs, the NAD(P)H-dependent medium-chain dehydrogenase/reductase superfamily (MDR) as well as the NAD(P)H-dependent short-chain dehydrogenase/reductase superfamily (SDR) are far less studied for biocatalytic applications.^[5,10,18,19,20]

An evaluation of their biocatalytic potential is almost lacking. Regarding other organisms, a promising portfolio of ERs with novel activities was shown via whole cell biotransformations of α,β -unsaturated substrates in various fungi from the phyla Ascomycota and Basidiomycota.^[21,22] This implicates a huge enzyme library with great potential in substituting conventional synthesis with environmentally friendly biocatalysts. So far, only one study targeted an ER from the yeast-like Basidiomycota *Sporidiobolus salmonicolor* that reduced unnatural large monocyclic enones like (*E*)-3-methylcyclopentadec-2-en-1-one, cyclopentadec-2-en-1-one, and cyclododec-2-en-1-one to their corresponding saturated ketones.^[23] Hence, this study investigated the biocatalytic value of the first ER from a filamentous fungi of the phylum Basidiomycota as a member of the MDR-superfamily. This ER turned out to exhibit novel biocatalytic activities displaying a valuable and versatile biocatalyst with high potential for future approaches.

Results and Discussion

Biochemical characterization and cofactor specificity

Following heterologous production in *E. coli* and purification, the effects of pH and temperature on CaeEnR1 (accession number: MW013782, *AAE3_13549* www.thines-lab.senckenberg.de/agrocybe_genome) activity was determined with oct-1-en-3-one (**1**) as substrate. CaeEnR1 showed maximum activity at pH 7.5 with more tolerance against acidic conditions. 50% of its activity left at pH 5.0 that increased with higher pH-values. Decreasing and increasing values (pH < 5 or > 7.5) resulted in a drastic loss of activity with ~25% left at pH 4.5 and < 10% at pH 8–10 (Figure 2A). CaeEnR1 showed maximum activity at 25–30°C. Increasing temperatures resulted in a steady loss with no activity left at 50°C. A low temperature of 4°C led also to a suppression of enzyme activity (Figure 2B).

Cofactor specificity with **1** as substrate was determined with NADPH and NADH, revealing a >700-fold higher preference for NADPH with 28.0 U·mg⁻¹ compared to NADH with

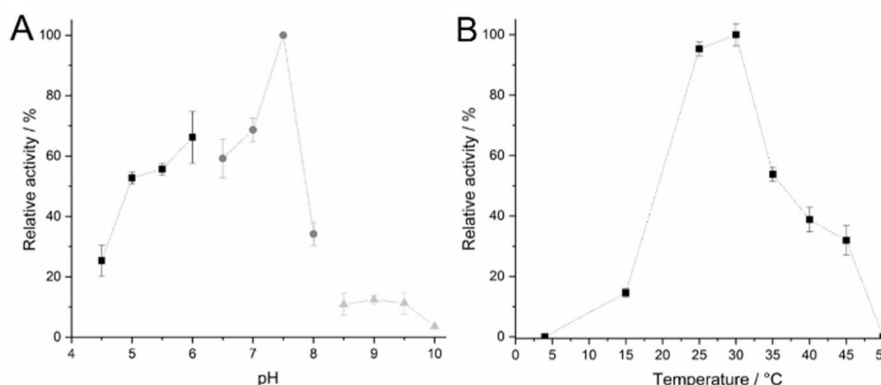


Figure 2. Influence of pH (A) (squares = 50 mM acetate buffer, circles = 50 mM phosphate buffer, triangles = 50 mM borate buffer) and of temperature (B) on CaeEnR1 activity.

0.04 U·mg⁻¹. Other ene-reductases from the MDR-superfamily as NtDBR (> 1,600-fold) or SsERD (no activity with NADH) also prefer NADPH as hydride donor.^[23,24] This is not surprising, due to the fact that these enzymes share several amino acids, such as G189, K193 and Y208, which were shown to be involved in NADPH binding by the crystal structures of NtDBR and AtDBR (Supporting information Figure S1A, B).^[4,20]

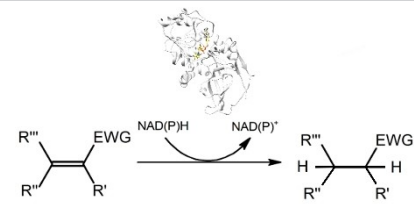
Reduction of alkenals and alkenones

To explore the substrate profile of CaeEnR1, the conversion rates (Table 1) of in total 21 different alkenals and alkenones were examined. These substrates were grouped according to their structure and physicochemical properties: aliphatic α,β -unsaturated alkenones: oct-1-en-3-one (1), oct-3-en-2-one (2), hex-1-en-3-one (3) (group I); aliphatic α,β -unsaturated alkenals: (*E*)-oct-2-enal (4), (*E*)-non-2-enal (5), (*E*)-hex-2-enal (6) (group II); aliphatic $\alpha,\beta,\gamma,\delta$ - and multiple- unsaturated alkenals: (*E,E*)-oct-2,4-dienal (7), (*E,E*)-non-2,4-dienal (8) (*E,E*)-non-2,6-dienal (9)

(group III); α,β -unsaturated alcohols: oct-1-en-3-ol (10), oct-2-en-1-ol (11) (group IV); cyclic α,β -unsaturated alkenones/alkynones: (*R,S*)-carvone (12), β -damascenone (13), 1,2-naphthoquinone (14), 4-phenyl-3-butene-2-one (15) (group V); cyclic α,β -unsaturated alkenals: coniferyl aldehyde (16), cinnamaldehyde (17), 2-phenyl-but-2-enal (18), β -cyclocitral (19) (group VI); cyclic α,β -unsaturated nitroalkenes: (*E*)- β -nitrostyrene (20), (*E*)- β -methyl- β -nitrostyrene (21) (group VII). Most conversion rates of group I and group II showed rates of up to 72% - 98%; only 2 and 6 were converted by 48% and 54%, respectively. While the conversion rates of group III showed values of up to 73% - 84% (Table 1). Remarkably, CaeEnR1 reduced selectively the double bond in α,β -position of 7, 8 and 9. However, no successful reduction of the substrates from group IV was detected. Compounds 15 (50%) and 17 (59%) were the only converted substrates of group V and VI, respectively. Related structures like 16 or 18 were either very poorly or not converted (Table 1).

This could be caused by steric effects of the methyl group adjacent to the double bond. Compared to 17, 16 has an additional phenolic hydroxy- and methoxy group, implicating

Table 1. Reduction of various activated alkenals/alkenones by CaeEnR1. A typical reaction mixture (1 mL) contained 0.2 mM NADPH, 0.1 mM substrate and 5 μ M CaeEnR1 in 50 mM phosphate buffer (pH 7.5). The reactions were incubated at 24 °C for 3 h at 160 rpm. CaeEnR1 did not catalyze the reduction of the substrates: oct-1-en-3-ol (10), oct-2-en-1-ol (11), (*R,S*)-carvone (12), β -damascenone (13), 2-phenyl-but-2-enal (18), β -cyclocitral (19).



Group	Substrate	Product	Conversion [%]
I	1	1b	98
	2	2b	48
	3	3b	95
II	4	4b	86
	5	5b	72
	6	6b	54
III	7	7b	73
	8	8b	84
	9	9b	27
VI	15	15b	50
VII	16	16b	3
	17	17b	59
VIII	20	20b	90
	21	rac-21b	26

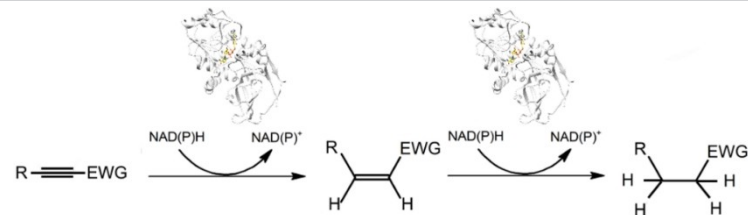
the necessity of an increased substrate tunnel or binding pocket. Possible steric effects were also observed for substrates of group VII. The non-substituted **20** was converted with good rates of 90%, whereas for **21** that contains a methyl group nearby the double bond a conversion of only 26% was achieved. A constriction due to bulky amino acid residues could explain the difference in conversion between substituted and non-substituted aromatic substrates. This was already pointed out for NtDBR, which reduced **17** and **21** with high conversion rates (100% and 71%) while **16**, similar to our study, was poorly reduced (~6%).^[20] The phenylalanine/serine substitution (NtDBR to AtDBR F285/S287, corresponding to S283 in CaeEnR1) was identified as potentially size restricting, allowing AtDBR to reduce substituted cinnamaldehyde-like substrates more efficiently. Especially, F285 in NtDBR was considered as the determinant for the limited reduction of substituted cinnamaldehyde-like substrates.^[4,20] Compared to NtDBR, CaeEnR1 harbors a serine (S283) at that position (Supporting Information S1) similar to AtDBR but shows very poor activity towards **16**, which indicates that this amino acid might not be the responsible determinant for the poor activities towards substituted cinnamaldehyde-like substrates. Furthermore, an efficient and regioselective reduction of the α,β -double bond in aliphatic $\alpha,\beta,\gamma,\delta$ -unsaturated aldehydes has not been pointed out so far (Table 1).

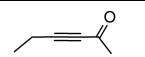
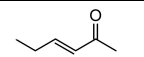
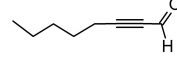
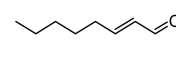
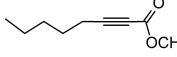
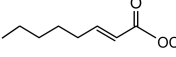
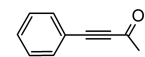
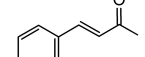
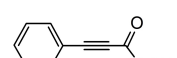
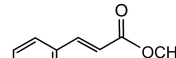
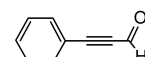
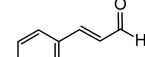
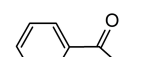
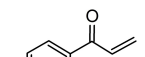
In general, CaeEnR1 showed the highest activities towards C8-alkenones and C8-alkenals among aliphatic substrates. With decreasing chain length, a ~2-fold loss was detected (Figure 3A). By comparing the aromatic substrates, the alkenone **15** and alkenal **17** were converted similarly while the nitroalkene counterpart **20** showed drastically higher conversion rates suggesting a higher activation of the C=C bond leading to a better conversion (Figure 3A).

Reduction of alkynals, alkynones and alkynoates

The reduction of alkynals, alkynones and alkynoates were examined by seven different substrates, divided in the two groups of aliphatic (group VIII): hex-3-yn-2-one (**22**), oct-2-ynal (**23**), methyl-oct-2-ynoate (**24**) and aromatic (group IX): 4-phenylbut-3-yne-2-one (**25**), methyl-3-phenylprop-2-ynoate (**26**), 3-phenylprop-2-ynal (**27**), 1-phenyl-2-propyn-1-one (**28**) compounds. CaeEnR1 successfully reduced the aliphatic and aromatic alkynals/alkynones **22**, **23**, **25**, **27** and **28** to their corresponding alkanals and alkanones (Table 2). While **23** showed a satisfactory conversion rate of 42%, the alkynoate counterpart **24** was not reduced to the corresponding alkanoate. Similarly, the aromatic alkynes **25**, **26** and **27** were differently converted depending on their carbonyl species. While the alkynone and alkynal **25** and **27** were converted by

Table 2. Reduction of various activated alkynals/alkynones by CaeEnR1. A typical reaction mixture (1 mL) contained 0.2 mM NADPH, 0.1 mM substrate and 5 μ M CaeEnR1 in 50 mM phosphate buffer (pH 7.5). The reactions were incubated at 24 °C for 3 h at 160 rpm.



Substrate	unsat. Product	sat. Product	Total conv. [%]	selectivity [%] alkene	selectivity [%] alkane
22			5	< 0.1	< 99.9
23			42	5	95
24			-	-	-
25			22	5	95
26			< 1	< 1	< 1
27			20	< 1	< 99
28			5	< 1	< 99

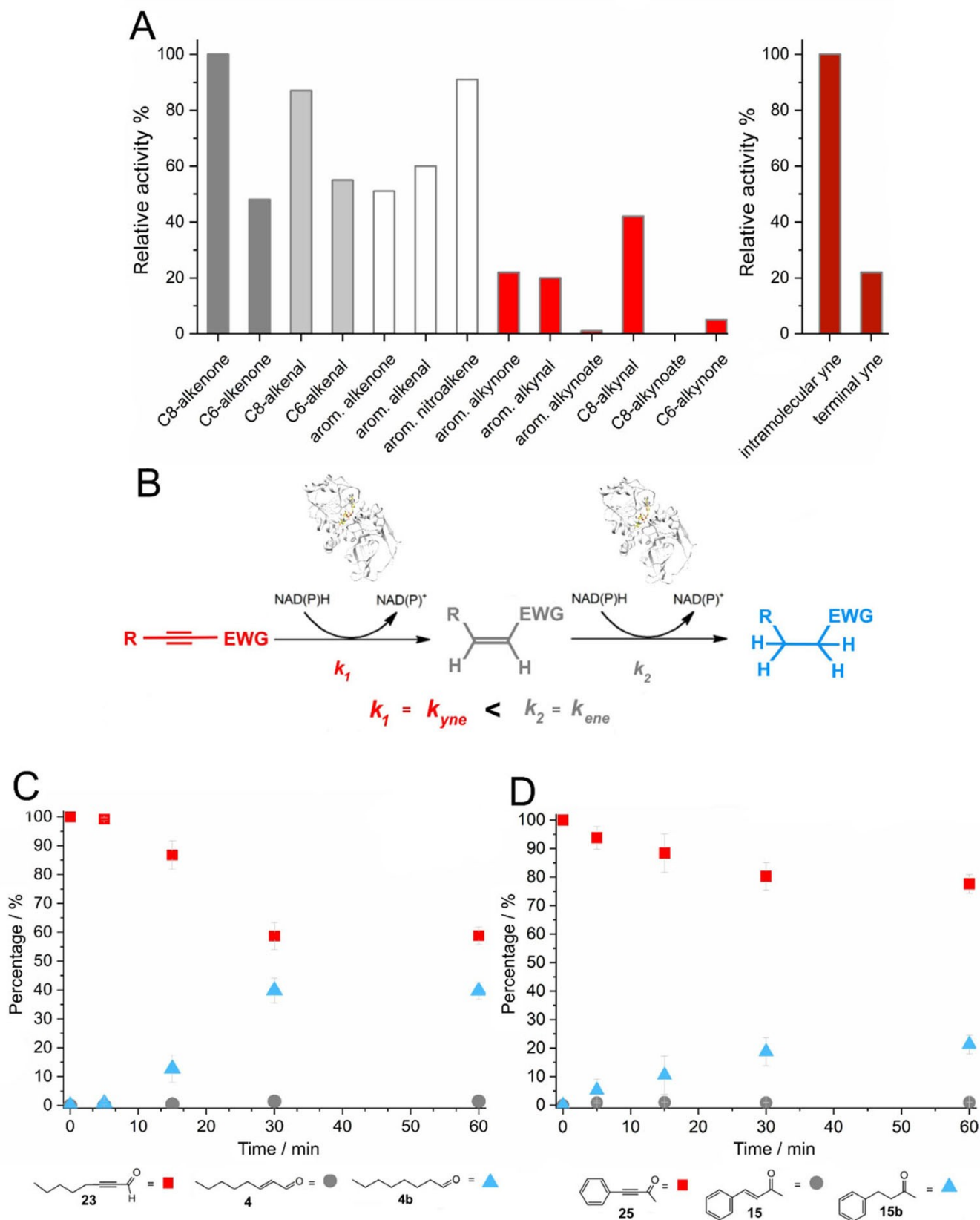
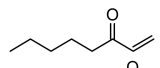
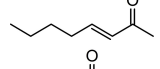
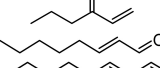

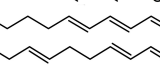
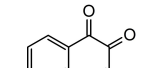
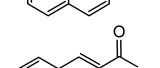
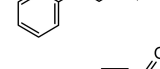
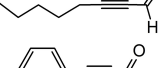
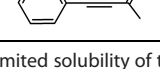
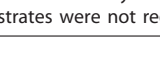
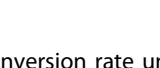
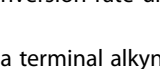


Figure 3. Time dependent reduction of alkynals/alkynones and comparison of the relative activity between alkenes and alkynes depending on chain length, electron withdrawing group and position of the unsaturated bond. (A) Comparison of the relative activities of CaeEnR1 towards various substrate types differing in chain length, carbonyl species and position of the unsaturated alkyne. (B) Two step reduction process with k_1 (alkyne reduction to the alkene), followed by k_2 (alkene reduction to the alkane). Reduction of **23** (C) and **25** (D) to their corresponding alkenals/alkenones **4**, **15** and alkanals/alkanones **4b**, **15b** with standard reaction conditions. Red square = alkyne, grey circle = alkene, blue triangle = fully saturated product.

Table 3. Steady-state kinetics of CaeEnR1 with alkenes. Given values are means \pm of triplicates.

Group	substrate	K_M [μM]	k_{cat} [s^{-1}]	k_{cat}/K_M [$\text{s}^{-1} \cdot \mu\text{M}^{-1}$]
I	1 	75.8 \pm 20.8	213.0 \pm 25.6	2.8 \pm 1.0
	2 	72.1 \pm 28.9	64.7 \pm 9.2	0.9 \pm 0.3
	3 	27.9 \pm 3.2	4.0 \pm 0.2	0.1 \pm 0.1
II	4 	211.2 \pm 61.2	41.1 \pm 5.1	0.2 \pm 0.1
	5 	180.5 \pm 29.5	10.2 \pm 1.0	0.1 \pm 0.0
	6 	n.d.	0.8 \pm 0.2 ^a	n.d.
	7 	n.d.	0.5 \pm 0.1 ^[a]	n.d.
III	8 	n.d.	1.0 \pm 0.1 ^[a]	n.d.
	9 	n.d.	0.8 \pm 0.2 ^[a]	n.d.
VI	14 	n.d.	1.2 \pm 0.8 ^a	n.d.
VI	15 	120.2 \pm 55.2	34.3 \pm 11.1	0.3 \pm 0.20
VIII	23 	n.d.	1.0 \pm 0.4 ^[a]	n.d.
IX	25 	n.d.	0.9 \pm 0.4 ^[a]	n.d.

[a] = rates (s^{-1}) with 0.25 mM substrate due to limited solubility of the substrates, significant absorption at 340/365 nm at higher concentrations or near zero-order kinetics. n.d., not determined. Other substrates were not reduced under steady-state conditions.

20–22%, the alkynoate **26** showed a conversion rate under 1% (Table 2).

Furthermore, the alkynoate **28** with a terminal alkyne group was poorly converted with 5% (Table 2). Collectively all reductions of the triple bond lead to minimum amounts (max. 2%) of the alkene intermediate (**22 a**, **4**, **15**, **27 a**, **28 a**) (Table 2). The reduction of the alkynone **25** was so far only described for OYE3.^[26] Generally, the successful reduction of alkynals and alkynones depicts a unique characteristic of CaeEnR1 among other described ERs. Compared to the tested alkenones and alkenals **4**, **15** and **17**, CaeEnR1 showed a \sim 2-fold lower conversion rate towards the alkyne counterparts **23**, **25** and **27** (Figure 3A). Similar observations were made for the aromatic alkenone and alkenal **15**, **17** and their counterparts **25**, **27** (Figure 3A). Furthermore, for compounds with an ester as electron withdrawing group (**24**, **26**) very poor or no conversions were detected. In addition, the position of the triple bond also seems to have a drastic impact on conversion. A \sim 5-fold difference in relative activity between the intramolecular alkyne in **25** and the terminal alkyne in **28** was detected (Figure 3A). To clarify whether the alkynes are first reduced to the corresponding alkene leading to its accumulation followed by the reduction to the fully saturated product, the reduction in a time lap of 60 min exemplarily for **23** and **25** was investigated (Figure 3C, D). Time dependent reduction of alkynals and alkynones revealed that the conversion rates were decent for **23** and **25** with \sim 40% and \sim 20% after 30 min, respectively (Figure 3). **22** was converted very poorly, showing a maximum after 30 min of only \sim 6%. However, the corresponding

alkenals/alkenones (**15**, **4** and **22 a**) never exceeded $<$ 2%. This suggests a rapid two-step mechanism including the reduction of the triple bond, leading to the alkenal/alkenone which is instantly further reduced to the saturated product. This is reasonable by comparing the reaction rates and specific activities against the alkynals/alkynones **23/25** and their alkenals/alkenones **4/15** differing by multiple magnitudes (Table 1 and 3). OYE3 from *S. cerevisiae* is also able to reduce **25**. However, this enzyme shows a higher affinity towards the alkyne, which first of all leads to an accumulation of the alkenone followed by a subsequent reduction to the alkanone.^[26]

Preparative scale biotransformation

For biotransformation in a preparative scale, **1** was used as a model substrate with a concentration of 25 mM. Reactions were carried out by using a NADP⁺/glucose dehydrogenase (GDH) recycling system as a source for NADPH. Within 1 h about \sim 30% of **1** was reduced to the corresponding product **1 b**. With ongoing reaction, the percentage of **1 b** plateaued at \sim 40% in the reaction mixture. No further reduction of **1** was detected after 6 h and 16 h (Figure 4). By comparing the conversion rates between the analytical and preparative scale reduction of **1**, a \sim 2.5-fold difference was noticed (Table 1, Figure 4). Due to the limited solubility of **1**, the solvent percentage was increased from 0.1% (analytical scale) to 10% (preparative scale) ethanol, which might have influenced the activity of CaeEnR1. Further-

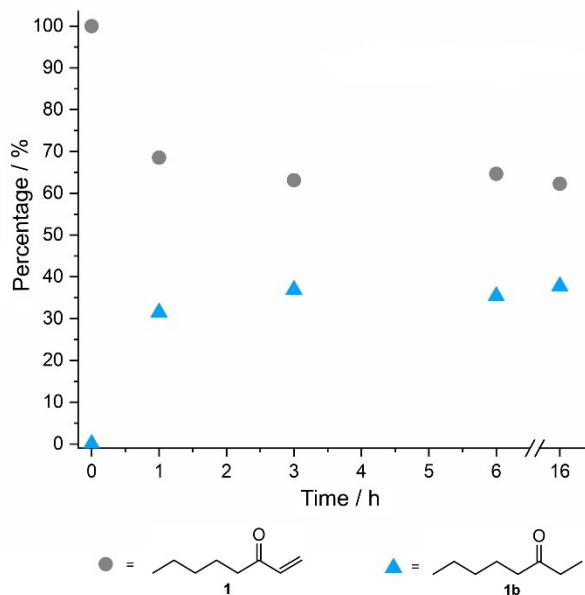


Figure 4. Time dependent reduction of substrate **1** (grey circles) to the corresponding product **1b** (blue triangles) in a preparative scale biotransformation. The reaction was monitored over 16 h at different time points.

more, it has to be noticed that several aspects and problems like heat transfer, transport phenomena, mass balance, proper mixing or the mentioned increasing amounts of organic solvents with higher substrate concentrations arise when it comes to sufficient up-scaling of biotransformations.^[30,31] Nevertheless, a promising first preparative scale biotransformation with CaeEnR1 was demonstrated.

Enzyme kinetics

Kinetic analysis revealed that the affinity of CaeEnR1 differed strongly between α,β -unsaturated ketones, α,β -unsaturated aldehydes and aromatic ketones (Table 3). In some cases (6, 7, 8, 9, 10, 11, 12, 13, 14, 16, 17, 18, 19, 20, 21, 22, 24, 26, 27), full steady-state kinetics were not determined due to either limited solubility, significant absorption at 340/365 nm, near zero-order kinetics or activity under the detection limit. However, the k_{cat} values with 0.25 mM of these substrates were calculated and ranged between 0.5–1.2 s⁻¹ (Table 3). All together, the aliphatic ketones were strongly preferred substrates with K_{M} values between 27.9–75.8 μM which are 2–3 times higher affinities compared to aldehydes (K_{M} = 180.5–211.2 μM). Interestingly, $\alpha,\beta,\gamma,\delta$ -unsaturated aldehydes with the same chain length compared to the tested α,β -unsaturated aldehydes showed presumable lower affinities (Table 3). In addition, a high affinity (K_{M} = 120.2 μM) and reaction rate (34.3 s⁻¹) towards the aromatic compound **15** was calculated. Surprisingly, **3** showed the lowest K_{M} with 27.9 μM among all tested substrates while the aldehyde analogue **6** showed lower reaction rates and assumingly shows a higher K_{M} . Furthermore, k_{cat} and $k_{\text{cat}}/K_{\text{M}}$ values of α,β -unsaturated substrates, particularly the ketones with eight

carbons were higher compared to the aldehydes and ketones with nine or six carbons (Table 3). The K_{M} values for **4** and **8** are similar with a slightly higher k_{cat} for **4**. With decreasing chain length of the aldehydes, the enzyme activity decreased as well, which suggests a correlation between chain length and affinity. Interestingly, the opposite was observed with α,β -unsaturated ketones, where CaeEnR1 showed the highest affinity towards **3** but coincidentally the lowest k_{cat} and $k_{\text{cat}}/K_{\text{M}}$ values compared to **1** and **2**. Similar findings were observed for AtDBR from *A. thaliana* that shows strikingly lower K_{M} values for α,β -unsaturated aldehydes with longer carbon chains (non-2-enal 5.9 μM , hex-2-enal 232 μM , pent-2-enal 1,420 μM).^[5] Another ER with strikingly lower affinities towards aliphatic substrates like **1** and **5** has been shown for NtDBR.^[20] To our knowledge, AtDBR is the only MDR-superfamily related enzyme that showed activity towards naphthoquinones like **14**.^[25] On consideration of the bioinformatic analysis, AtDBR and CaeEnR1 share the serine residue located in the binding pocket/substrate entrance (Supporting Figure S1B), suggesting that this residue could be crucial for 1,2-naphthoquinone reduction.

Conclusion

Despite their overall potential, research on new biocatalysts from promising specimens of the phyla Basidiomycota is underrepresented. Hence, the first ER from a fungus of the phylum Basidiomycota with high activities towards aliphatic and aromatic α,β -unsaturated compounds was comprehensively characterized. Compared to the very few known ERs of the MDR-superfamily, CaeEnR1 exhibited highly efficient and regioselective reductions of $\alpha,\beta,\gamma,\delta$ -unsaturated aldehydes and is able to reduce activated alkynes to their saturated compounds. This first report on such biocatalytic reductions underlines the uniqueness of CaeEnR1. Collectively, this study introduces a new type of ER with a broad substrate scope including aliphatic and aromatic alkenals/alkenones, alkynals/alkynones and aromatic nitro alkenes. Moreover, the discovery of alkyne reduction and future investigations of the reaction mechanism will also have an impact on “new-to-nature” reactions like the recently described photocatalytic deacetylation by MDR-related ERs. For the development of such reactions, knowledge about the mechanism of C=C reductions was crucial.^[28] Furthermore, with this ene/yne-reductase the biocatalytic gap of C≡C reductions is filled, which enables a new field of opportunities and challenges for protein engineering approaches, aiming for novel biocatalytic cascades or enzyme improvement via co-factor recycling systems.

Experimental Section

Cloning and protein expression of CaeEnR1

The codon optimized *ENR1* gene (accession number: MW013782, AAE3_13549 www.thines-lab.senckenberg.de/agrocybe_genome) was commercially purchased and cloned into the plasmid pET28a (BioCat GmbH, Heidelberg, Germany). For protein expression,

pET28a/CaeEnR1 plasmid was transformed into *E. coli* BL21 Gold (DE3). *E. coli* cells were cultivated in Terrific Broth medium (TB) containing 12 g tryptone, 24 g yeast extract and 5 g glycerol, supplemented with an equivalent of 1x TB-salts from a 10x stock solution (0.17 M KH_2PO_4 and 0.72 M K_2HPO_4) and 50 $\text{mg}\cdot\text{L}^{-1}$ kanamycin as selection marker at 37 °C until an OD_{600} of 0.4–0.6 was reached. Expression was induced by adding isopropyl- β -D-thiogalactopyranoside to a final concentration of 0.1 mM. Cultivation was continued for another 24 h at 24 °C. Cells were harvested by centrifugation (4,000 g, 30 min, 4 °C) and stored at –20 °C until further use or directly processed.

Protein purification

The cell pellet was thawed on ice and resuspended in lysis-buffer (50 mM phosphate, 300 mM NaCl, 20 mM imidazole, pH 7.5). Disruption of cells was carried out by sonification (3 cycles for 60 s on, 60 s rest) on ice using a sonifier (Bandelin Sonopuls, Berlin, Germany). After complete disruption, cell debris was removed by centrifugation (11,000 g, 45 min, 4 °C). The resulting supernatant was further processed, by either using Ni-NTA spin columns, following the instruction of the manufacturer (Qiagen, Venlo, Netherlands) or by using a 5 mL HisTrap column (GE-Healthcare). The HisTrap columns were equilibrated with 5 column volumes (CV) lysis-buffer and then loaded with the supernatant, washed twice with 5 CV lysis buffer and eluted with an increasing imidazole concentration from 20 mM imidazole (lysis-buffer) to 500 mM imidazole (elution-buffer, 50 mM phosphate, 300 mM NaCl, 500 mM imidazole, pH 7.5). Fractions with purified CaeEnR1 were analyzed via SDS-PAGE, concentrated and rebuffed with Amicon[®] Ultra 4 mL centrifugal filters (Merck KGaA, Darmstadt, Germany). Protein concentration was photometrically determined by using the 260/280 ratio and the specific extinction coefficient ($E_{260} = 40340 \text{ M}^{-1}\cdot\text{cm}^{-1}$), calculated with the ExpASY ProtParam tool.^[29]

Enzyme assay

UV method: CaeEnR1 activity was determined by recording the oxidation of NADH/NADPH at 340 nm ($E_{340} = 6620 \text{ M}^{-1}\cdot\text{cm}^{-1}$) on a Nanophotometer (Implen, Munich, Germany). The typical reaction mixture contained 0.2 mM NADPH, 0.2 mM substrate and an appropriate amount of enzyme in a total volume of 1 mL. For pH dependency, the mixture was incubated in either 50 mM acetate buffer (pH 4.5–6.0), 50 mM phosphate buffer (pH 6.5–8.0) or 50 mM borate buffer (pH 8.5–10.0) to determine the pH-optimum. Effects of the temperature were measured by incubating the reaction mixture at different temperatures, ranging from 4 °C–50 °C. One unit of enzyme activity was defined as the conversion of μmol substrate per minute.

GC-MS method: A typical reaction mixture of 1 mL contained 0.2 mM NADPH, 0.1 mM substrate, an appropriate amount of enzyme in 50 mM phosphate buffer, pH 7.5. The mixture was incubated at 24 °C for 3 h.

Preparative scale biotransformation

Biotransformation in a preparative scale contained 25 mM of substrate 1 (solved in ethanol, 10% final solvent concentration), 0.1 mM NADP^+ , 100 mM glucose, 100 U glucose dehydrogenase from *Pseudomonas sp.* (Sigma Aldrich) and an appropriate amount enzyme in 50 mM phosphate buffer, pH 7.5 with a final volume of 100 mL. The mixture was incubated for 16 h at 24 °C. After defined times (1 h, 3 h, 6 h and 16 h) an aliquot was taken to monitor the reaction progress.

Kinetic parameters

Steady-state kinetic parameters were calculated by incubating purified CaeEnR1 with different concentrations according to the used substrates ranging from 7.5–300 μM and 0.2 mM NADPH. Resulting data was fitted with the Michaelis-Menten equation in OriginPro 2018 software.

Product analysis

The reaction products were extracted with 400 μL ethyl acetate, followed by mixing on a vortexer and centrifugation for 2 min at 13000 g. Analysis of the reaction products in the organic layer was carried out on an Agilent Technologies 7890 A GC-MS-system (Santa Clara, USA), equipped with a VFWax column (30 $\text{m}\times 0.25 \text{ mm}\times 0.25 \mu\text{m}$ film thickness, Santa Clara, USA) operated in splitless mode under the following parameters: carrier gas, Helium with a constant flow of 1.2 $\text{mL}\cdot\text{min}^{-1}$. Oven temperature was at 40 °C (3 min), 10 °C $\cdot\text{min}^{-1}$ to 240 °C and hold for 7 min. The mass spectrometer operated in electron impact mode with an electron energy of 70 eV and scanned in a range of m/z 33–300. Conversion rates were calculated by using the peak areas. Retention times and mass spectrum was compared with authentic standards, the NIST database or by the characteristic fragmentation pattern and molecule ion.

In silico analysis of CaeEnR1

Phylogenetic analysis and amino acid alignments: Sequences for phylogenetic analysis and sequence alignments were obtained via the National Center of Biotechnology Information (NCBI, <https://www.ncbi.nlm.nih.gov/>). Amino acid alignments and tree building were performed with the Clustal Omega web tool (<https://www.ebi.ac.uk/Tools/msa/clustalo/>). Visualization of the phylogenetic tree was carried out via the online tools, interactive tree of life (iTOL, <https://itol.embl.de/>) and <http://www.phylogeny.fr>.

Acknowledgements

We gratefully acknowledge the financial support by the Deutsche Forschungsgemeinschaft (DFG, German Research Foundation)-Funder Id: <https://doi.org/10.13039/501100001659>, Grant Number: RU 2137/1-1. Open access funding enabled and organized by Projekt DEAL.

Conflict of Interest

The authors declare no conflict of interest.

Keywords: ene-reductase · biocatalysis · regioselectivity · double bond reductase · alkynes

- [1] R. A. Sheldon, J. M. Woodly, *Chem. Rev.* **2018**, *118*, 801–838.
- [2] M. C. Bryan, P. J. Dunn, D. Entwistle, F. Gallou, S. G. Koenig, J. D. Hayler, M. R. Hickey, S. Hughes, M. E. Kopach, G. Moine, P. Richardson, F. Roschangar, A. Steven, F. J. Weiberth, *Green Chem.* **2018**, *20*, 5082–5103.
- [3] H. S. Toogood, N. S. Scrutton, *ACS Catal.* **2018**, *8*, 3532–3549.
- [4] B. Youn, S.-J. Kim, S. G. A. Moinuddin, C. Lee, D. L. Bedgar, A. R. Harper, L. B. Davin, N. G. Lewis, C. Kang, *J. Biol. Chem.* **2006**, *281*, 40076–40088.

- [5] J. Mano, Y. Torii, S. Hayashi, K. Takimoto, K. Matsui, D. Inzé, E. Babiychuk, S. Kushnir, K. Asada, *Plant Cell Physiol.* **2002**, *43*, 1445–1455.
- [6] P. C. Guo, P. X. Ma, Z. Z. Bao, J. D. Ma, Y. Chen, C. Z. Zhou, *J. Struct. Biol.* **2011**, *176*, 112–118.
- [7] D. Karrer, M. Rühl, *PLoS One* **2019**, e0218625.
- [8] Y.-J. Liu, X.-Q. Pei, H. Lin, P. Gai, Y.-C. Liu, Z.-L. Wu, *Appl. Microbiol. Biotechnol.* **2012**, *95*, 635–645.
- [9] S. Raimondi, D. Romano, A. Amaretti, F. Molinari, M. Rossi, *J. Biotechnol.* **2011**, *156*, 279–285.
- [10] Y. Fu, K. Castiglione, D. Weuster-Botz, *Biotechnol. Bioeng.* **2013**, *110*, 1293–1301.
- [11] R. A. Sheldon, D. Brady, *ChemSusChem* **2019**, *12*, 2859–2881.
- [12] R. Shen, T. Chen, Y. Zhao, R. Qiu, X. Zhou, S. Yin, X. Wang, M. Goto, L. B. Han, *J. Am. Chem. Soc.* **2011**, *133*, 17037–17044.
- [13] A. Mori, Y. Miyakawa, E. Ohashi, T. Haga, T. Maegawa, H. Sajiki, *Org. Lett.* **2006**, *8*, 3279–3281.
- [14] L. Longwitz, T. Werner, *Angew. Chem. Int. Ed.* **2020**, *132*, 2792–2785.
- [15] Y. Wang, Z. Huang, X. Leng, H. Zhu, G. Liu, Z. Huang, *J. Am. Chem. Soc.* **2018**, *140*, 4417–4429.
- [16] I. Schnetmann-Göttker, P. White, M. Brookhart, *J. Am. Chem. Soc.* **2003**, *126*, 1804–1811.
- [17] M. Gupta, C. Hagen, W. C. Kaska, R. E. Cramer, C. M. Jensen, *J. Am. Chem. Soc.* **1997**, *119*, 840–841.
- [18] H. Kasahara, Y. Jiao, D. L. Bedgar, S.-J. Kim, A. M. Patten, Z.-Q. Xia, L. B. Davin, N. G. Lewis, *Phytochemistry* **2006**, *67*, 1765–1780.
- [19] K. L. Ringer, M. E. McConkey, E. M. Davis, G. W. Rushing, R. Croteau, *Arch. Biochem.* **2003**, *418*, 80–92.
- [20] D. J. Mansell, H. S. Toogood, J. Waller, J. M. X. Hughes, C. W. Levy, J. Gardiner, N. S. Scrutton, *ACS Catal.* **2013**, *3*, 370–379.
- [21] A. Skrobiszewski, R. Ogórek, E. Płaskowska, W. Gładkowski, *Biocatal. Agric. Biotechnol.* **2013**, *2*, 26–31.
- [22] A. Romagnolo, F. Spina, E. Brenna, M. Crotti, F. Parmeggiani, G. C. Varese, *Fungal Biol. Rev.* **2015**, *119*, 487–493.
- [23] K. Yamamoto, Y. Oku, A. Ina, A. Izumi, M. Doya, S. Ebata, Y. Asano, *ChemCatChem* **2017**, *9*, 3697–3704.
- [24] Y. Wang, Z. Huang, X. Leng, H. Zhu, G. Liu, Z. Huang, *Appl. Microbiol. Biotechnol.* **2014**, *98*, 705–715.
- [25] J. Mano, E. Babiychuk, E. Belles-Boix, J. Hiratake, A. Kimura, D. Inzé, S. Kushnir, K. Asada, *Eur. J. Biochem.* **2000**, *267*, 3661–3671.
- [26] A. Müller, R. Stürmer, B. Hauer, B. Rosche, *Angew. Chem. Int. Ed.* **2007**, *46*, 3316–3318; *Angew. Chem.* **2007**, *119*, 3380–3382.
- [27] Y. Wu, Y. Cai, Y. Sun, R. Xu, H. Yu, X. Han, H. Lou, A. Cheng, *FEBS Lett.* **2013**, *587*, 3122–3128.
- [28] K. F. Biegasiewicz, S. J. Cooper, M. A. Emmanuel, D. C. Miller, T. K. Hyster, *Nature* **2018**, *10*, 770–775.
- [29] E. Gasteiger, C. Hoogland, A. Gattiker, S. Duvaud, M. R. Wilkins, R. D. Appel, A. Bairoch, *The Proteomics Protocols Handbook* (Ed.: John M. Walker), Humana Press, **2005**, pp. 571–607.
- [30] F. R. Schmidt, *Appl. Microbiol. Biotechnol.* **2005**, *68*, 425–435.
- [31] D. Vasić-Rački, Z. Findrik, A. Vrsalović Presečki, *Appl. Microbiol. Biotechnol.* **2011**, *91*, 845–856.

Manuscript received: December 18, 2020

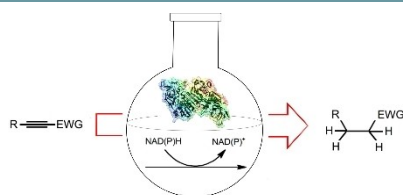
Revised manuscript received: January 22, 2021

Accepted manuscript online: February 1, 2021

Version of record online: ■■■, ■■■■

FULL PAPERS

Fun with fungus! The first characterized ene-reductase from a filamentous fungus has an interesting substrate portfolio. Besides its original substrates from the fungal oxylipin biosynthesis, the aliphatic C8-alkenones and C8-alkenals, EnR1 from the black poplar mushroom *Cyclocybe aegerita* is capable of reducing a number of alkynes into their alkanes, representing a novel activity in MDR-superfamily related ERs.



*D. Karrer, Dr. M. Gand, Dr. M. Rühl**

1 – 10

Expanding the Biocatalytic Toolbox with a New Type of ene/yne-Reductase from *Cyclocybe aegerita*



Supporting Information

Expanding the biocatalytic toolbox with a new type of ene/yne-reductase from *Cyclocybe aegerita*

Dominik Karrer^[a], Martin Gand^[a], Martin Rühl^{[a, b]*}

[a] Dominik Karrer, Dr. Martin Gand, Dr. Martin Rühl
Department of Biology and Chemistry, Justus-Liebig University Giessen
Institute of Food Chemistry and Food Biotechnology
Heinrich-Buff Ring 17
35392 Giessen, Germany

[b] Dr. Martin Rühl
Fraunhofer Institute for Molecular Biology and Applied Ecology IME Business Area
Bioresources
35392 Giessen, Germany.

Supporting Figures

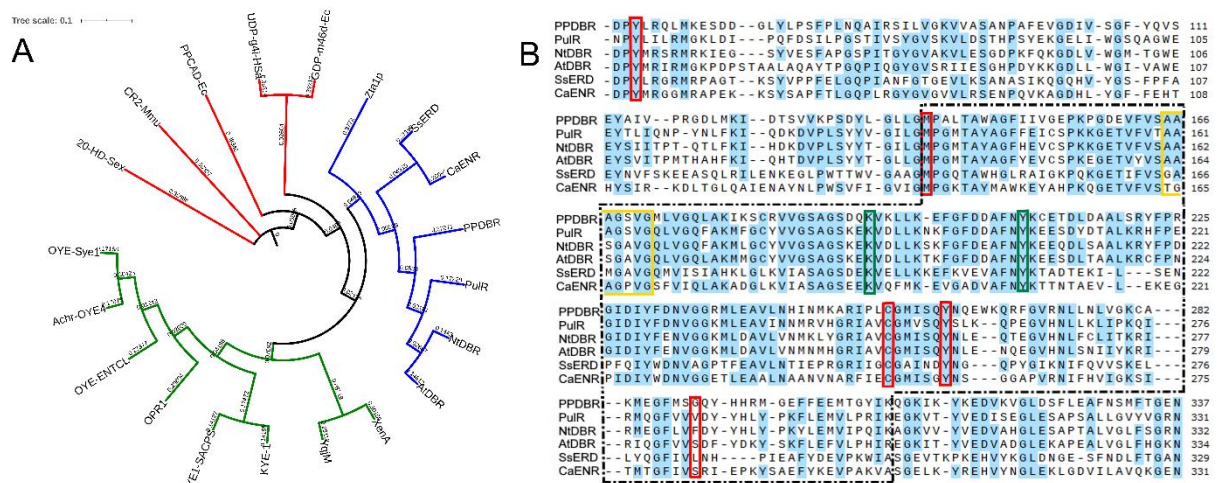


Figure S1. (A) Phylogenetic analysis of different ene-reductases belonging to OYEs (green), MDRs (blue) and SDRs (red). SsERD *Sporidiobolus salmonicolor* (A0A224AG05), NtDDBR *Nicotiana arabicum* (Q9SLN8), CaeEnR1 *Cyclocybe aegerita*, AtDDBR *Arabidopsis thaliana* (Q39172), PulR *Mentha piperita* (Q6WUAU), PPDBR *Pinus taeda* (Q0PIN2), Zta1p *Saccharomyces cerevisiae* (A6ZKZ0), 20-HD-S.ex *Streptomyces exfoliates* (P19992), UDP-g4i-H.Sa *Homo sapiens* (Q14376), GDP-m46d-Ec *Escherichia coli* (P0AC88), CR2-Mmu *Mus musculus* (P08074), PPCAD-Ec *Escherichia coli* (P0CI31), Achr-OYE4 *Achromobacter sp. JA81* (I3V5V6), OYE-Sye1 *Shewanella-oneidensis* (Q8EEC8), KYE-1 *Kluyveromyces lactis* (P40952), OYE1-SACPS *Saccharomyces pastorianus* (Q02899), OPR1 *Arabidopsis thaliana* (Q8LAH7), OYE-ENTCL *Enterobacter cloacae* (P71278), XenA *Pseudomonas putida* (88NF7), YqjM *Bacillus subtilis* (P54550). (B) Partial amino acid alignment of different ERs. SsERD *S. salmonicolor* (A0A224AG05), NtDDBR *N. tabacum* (Q9SLN8), CaeEnR1 *C. aegerita*, AtDDBR *A. thaliana* (Q39172), PulR *M. piperita* (Q6WUAU), PPDBR *P. taeda* (Q0PIN2). Dotted lines: nucleotide-binding domain. Yellow: conserved A[AG]XGXXG motif. Green: amino acids suggested binding NADPH. Red: conserved amino acids located in the active site.

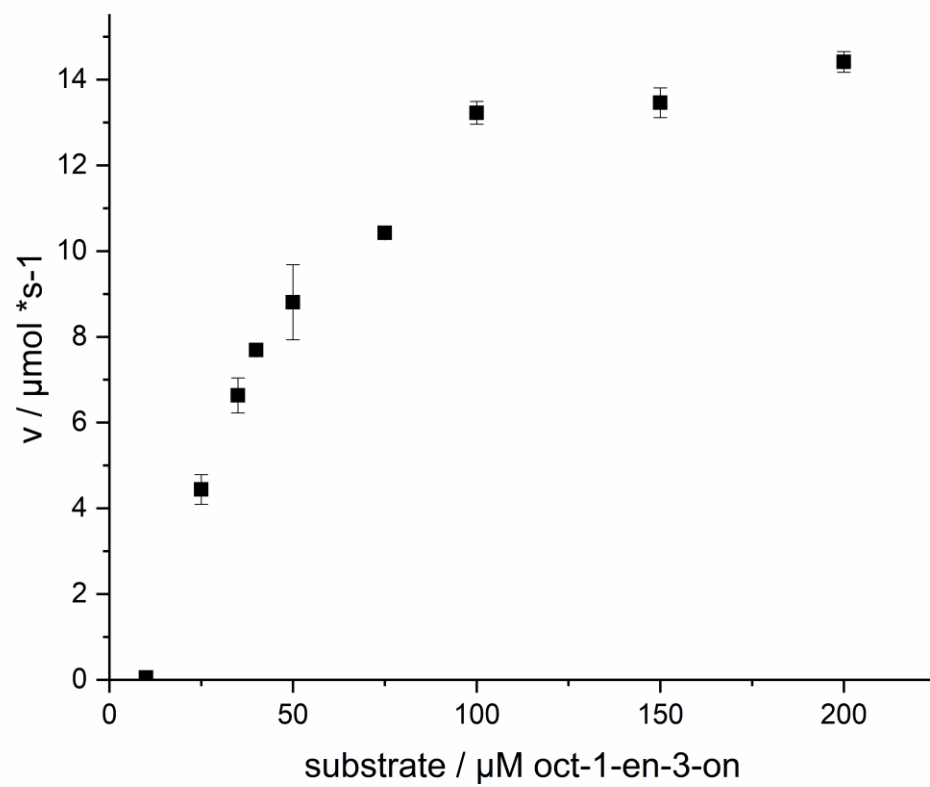


Figure S2. Michaelis-Menten plot of CaeEnR1 with oct-1-en-3-one.

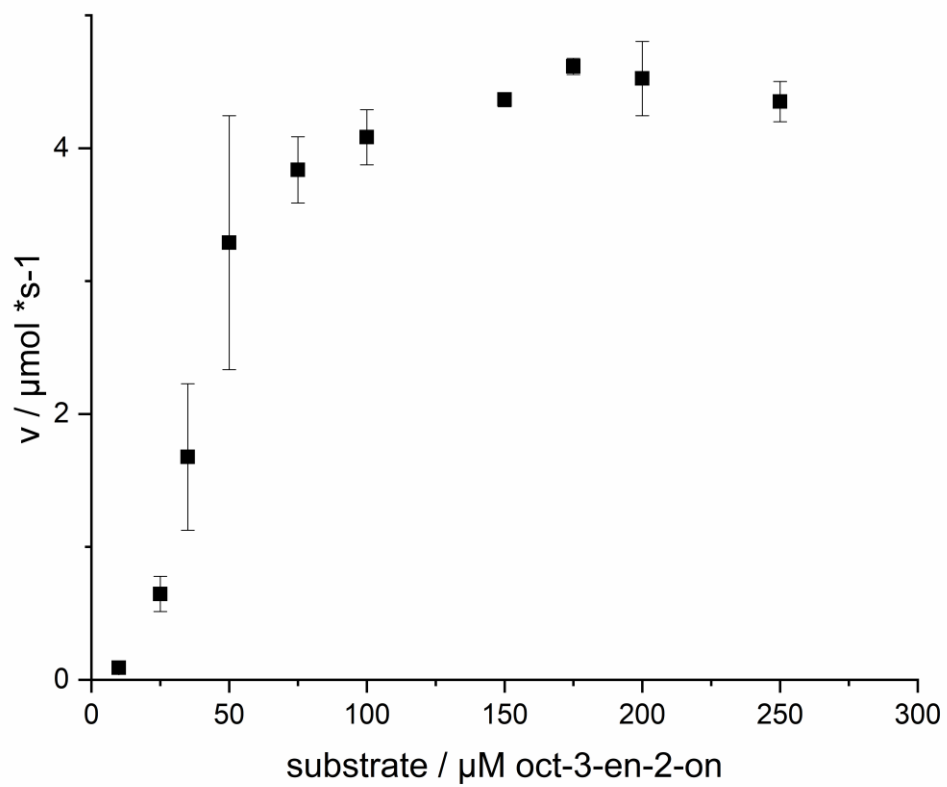


Figure S3. Michaelis-Menten plot of CaeEnR1 with oct-3-en-2-one.

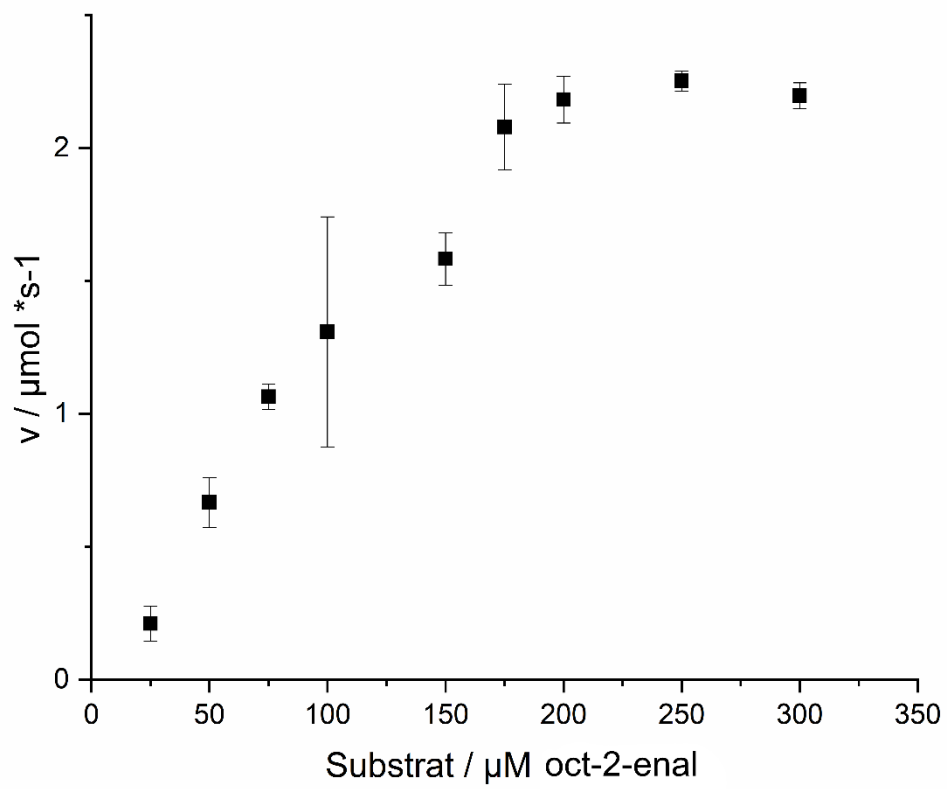


Figure S4. Michaelis-Menten plot of CaeEnR1 with oct-2-enal.

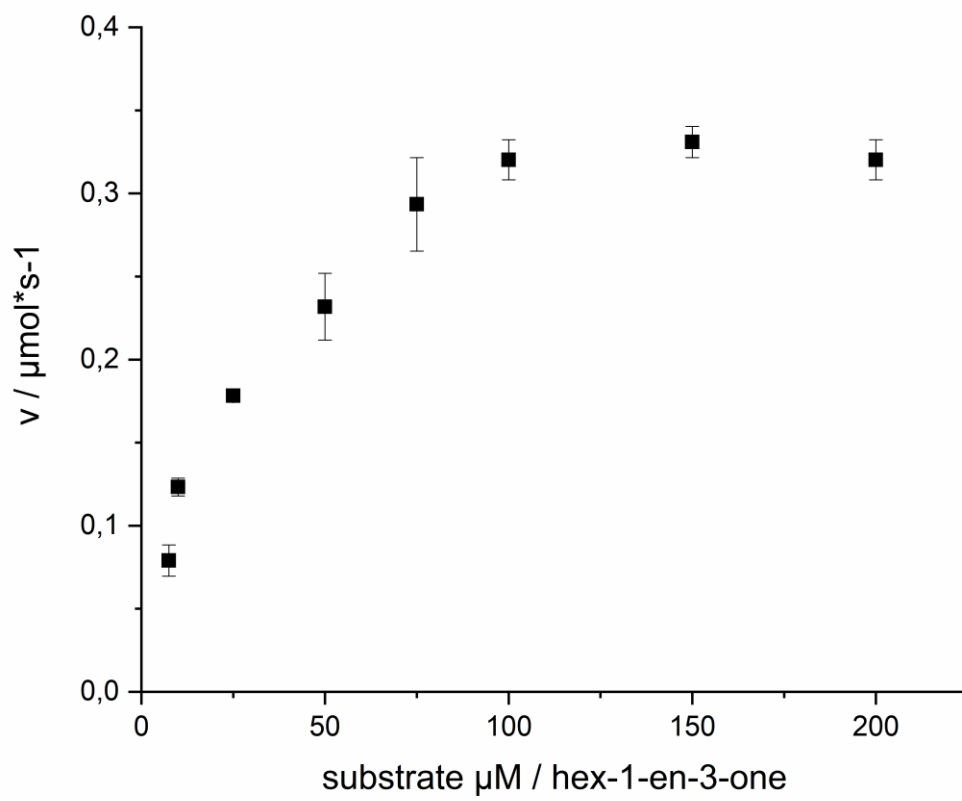


Figure S5. Michaelis-Menten plot of CaeEnR1 with hex-1-en-3-one.

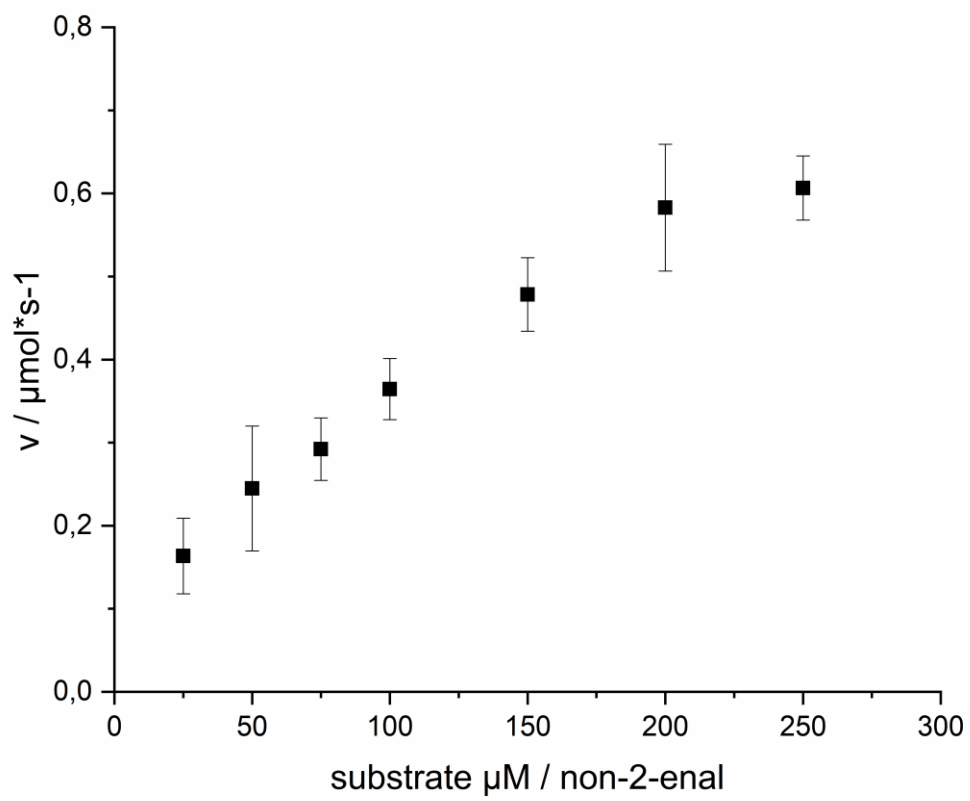


Figure S6. Michaelis-Menten plot of CaeEnR1 with non-2-enal.

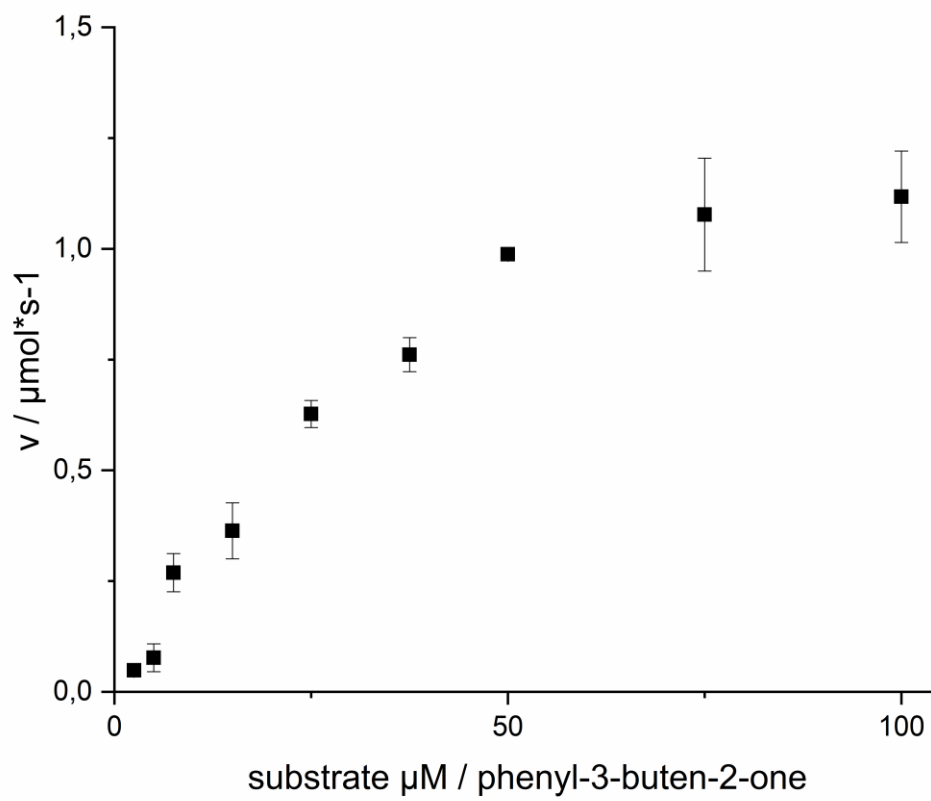


Figure S7. Michaelis-Menten plot of CaeEnR1 with phenyl-3-buten-2-one.

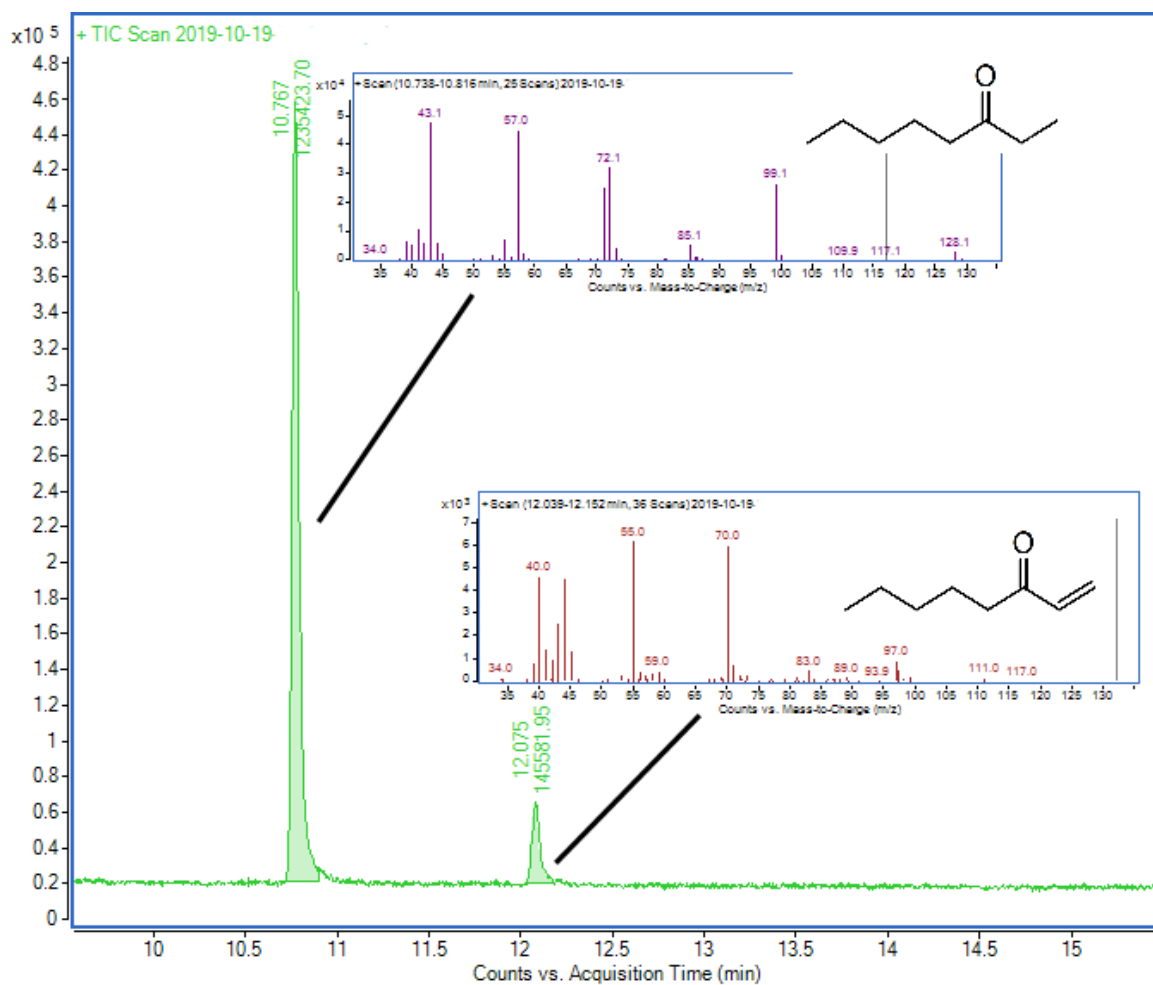


Figure S8. GC-MS analysis of the biocatalytic reduction of oct-1-en-3-one by CaeEnR1.

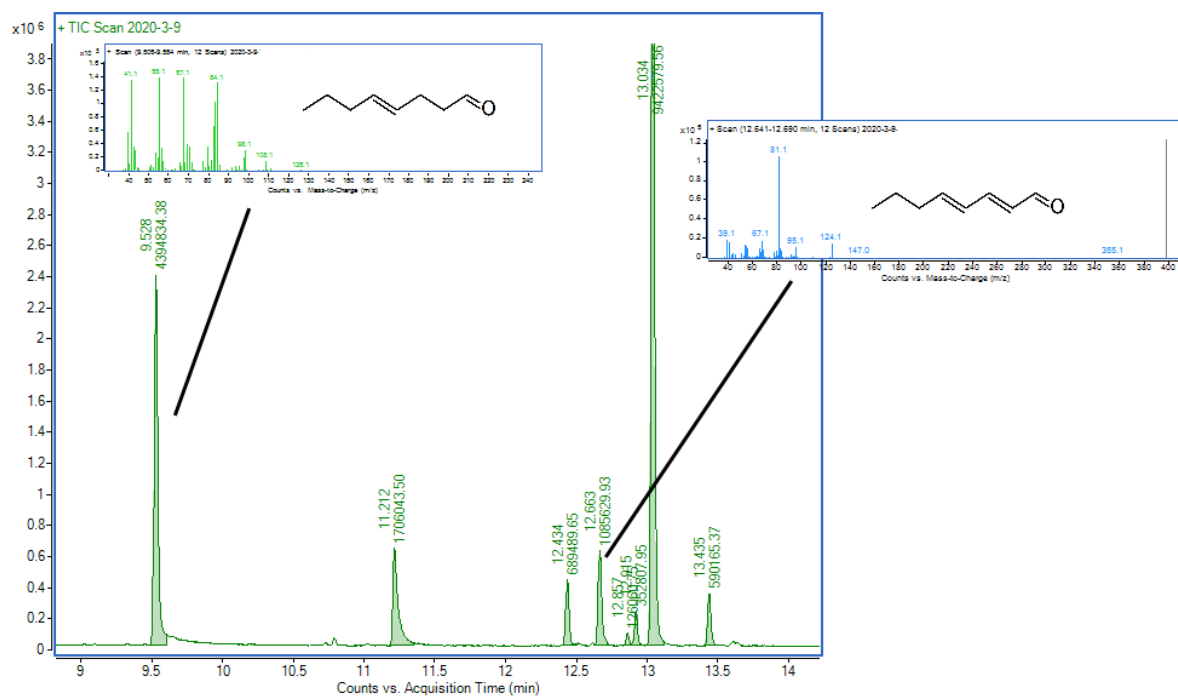


Figure S9. GC-MS analysis of the biocatalytic reduction of (*E,E*)-oct-2,4-dienal by CaeEnR1.

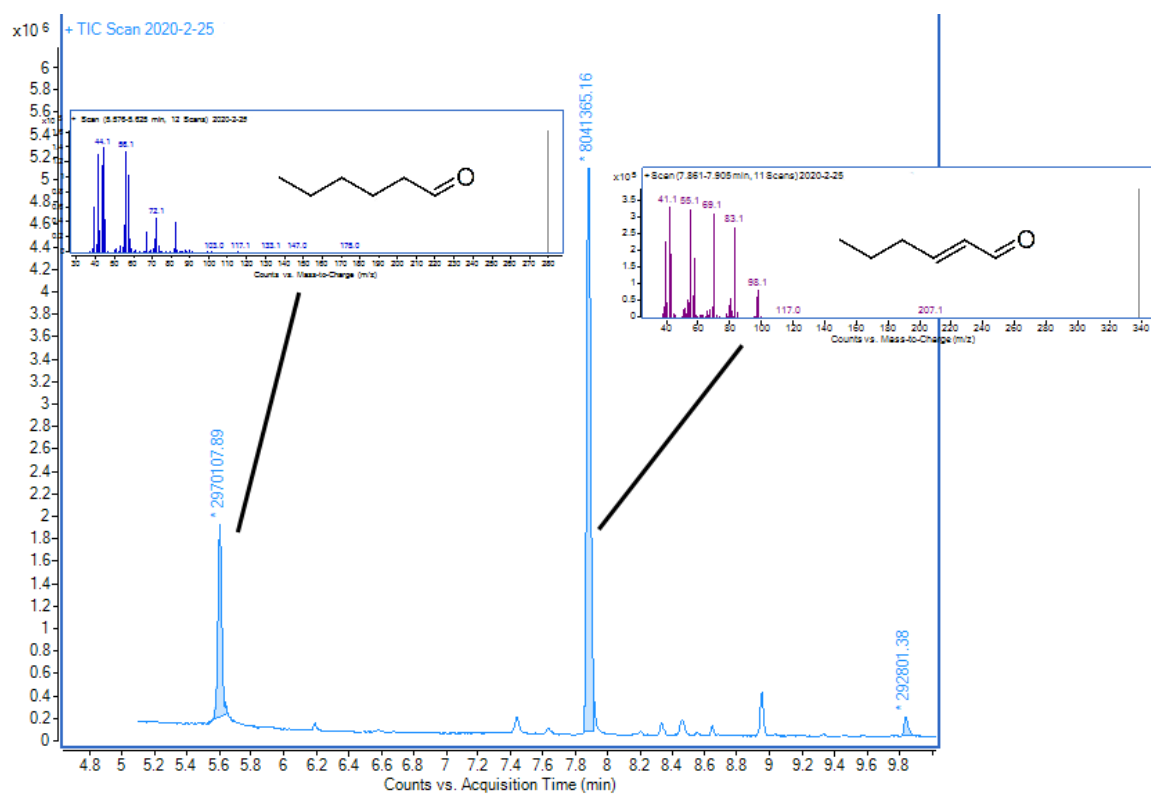


Figure S10. GC-MS analysis of the biocatalytic reduction of (*E*)-hex-2-enal by CaeEnR1.

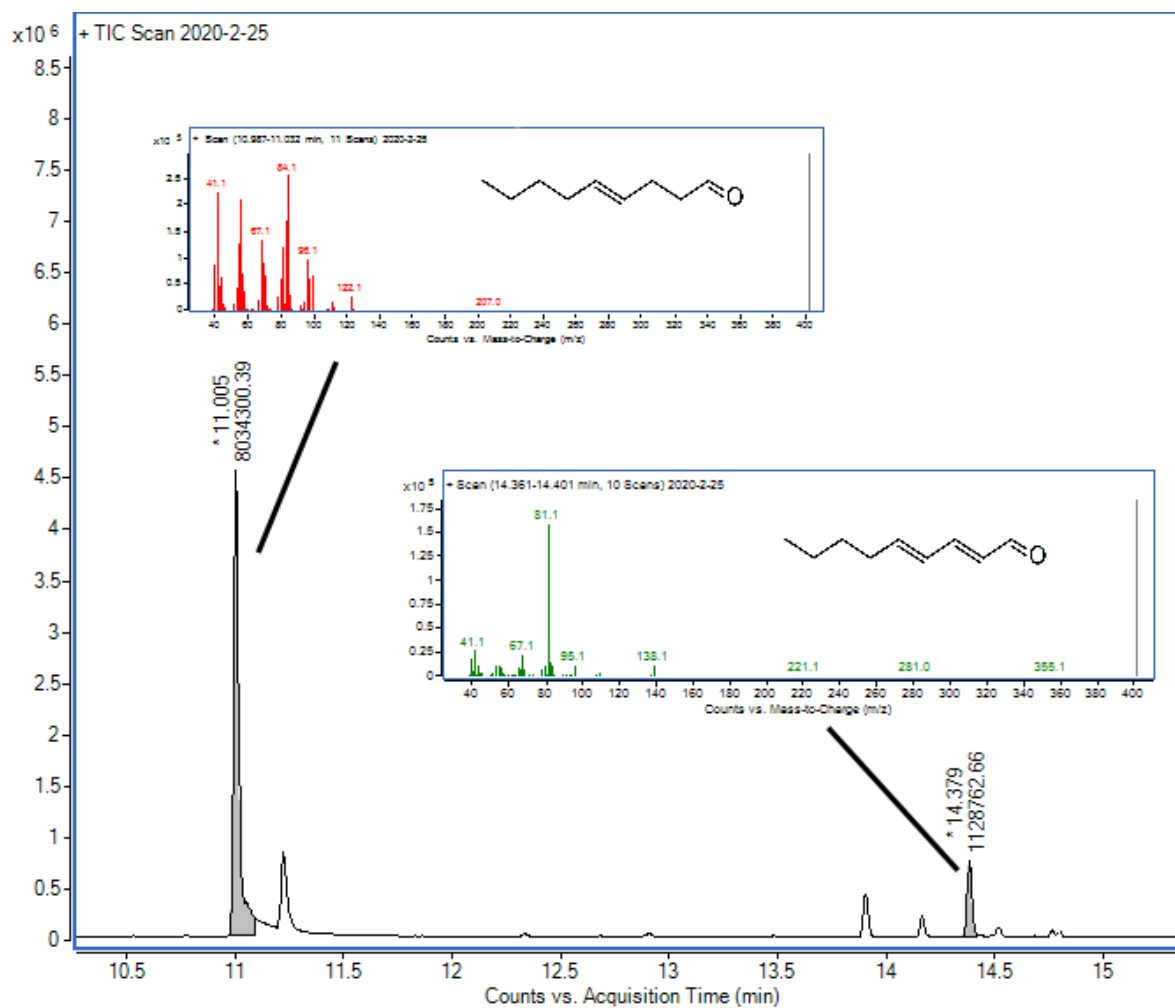


Figure S11. GC-MS analysis of the biocatalytic reduction of (E,E)-non-2,4-dienal by CaeEnR1.

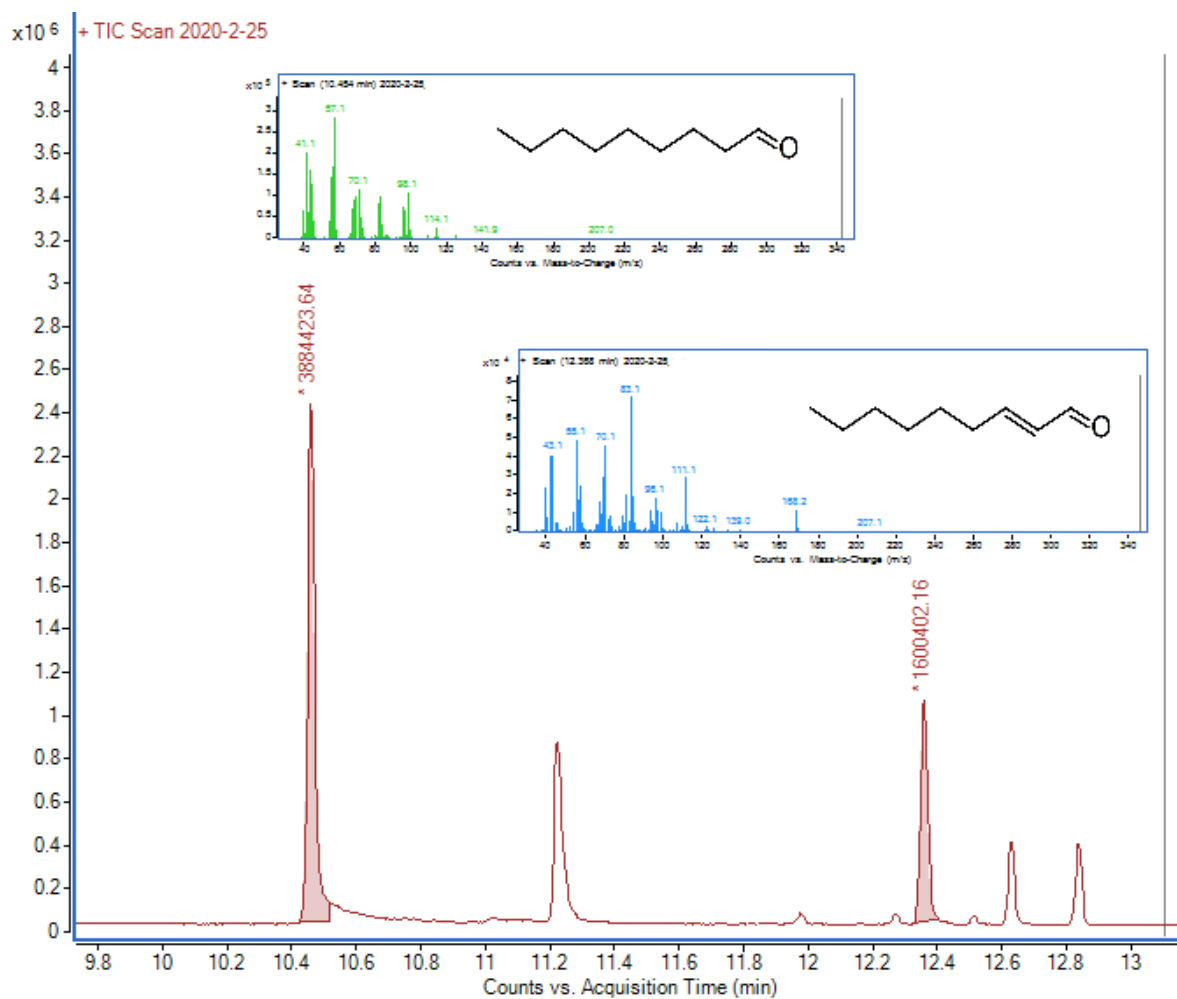


Figure S12. GC-MS analysis of the biocatalytic reduction of (*E*)-non-2-enal by CaeEnR1.

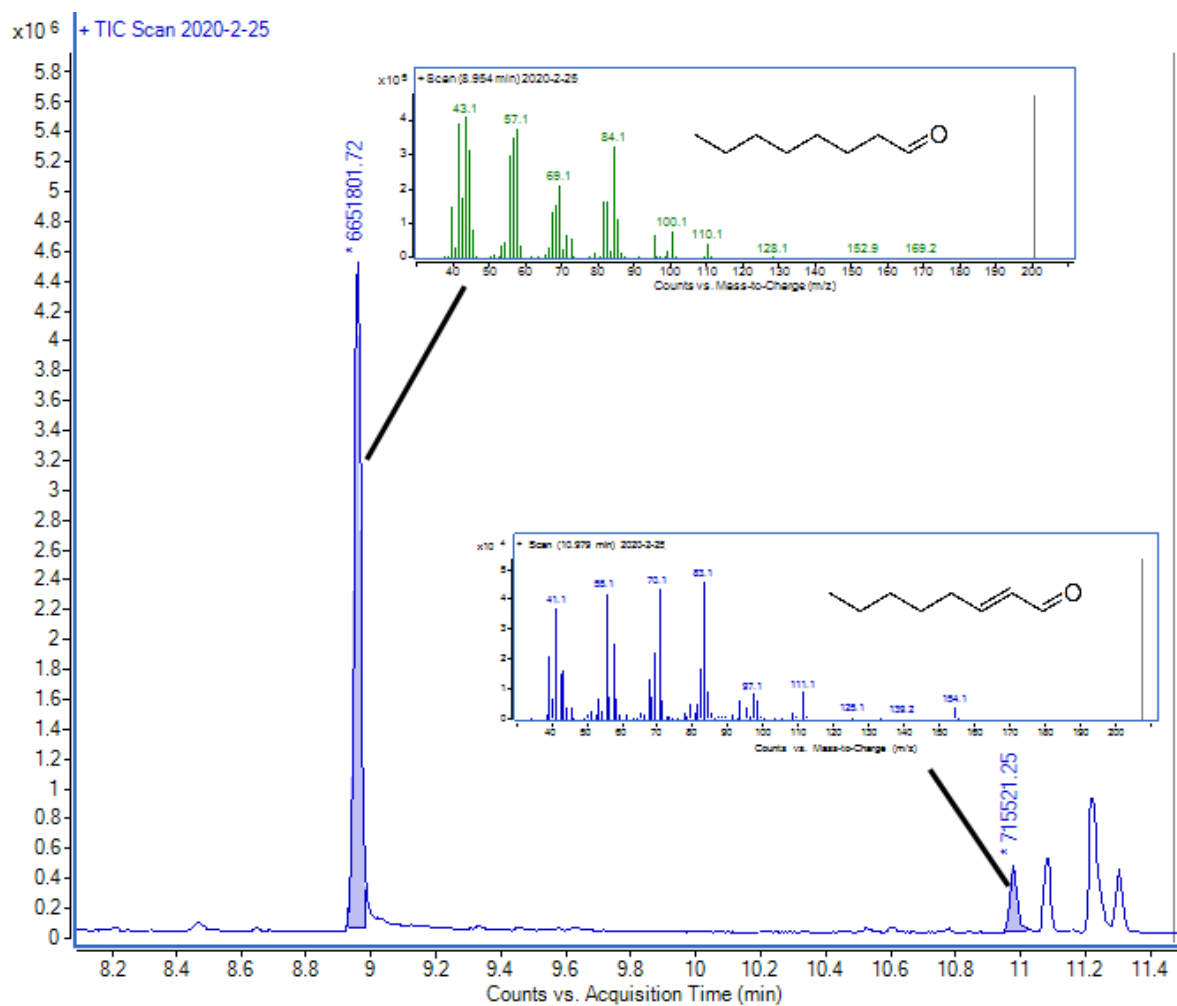


Figure S13. GC-MS analysis of the biocatalytic reduction of (*E*)-oct-2-enal by CaeEnR1.

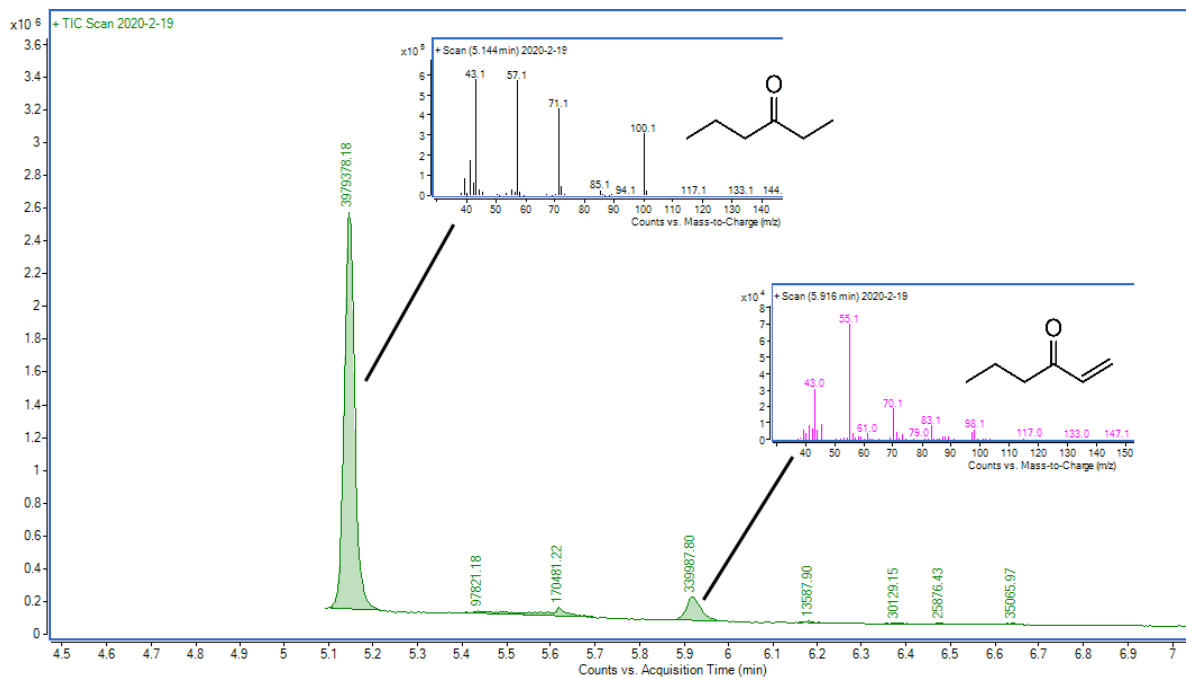


Figure S14. GC-MS analysis of the biocatalytic reduction of hex-1-en-3-one by CaeEnR1.

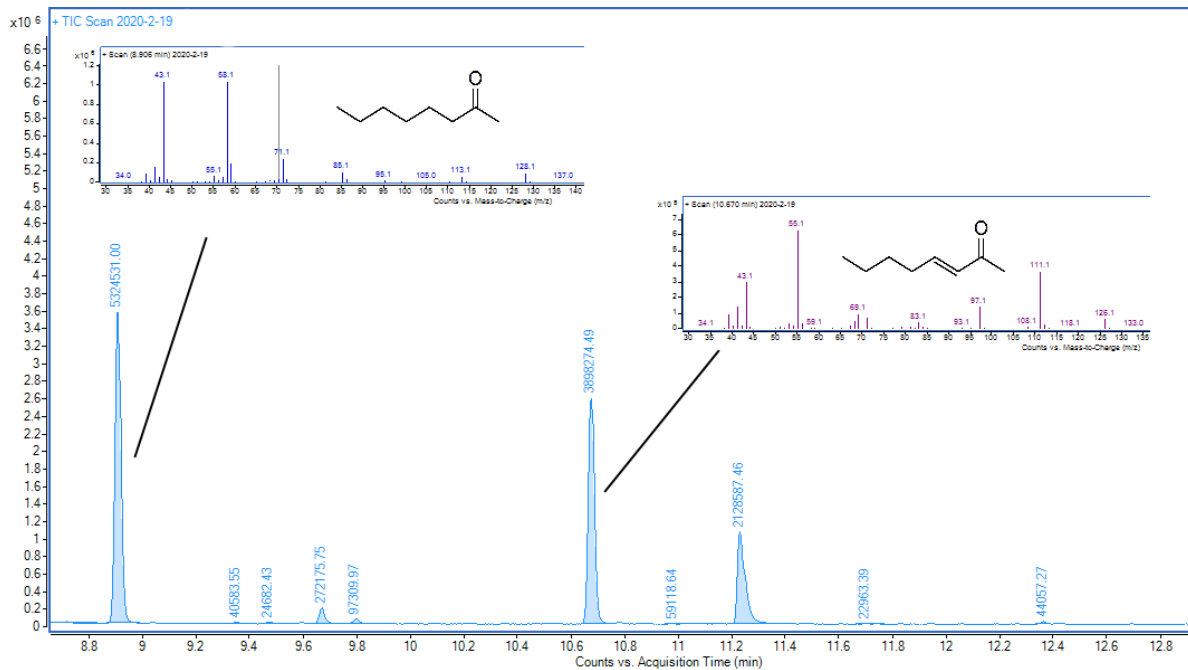


Figure S15. GC-MS analysis of the biocatalytic reduction of oct-2-en-3-one by CaeEnR1.

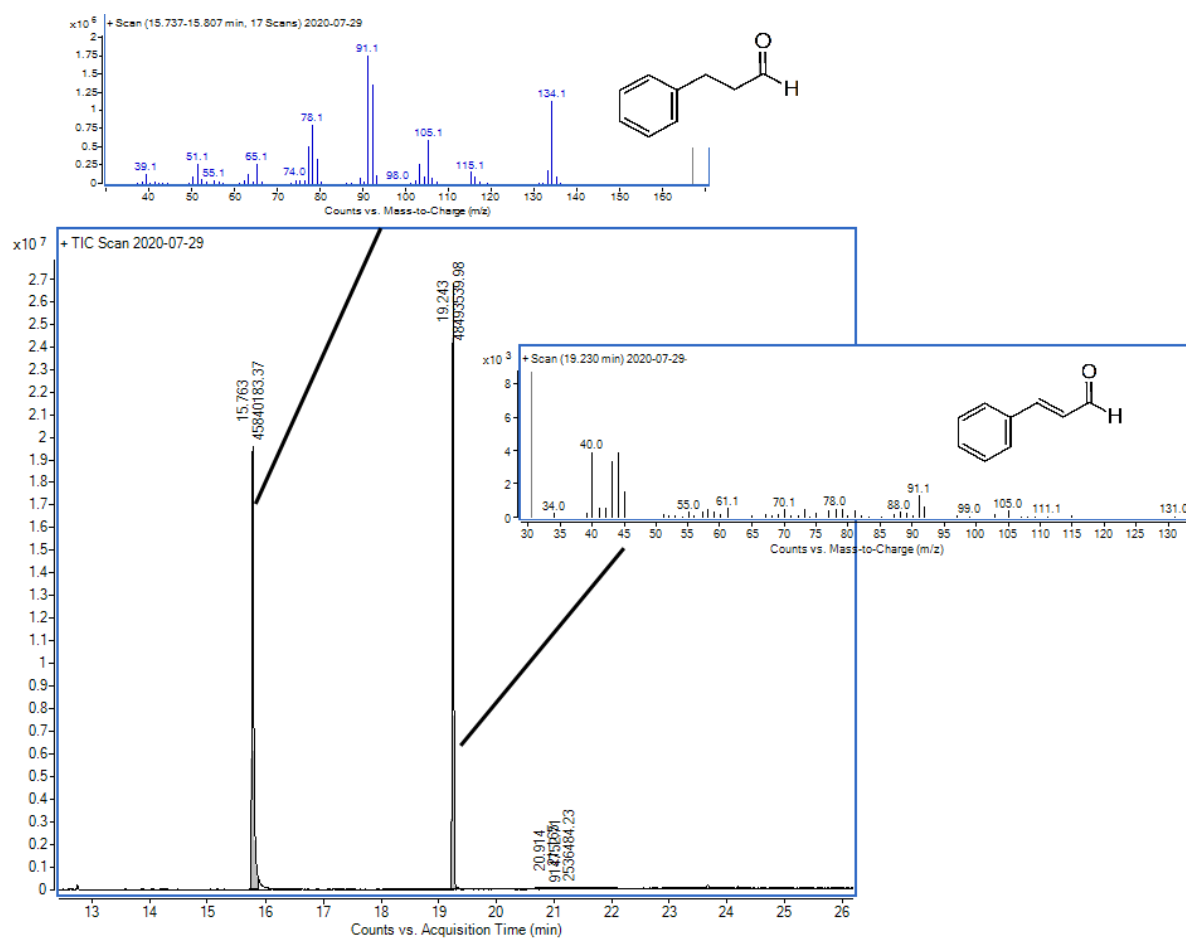


Figure S16. GC-MS analysis of the biocatalytic reduction of cinnamaldehyde by CaeEnR1.

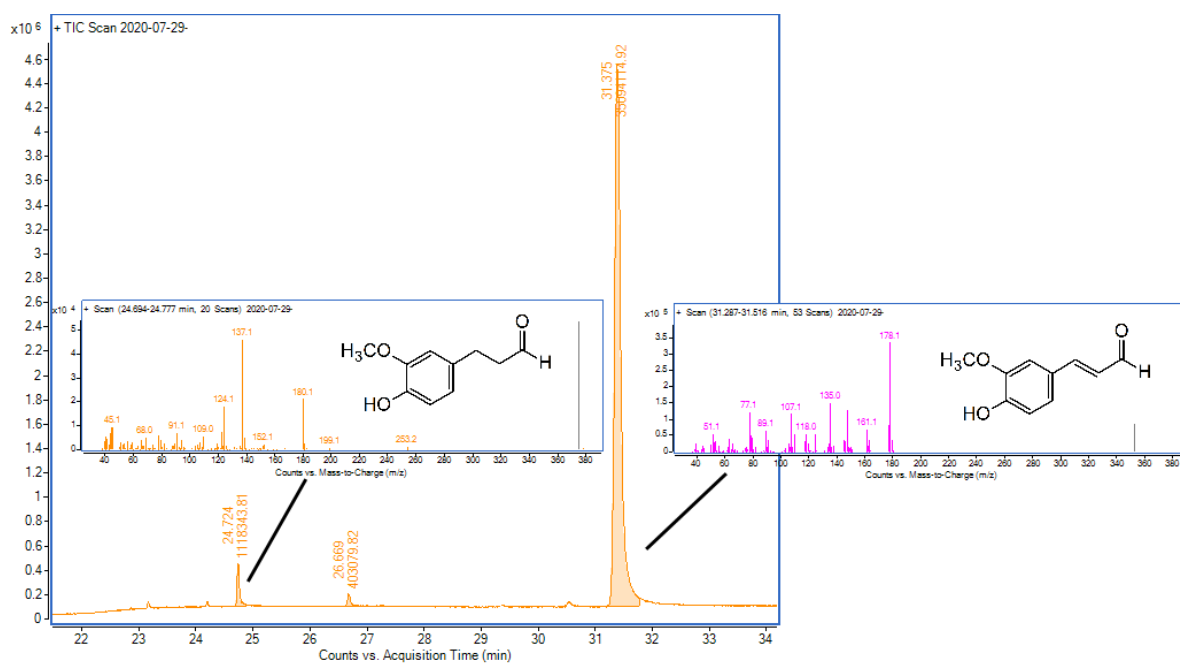


Figure S17. GC-MS analysis of the biocatalytic reduction of coniferyl aldehyde by CaeEnR1.

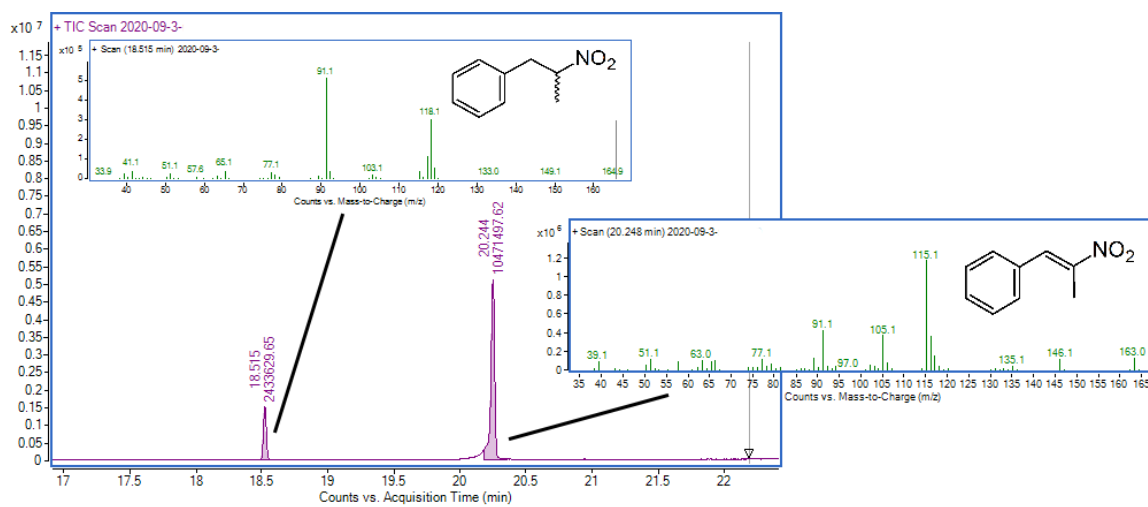


Figure S18. GC-MS analysis of the biocatalytic reduction of (*E*)- β -methyl- β -nitrostyrene by CaeEnR1.

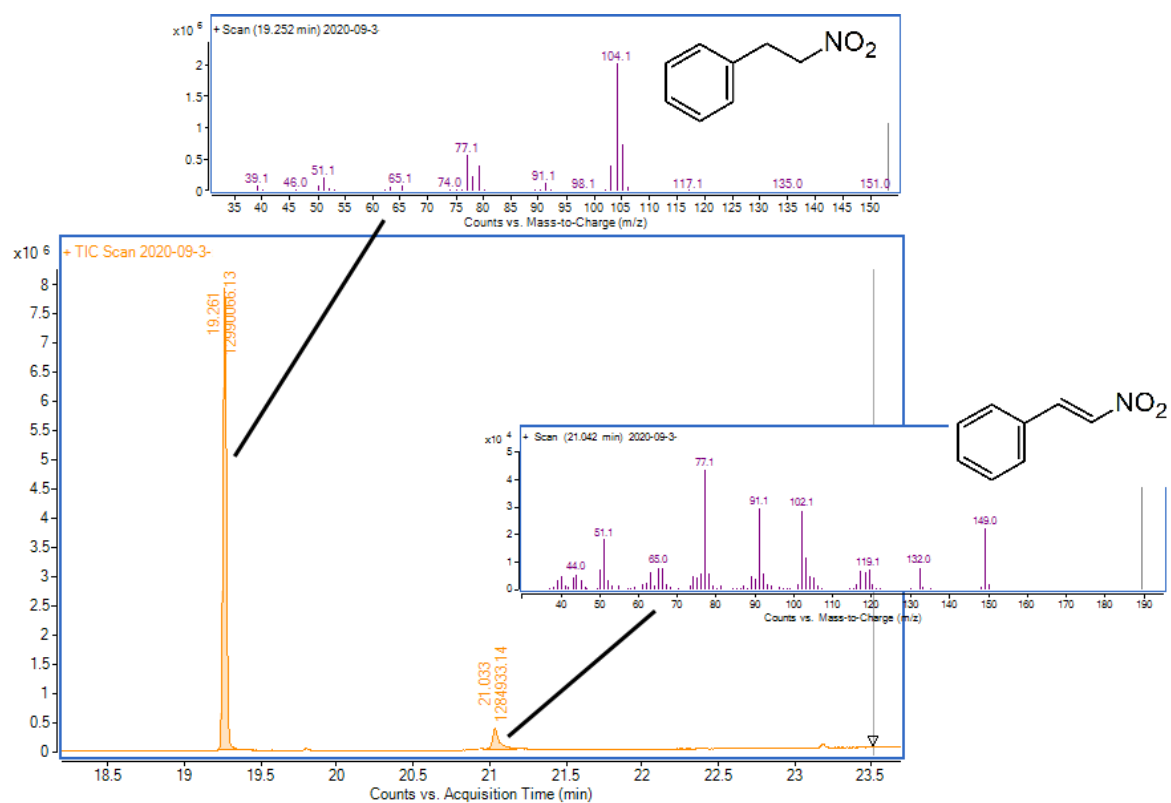


Figure S19. GC-MS analysis of the biocatalytic reduction of *(E)*-β-nitrostyrene by CaeEnR1.

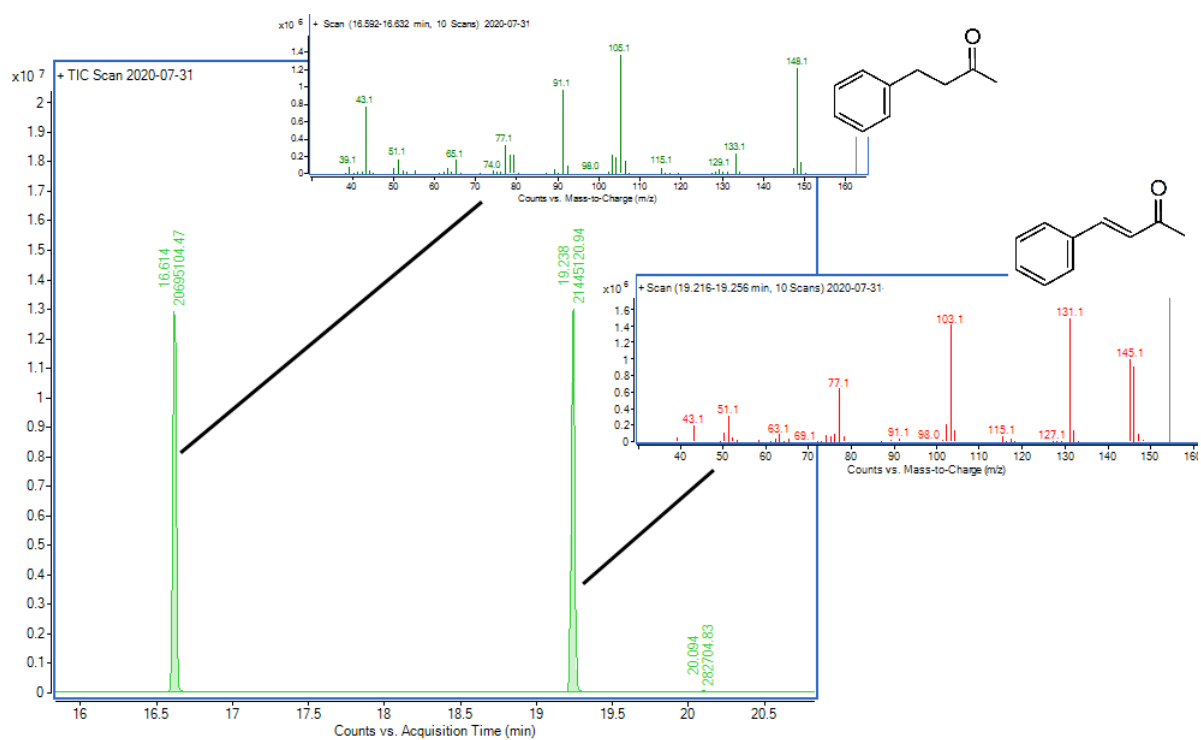


Figure S20. GC-MS analysis of the biocatalytic reduction of 4-phenyl-3-butene-2-one by CaeEnR1.

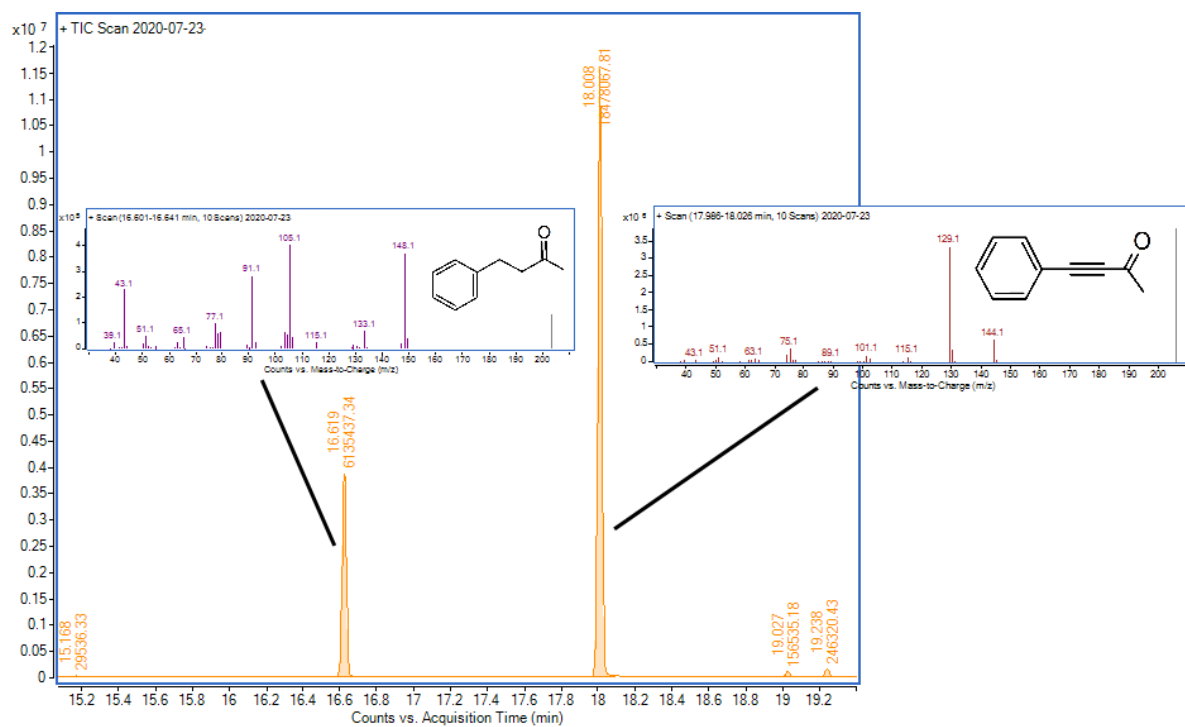


Figure S21. GC-MS analysis of the biocatalytic reduction of 4-phenylbut-3-yne-2-one by CaeEnR1.

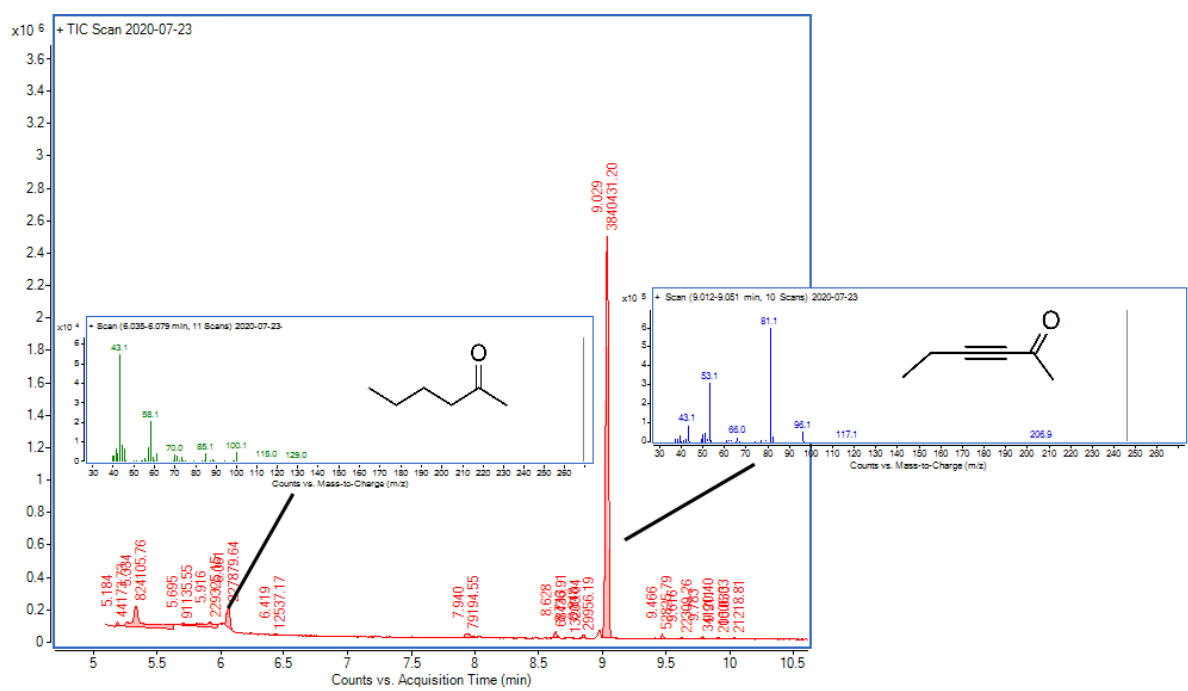


Figure S22. GC-MS analysis of the biocatalytic reduction of hex-3-yn-2-one by CaeEnR1.

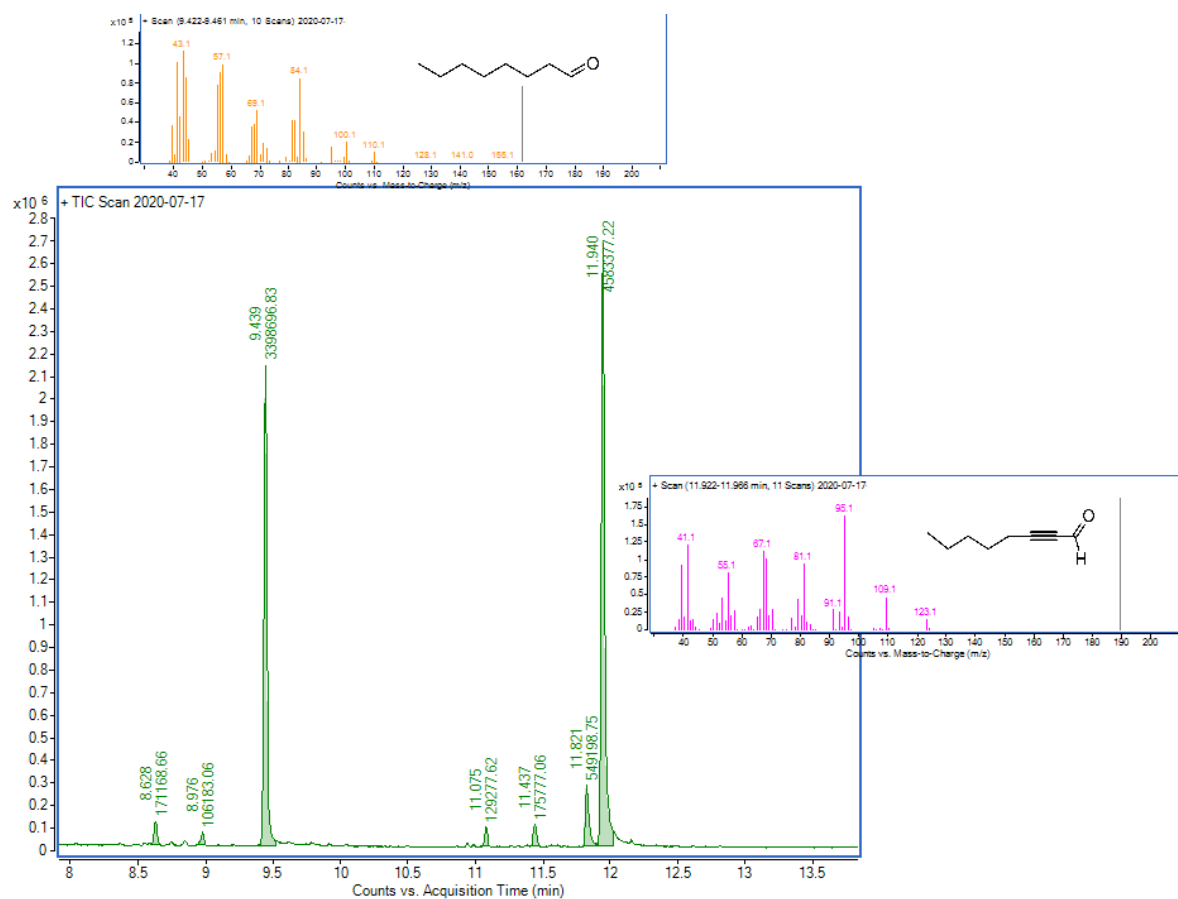


Figure S23. GC-MS analysis of the biocatalytic reduction of oct-2-ynal by CaeEnR1.

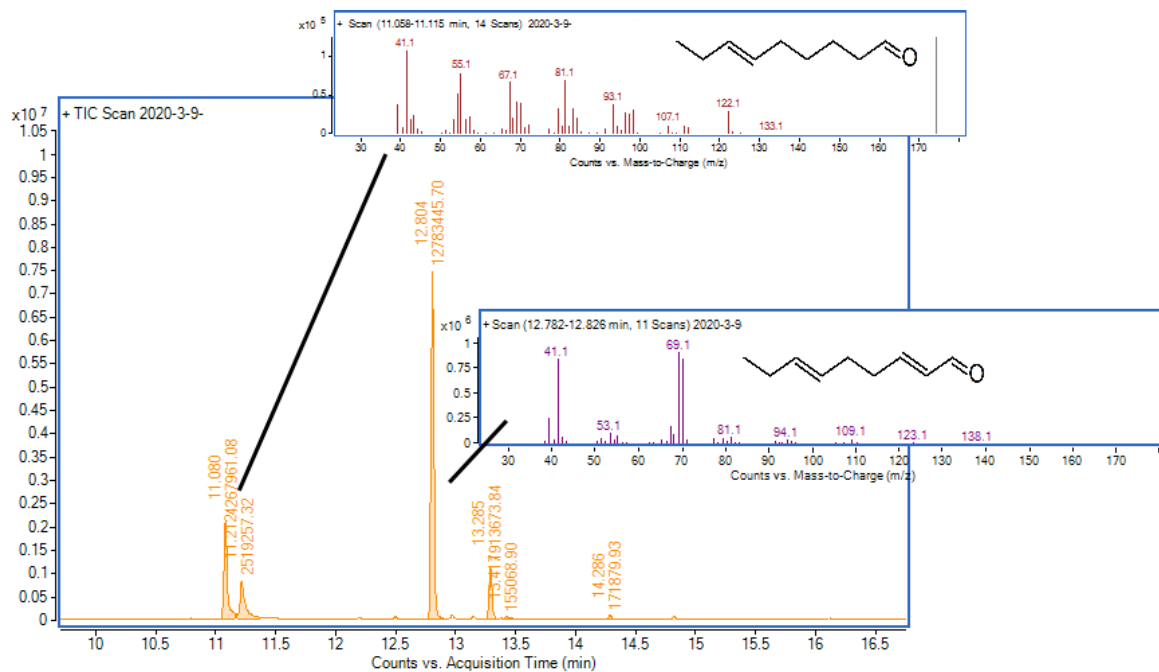


Figure S24. GC-MS analysis of the biocatalytic reduction of (E,E)-non-2,6-dienal by CaeEnR1.

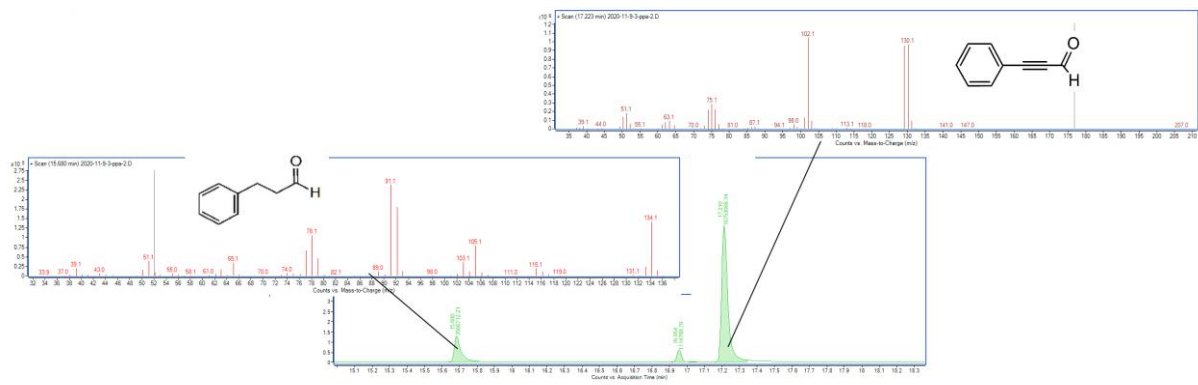
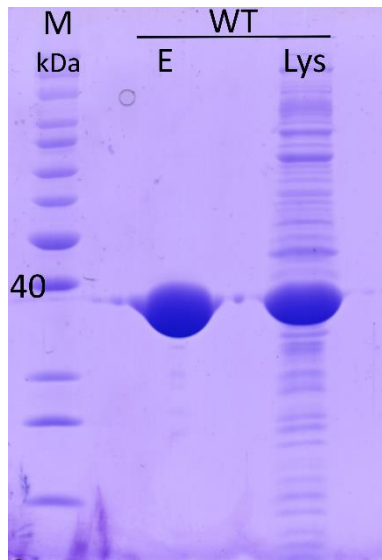


Figure S25. GC-MS analysis of the biocatalytic reduction of 3-phenylprop-2-ynal by CaeEnR1.



S26. SDS-PAGE of the purified CaeEnR1. Lys = lysate, E = eluate.

2.3 Publication 3: Engineering a lipoxygenase from *Cyclocybe aegerita* towards long chain polyunsaturated fatty acids

Dominik Karrer, Dr. Martin Gand, Dr. Martin Rühl

AMB Express (2021), 11, 37.

DOI: [10.1186/s13568-021-01195-8](https://doi.org/10.1186/s13568-021-01195-8)

ORIGINAL ARTICLE

Open Access



Engineering a lipoxygenase from *cyclocybe aegerita* towards long chain polyunsaturated fatty acids

Dominik Karrer¹, Martin Gand¹ and Martin Rühl^{1,2*} 

Abstract

The basidiomycetous lipoxygenase Lox1 from *Cyclocybe aegerita* catalyzes the oxygenation of polyunsaturated fatty acids (PUFAs) with a high preference towards the C18-PUFA linoleic acid (C18:2 (ω-6)). In contrast, longer PUFAs, generally not present in the fungal cell such as eicosatrienoic acid (C20:3(ω-3)) and docosatrienoic acid (C22:3 (ω-3)), are converted with drastically lower activities. With site-directed mutagenesis, we were able to create two variants with enhanced activities towards longer chain PUFAs. The W330L variant showed a ~20% increased specific activity towards C20:3(ω-3), while a ~2.5-fold increased activity against C22:3 (ω-3) was accomplished by the V581 variant.

Keywords: Lipoxygenase, Mutagenesis, Biocatalysis, Protein engineering, *Cyclocybe aegerita*

Introduction

Lipoxygenases (LOX) are non-heme iron dependent dioxygenases that catalyze the insertion of molecular oxygen at a (1Z,4Z)-pentadiene motif, which occurs e.g. in polyunsaturated fatty acids (PUFAs), in a regio- and stereospecific manner (An et al. 2018; Liavonchanka and Feussner 2006). In higher fungi of the phyla *Basidiomycota*, C18-PUFAs and especially linoleic acid are predominant, whereas C20-PUFAs like arachidonic acid and eicosapentaenoic acid were either found in very low amounts or in traces in fungi of the phyla *Basidiomycota*, such as in *Cyclocybe aegerita* (syn. *Agroycbe aegerita*), and *Ascomycota* like *Phellinus* sp. and *Romaria* sp. (Brodhun and Feussner 2011, Dembitsky et al. 1991, Landi et al. 2017). In general, studies on purified basidiomycetous LOX are scarce with only LOX from *Pleurotus* spp. and *Cyclocybe aegerita* described so far (Karrer and Rühl 2019; Kuribayashi et al. 2002; Leonhardt et al. 2013;

Plagemann et al. 2013). For three of them it is known that they primarily produce 13-hydroperoxy-9Z,11E-octadecadienoic acid (13-HPOD) and minor levels of 9-hydroperoxy-10E,12Z-octadecadienoic acid (9-HPOD) (Karrer and Rühl 2019; Kuribayashi et al. 2002; Plagemann et al. 2013). Furthermore, basidiomycetous LOX share a high preference towards C18-PUFAs of which linoleic acid was converted with the highest preference. With increasing chain length, the activity drastically decreases (Karrer and Rühl 2019). Yet, no study focused on the question which amino acids are the determining factors of the inefficient oxygenation of C20-C22-PUFAs. This shortcoming is addressed in this study by site-directed mutagenesis of three amino acid residues located in the substrate tunnel of the Lox1 from *Cyclocybe aegerita*.

Materials and methods

Cloning and protein expression of CaeLOX1

The codon optimized *LOX1* gene (accession number: MW013781), whose original cDNA was commercially purchased and cloned into the plasmid pET28a (Bio-Cat GmbH, Heidelberg, Germany). For protein expression, pET28a/Lox1 plasmid was transformed into *E. coli* BL21-Gold (DE3) by adding ~100 ng of plasmid-DNA

*Correspondence: martin.ruehl@uni-giessen.de

² Fraunhofer Institute for Molecular Biology and Applied Ecology IME Branch for Bioresources, Department of Biology and Chemistry, Justus-Liebig University Giessen, Institute of Food Chemistry and Food Biotechnology, Heinrich-Buff Ring 17, Giessen, Hesse 35392, Germany
Full list of author information is available at the end of the article

to chemically competent cells. The mixture was incubated on ice for 30 min, followed by a heat shock for 45 s at 42 °C. After 5 min rest on ice, 500 µL of LB-medium was added to the competent cells with a subsequent incubation period of 30 min at 37 °C. 200 µL of the cell suspension was plated on LB-Agar, supplemented with kanamycin (50 mg L⁻¹). After incubation over night at 37 °C, the obtained clones were used for protein expression. Recombinant *E. coli* cells were cultivated in auto-induction medium containing 10 g tryptone, 5 g yeast extract, supplemented with 50 mM Na₂HPO₄, 50 mM KH₂PO₄, 25 mM (NH₄)₂SO₄, 0.5% (w/v) glycerol, 0.025% (w/v) glucose, 0.2% (w/v) lactose and 50 mg L⁻¹ kanamycin as selection marker, at 24 °C for 16 h. Cells were harvested by centrifugation (4.000g, 30 min, 4 °C) and stored at -20 °C until further use.

Protein purification

The cell pellet was thawed on ice and resuspended in lysis-buffer (50 mM phosphate, 300 mM NaCl, pH 7.5). Disruption of cells was carried out by sonification (3 cycles for 60 s each with 60 s rest in between) on ice using a sonifier (Bandelin Sonopuls, Berlin, Germany). After complete disruption, cell debris was removed by centrifugation (14.000 g, 30 min, 4 °C). The resulting supernatant was further processed by using Ni-NTA spin columns (Qiagen, Hilden, Germany) following manufacturer instructions. The eluted protein (using 500 mM imidazole in the elution buffer) was collected and subsequently concentrated and rebuffed in 50 mM phosphate buffer (pH 7.5) by using Pall Nanosep® omega centrifugal devices (10 kDa cut off). The concentrated protein was analyzed via SDS-PAGE. Fractions with purified CaeLox1 were used for further analysis. Protein concentration was photometrically determined by using the 260/280 ratio and the specific extinction coefficient ($\epsilon_{280} = 102,135 \text{ M}^{-1} \text{ cm}^{-1}$), calculated with the ExpASy ProtParam tool (Gasteiger et al. 2005).

Lipoxygenase assay

LOX activity was determined by recording the formation of the conjugated double bond at 234 nm ($\epsilon = 25,000 \text{ M}^{-1} \text{ cm}^{-1}$) on a Nanophotometer (Implen, Munich, Germany). The reaction mixture contained 1.25 mM PUFA (Acros Organics: linoleic acid, linolenic acid, Cayman Chemicals: eicosatrienoic acid, docosatrienoic acid), 20 µL enzyme solution and 50 mM phosphate buffer, pH 7.5 to a final volume of 1 mL.

Determination of pH- and temperature-optimum

For the determination of the pH-optimum, three different buffers were used: 50 mM acetate buffer, pH 4.5–6.0; 50 mM phosphate buffer, pH 6.5–7.5 and 50 mM

borate buffer, pH 8.0–10.0. Effects of the temperature were determined by incubating the reaction mixture at different temperatures, ranging from 4 °C – 60 °C.

Site-directed mutagenesis

For mutagenesis a modified QuikChange® protocol was used (Gand et al. 2016). The modified QuikChange® reaction mixture contained 1 µL pET28a-Lox1-WT (~50 ng/µL), 2.5 µL forward primer, 2.5 µL reverse primer (Table 1), 1 µL dNTPs, 0.5 µL Phusion-polymerase (Thermo Fisher Scientific), 10 µL 5× GC-buffer, 1 µL dimethylsulfoxide and 35 µL ddH₂O. PCR conditions with Phusion polymerase: initial denaturation for 3 min at 98 °C, 30 s denaturation at 98 °C, 30 s annealing at 62/64/66/68 °C, elongation at 72 °C for 3:30 min, final elongation for 5 min at 72 °C. Then, 2 µL *DpnI* (Thermo Fisher Scientific, Waltham, MA, USA) was added and the samples were incubated for 2 h at 37 °C, followed by *DpnI* inactivation at 80 °C for 10 min. Chemically competent *E. coli* Zymo 10β (Zymo Research Europe GmbH, Freiburg, Germany) were transformed via heat shock with the PCR-products and plated out on LB-plates containing kanamycin as selection marker (50 mg L⁻¹). After incubation over night at 37 °C, the obtained colonies were picked and used to inoculate fresh LB-medium with the according selection marker. After another incubation period over night at 37 °C, the success of site-directed mutagenesis was confirmed via DNA-sequencing (Microsynth Seqlab, Göttingen, Germany).

Homology modelling

The crystal structure of the lipoxygenase from *Glycine max* (PDB: 1IK3) was used as template, sharing 43 % sequence similarity. Models were calculated with SWISS-MODEL () (Guex et al. 2009) and visualized with Chimera 1.13.1 (Pettersen et al. 2004).

Table 1 Primer sequences for site-directed mutagenesis

primer	sequence
fw_Lox1-I393F	5'-ccgagatggtgcccgtttatgttttaaaatccgg-3'
rv_Lox1-I393F	5'-ccggaattttaaaataactaaacggggcaaccatactcgg-3'
fw_Lox1-V581A	5'-gatgatggcagcagggcgcgtatctgctgag-3'
rv_Lox1-V581A	5'-ctcagcagatacggcgctgtgacctatc-3'
fw_Lox1-V581F	5'-gatgatggcagcagttccgtatctgctgag-3''
rv_Lox1-V581F	5'-ctcagcagatacggaaactgtgacctatc-3'
fw_Lox1-W330L	5'-caggtgagcagctgaccctgcatgaactg-3'
rv_Lox1-W330L	5'-cagttcatgacgggtcagatcgctcacctg-3'

Molecular docking

Autodock Vina was used for docking analysis. For each docking run, a box was defined which covered the active site with a grid of $22 \times 18 \times 26$ Å. All parameters were set on standard (Trott et al. 2010).

Results

Bioinformatic analysis and homology modelling

Shape and specificity of mammalian LOX or the regioselectivity of LOX from plants were investigated by various studies. It was pointed out that specific bulky/aliphatic amino acid residues in the substrate tunnel can affect substrate orientation and, therefore, be crucial for substrate specificity (Borngräber et al. 1999; Brodhun et al. 2013; Hornung et al. 2008). A comparison of sequence alignments of already characterized basidiomycetous LOX, assisted by the homology model of CaeLox1, shows that in their substrate tunnel the amino acid W330 is highly conserved and the amino acid hydrophobicity at the positions I393 and V581 are very similar (Fig. 1a, b). Furthermore, molecular docking in a carboxyl-end towards the stabilizing K540 orientation was calculated for the widely occurring linoleic acid (C18:2 ω -6), linolenic acid (C18:3 ω -3) as well as for the rare PUFAs eicosatrienoic acid (C20:3 ω -3) and docosatrienoic acid (C22:3 ω -3). This revealed that the residues W330, I393 and V581 are indeed in interacting distance, with less than 5 Å, to the carboxy-end and middle section of the tested PUFAs (Fig. 2a–d).

Temperature and pH optimum

In acidic environment (pH 4.5–6.0), the CaeLox1 activity remained very low with about 10% of the maximum activity. A drastic increase in activity was detected with increasing pH reaching its maximum at 7.5. Further increase of the pH resulted in a drastic loss with no detectable activity from pH 9.5 and above (Fig. 3a). The effect of the temperature on the activity of CaeLox1 was determined in a temperature range between 4 °C and 60 °C. The highest activity was detected at 25 °C. A steady loss of activity to about 80% was detected when increasing the temperature from 25 to 45 °C. With a further temperature increase to 50 °C and 60 °C no activity could be detected. At 4 °C 10% of the maximal LOX activity remained (Fig. 3b). Based on these results, any further experiments were conducted at pH 7.5 and 25 °C.

Specific activities towards various PUFAs

To experimentally verify the role of W330, I393 and V581 in PUFA oxygenation, we investigated the specific activities of PUFAs occurring (linoleic acid, linolenic acid) and non-occurring (eicosatrienoic- and docosatrienoic acid)

in fungi of the phylum *Basidiomycota*. Expanding the size of the substrate tunnel (V581A), putatively stabilizing the middle-section of the substrate in a carboxylate-end first orientation (Fig. 1), led to a ~3-fold loss of activity, while a reduced size (V581F) resulted in a ~2.5-fold decrease of activity towards linoleic acid (Fig. 4a). With the same mutations, similar differences in activities towards linolenic acid were observed in comparison to the wild type. Interestingly, the observed effects of the V581A/F mutations changed with increasing chain length of the fatty acid. Compared to C18-PUFAs, the V581F variant showed only a <2-fold difference in activity towards C20-22:3(ω -3)-PUFAs eicosatrienoic acid and docosatrienoic acid (Fig. 4c, d). Furthermore, a ~2.5-fold increased activity against docosatrienoic acid was detected for the V581A variant, representing 50% of the WT activity towards the natural substrate linoleic acid. Tightening the substrate tunnel receiving the carboxy-end of the PUFAs with the I393F variant, a ~3-fold decrease was observed against C18-PUFAs while C20- and C22-PUFAs were less affected by this mutation. CaeLox1 mutation W330L, which leads to a widening of the substrate tunnel, resulted in only ~15% of the activity towards linoleic acid in comparison to the wild type LOX CaeLox1. Surprisingly in this mutant (W330L), the conversion of eicosatrienoic acid was increased by ~20% compared to linoleic acid. However, the W330L variant showed a ~60% reduction in the activity to docosatrienoic acid (Fig. 4c, d). Due to the increased specific activity of the W330L and V581A variants towards the C20-22:3(ω -3)-PUFAs, the double mutant W330L/V581A was created. This variant exhibited similar or even lower specific activities towards C18- as well as C20-22-PUFAs, compared to the single mutations V581A and W330L (Fig. 4a–d).

Discussion

Both variants V581A and V581F showed similar activities to the fungal occurring PUFAs (linoleic acid and linolenic acid) compared to the wild type LOX, which suggests that neither increasing or decreasing space at that position leads to significantly higher activities but rather interfere with an efficient substrate binding of C18-PUFAs (Fig. 4a, b). The observed effects of the V581A/F mutations changed with increasing chain length, suggesting that alteration of space inside the tunnel seems to get relevant for longer chain PUFAs (Fig. 4c, d). Due to an additional C=C double bond in long chain PUFAs like C20(ω -3), which leads to lessened flexibility of the alkyl-chain, providing extra space seems to be beneficial. On the other hand, linoleic acid that harbors two C=C bonds resulting in increased flexibility of the alkyl-chain, seems to require a tighter substrate tunnel for an optimal substrate orientation.

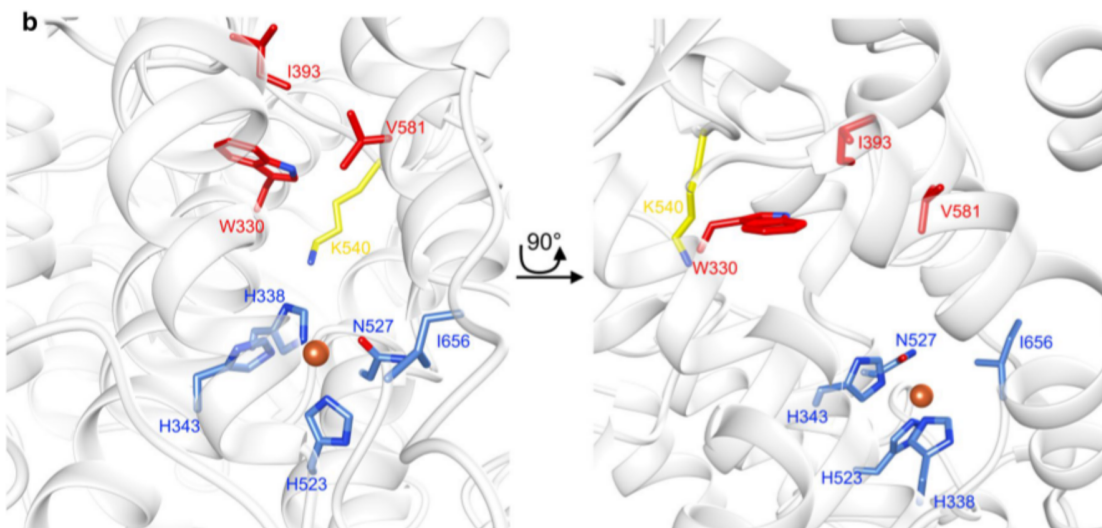
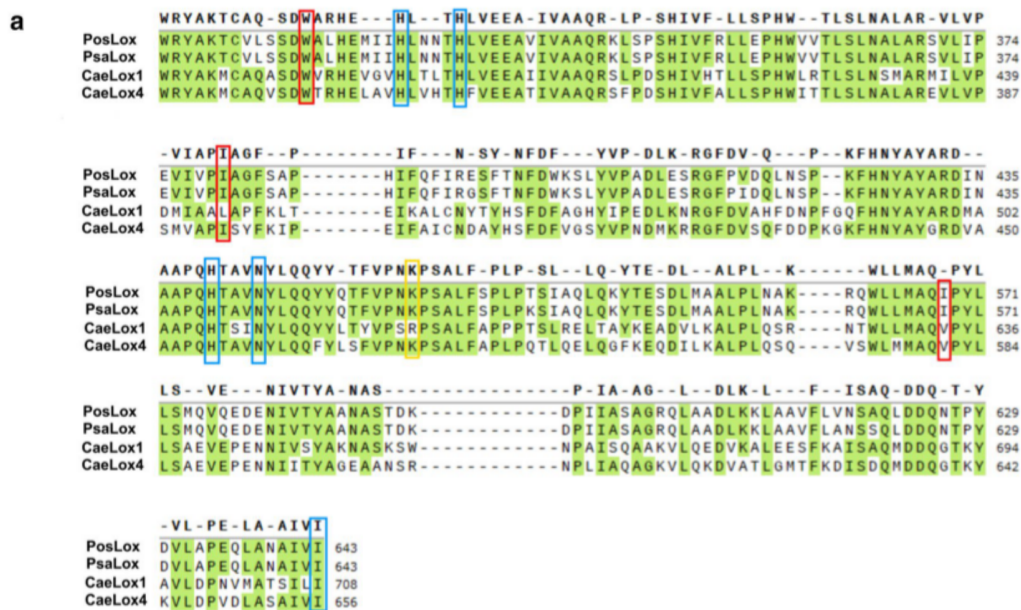


Fig. 1 a Partial sequence alignment of various LOX. *Cyclocybe aegerita* CaeLox1 (MW013781), CaeLox4 (MK451709), *Pleurotus sapidus* PsaLox (CCV01580), *Pleurotus ostreatus* PosLox (CCV01578). Alignment was carried out by using Clustal Omega with default parameters. The highlighted amino acid residues involved in iron binding are highlighted in blue. Amino acids considered to be involved in selectivity and activity by shaping the substrate tunnel are highlighted in red. Amino acid residues considered to interact with the carboxylate end of the substrate via ionic interactions are highlighted in yellow. **b** Substrate tunnel of the homology model of CaeLox1. Iron (orange) binding amino acid residues are highlighted as blue sticks (H338, H343, H523, N527, I656) and the positively charged amino acid at the bottom of the substrate tunnel is highlighted in yellow sticks. Amino acid residues involved in shaping the substrate tunnel are shown as red sticks (V581, I393 and W330). Oxygen inside the amino acid side chains are colored in red and nitrogen in blue

Although the increased chain length in comparison to the eicosatrienoic acid leads to a higher flexibility, the conformation of docosatrienoic acid in the substrate tunnel without a tryptophan might be unsuitable (Fig. 4c, d). Previous studies investigated the role of the amino acid residues W500 and W523, located in the

substrate tunnel of LOX-1 from soybeans and a LOX from pea seeds (Hughes et al. 2001; Ruddat et al. 2004). Increasing space at position W500 of LOX-1 from soybeans revealed a decrease of activity towards linoleic acid and arachidonic acid (Ruddat et al. 2004). Furthermore, the W523A variant of a LOX from pea seeds

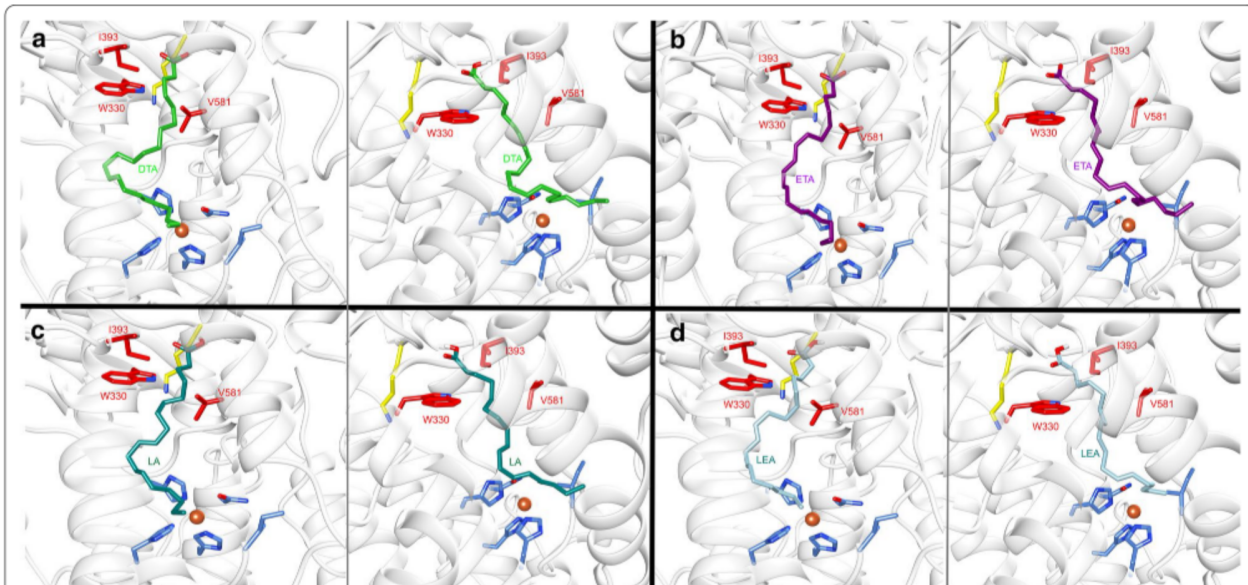


Fig. 2 Molecular docking of **a** docosatrienoic acid (DTA, green sticks), **b** eicosatrienoic acid (ETA, magenta sticks), **c** linoleic acid (LA, cyan sticks) and **d** linolenic acid (LEA, light blue sticks) into the homology model of CaeLox1. Iron (orange) binding amino acid residues are highlighted as blue sticks (H338, H343, H523, N527, I656) and the positively charged amino acid at the bottom of the substrate tunnel is highlighted in yellow sticks. Amino acid residues involved in shaping the substrate tunnel are shown as red sticks (V581, I393 and W330). Oxygen inside the amino acid side chains are colored in red and nitrogen in blue

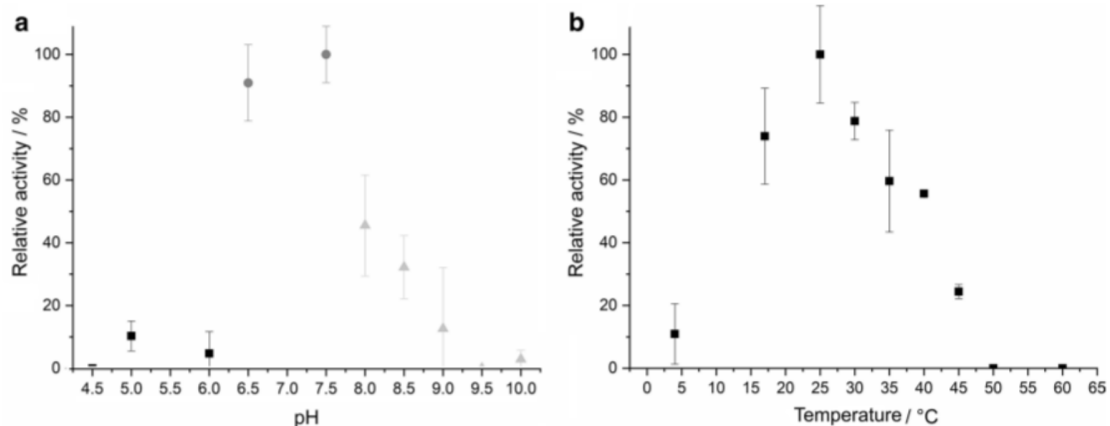
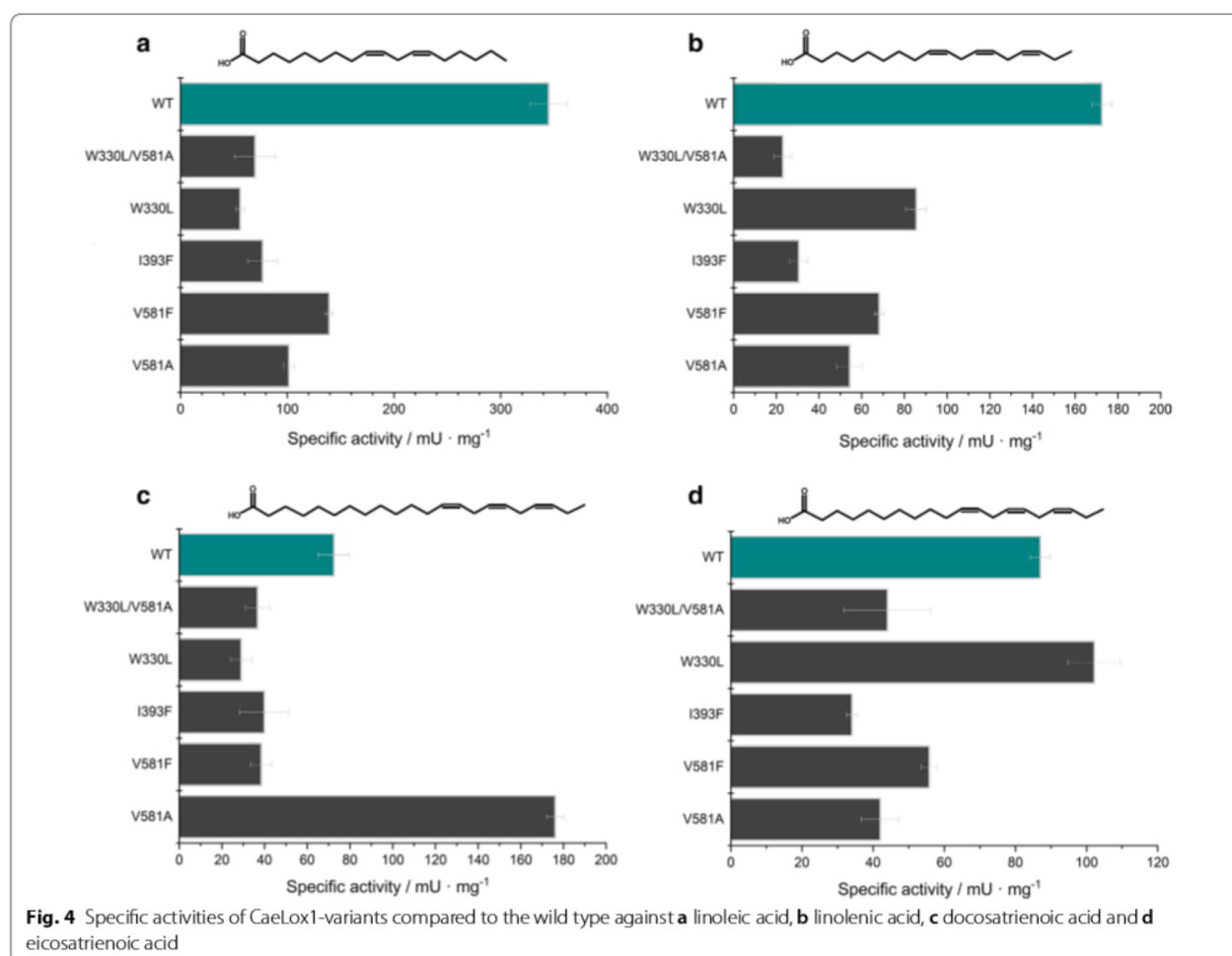


Fig. 3 Effects of pH (**a**) and temperature (**b**) on CaeLox1 activity. buffers used: 50 mM acetate (squares) from pH 4.5–6.0, 50 mM phosphate (circles) from pH 6.5–7.5, 50 mM borate (triangles) from pH 8.0–10.0

showed no difference in activity towards linolenic acid but a ~6-fold decrease towards the longer arachidonic acid (Hughes et al. 2001). This is partly in accordance with our results, since we were able to show spacing at this position (corresponds to W330 in CaeLox1) plays a beneficial role for the C-20(ω -3)-PUFA eicosatrienoic acid. By combining the mutations V581A and W330L to the V581A/W330L variant, the beneficial effects of

the single mutations for C-20-22(ω -3)-PUFAs seem to neutralize each other (Fig. 4c, d). This demonstrates the challenges in efficient protein engineering of lipoxygenases. Due to the long carbon chain of fatty acids, a large number of substrate conformations, their interactions with the residues of the tunnel as well as physicochemical effects have to be taken into account which makes a general prediction of important amino acid



residues in the substrate tunnel difficult. Besides the mentioned studies, no other mutagenesis studies with long chain PUFAs are existent.

Acknowledgements

We thank Niklas Broel and Alexander Atamasov for their support in the experiments.

Authors' contributions

DK, MG and MR conceived and designed research. DK and MG conducted experiments. DK analyzed data. DK, MG and MR wrote the manuscript. All authors read and approved the manuscript.

Funding

Open Access funding enabled and organized by Projekt DEAL. Not applicable.

Availability of data and materials

All relevant data for this article are included within this manuscript. The GenBank accession number for the *LOX1* gene is MW013781.

Consent of publication

Not applicable.

Competing interests

No relevant financial or non-financial competing interests are to report.

Author details

¹ Institute of Food Chemistry and Food Biotechnology, Justus-Liebig University Giessen, Institute of Food Chemistry and Food Biotechnology, Heinrich-Buff Ring 17, Giessen, Hesse 35392, Germany. ² Fraunhofer Institute for Molecular Biology and Applied Ecology IME Branch for Bioresources, Department of Biology and Chemistry, Justus-Liebig University Giessen, Institute of Food Chemistry and Food Biotechnology, Heinrich-Buff Ring 17, Giessen, Hesse 35392, Germany.

Received: 26 October 2020 Accepted: 16 February 2021

Published online: 04 March 2021

References

- An JU, Hong SH, Oh DK (2018) Regiospecificity of a novel bacterial lipoxygenase from *Myxococcus xanthus* for polyunsaturated fatty acids. *Biochim Biophys Acta Mol Cell Biol Lipids* 8:823–833
- Borngräber S, Browner M, Gillmor S, Gerth C, Anton M, Fletterick R, Kühn H (1999) Shape and specificity in mammalian 15-Lipoxygenase active site. *J Biol Chem* 52:37345–37350
- Brodhun F, Feussner I (2011) Oxylipins in fungi. *FEBS J* 278:1047–1063
- Brodhun F, Cristobal-Sarramian A, Zabel S, Newie J, Hamberg M, Feussner I (2013) An α -linolenic acid specific hydroperoxidase activity from *Fusarium oxysporum*. *PLoS ONE* e64919

- Gand M, Thöle C, Müller H, Brundiek H, Bashiri G, Höhne M (2016) A NADH-accepting imine reductase variant: Immobilization and cofactor regeneration by oxidative deamination. *J Biotechnol* 230:11–18
- Gasteiger E, Hoogland C, Gattiker A, Duvaud S, Wilkins M, Appel RD, Bairoch A (2005) Protein Identification and Analysis Tools on the ExPASy Server. In: Ed.: John M, Walker The Proteomics Protocols Handbook. Humana Press, Totowa New Jersey
- Guex N, Peitsch MC, Schwede T (2009) Automated comparative protein structure modeling with SWISS-MODEL and swiss-PdbViewer: A historical perspective. *Electrophoresis* 30:162–173
- Hornung E, Kunze S, Liavonchanka A, Zimmermann G, Kühn D, Fritsche K (2008) Identification of an amino acid determinant of pH regioselectivity in a seed lipoxygenase from *Momordica charantia*. *Phytochemistry* 69:2774–2780
- Hughes RK, Lawson DM, Hornostay AR, Fairhurst SA, Casey R (2001) Mutagenesis and modelling of linoleate binding pea seed lipoxygenase. *Eur J Biochem* 268:1030–1040
- Karrer D, Rühl M (2019) A new lipoxygenase from the agaric fungus *Agrocybe aegerita*: Biochemical characterization and kinetic properties. *PLoS ONE* 15:e0218625
- Kuribayashi T, Kaise H, Uno C, Hara T, Hayakawa T, Joh T (2002) Purification and characterization of lipoxygenase from *Pleurotus ostreatus*. *J Agric Food Chem* 50:1247–1253
- Leonhardt R-B, Plagemann I, Linke D, Zelena K, Berger RG (2013) Orthologous lipoxygenases of *Pleurotus* spp. – A comparison of substrate specificity and sequence homology. *J Mol Catal B: Enzym* 97:189–195
- Liavonchanka A, Feussner I (2006) Lipoxygenases: occurrence, functions and catalysis. *J Plant Physiol* 163:348–357
- Plagemann I, Zelena K, Arendt P, Ringel PD, Krings U, Berger R (2013) LOXPsa1, the first recombinant lipoxygenase from a basidiomycete fungus. *J Mol Catal B: Enzym* 8/99–104
- Pettersen EF, Goddard TD, Huang CC, Couch GS, Greenblatt DM, Meng EC, Ferrin TE (2004) UCSF Chimera - a visualization system for exploratory research and analysis. *J Comput Chem* 25:1605–1612
- Ruddat VC, Mogul R, Chorny I, Chen C, Perrin N, Whitman S, Kenyon V, Jacobson MP, Bernasconi CF, Holman TR (2004) Tryptophane 500 and arginine 707 define product and substrate active site binding in soybean lipoxygenase-1. *Biochemistry* 41:13063–13071
- Trott O, Olson AJ (2010) AutoDock Vina: improving the speed and accuracy of docking with a new scoring function, efficient optimization and multi-threading. *J Comput Chem* 2010 31:455–461

Publisher's note

Springer Nature remains neutral with regard to jurisdictional claims in published maps and institutional affiliations.

Submit your manuscript to a SpringerOpen® journal and benefit from:

- Convenient online submission
- Rigorous peer review
- Open access: articles freely available online
- High visibility within the field
- Retaining the copyright to your article

Submit your next manuscript at ► [springeropen.com](https://www.springeropen.com)

**2.4 Publication 4: Biotransformation of
[U-¹³C]linoleic acid suggests two independent
ketonic- and aldehydic cycles within C8-oxylin
biosynthesis in *Cyclocybe aegerita* (V. Brig.)
Vizzini**

Dominik Karrer, Vanessa Weigel, Nikolas Hoberg, Alexander Atamasov, Dr.
Martin Rühl

Mycological Progress (2021), 20, 929-940.

DOI: 10.1007/s11557-021-01719-3



Biotransformation of [U-¹³C]linoleic acid suggests two independent ketonic- and aldehydic cycles within C8-oxylipin biosynthesis in *Cyclocybe aegerita* (V. Brig.) Vizzini

Dominik Karrer¹ · Vanessa Weigel¹ · Nikolas Hoberg¹ · Alexander Atamasov¹ · Martin Rühl^{1,2}

Received: 13 May 2021 / Revised: 15 June 2021 / Accepted: 16 June 2021
© The Author(s) 2021

Abstract

Although the typical aroma contributing compounds in fungi of the phylum Basidiomycota are known for decades, their biosynthetic pathways are still unclear. Amongst these volatiles, C8-compounds are probably the most important ones as they function, in addition to their specific perception of fungal odour, as oxylipins. Previous studies focused on C8-oxylipin production either in fruiting bodies or mycelia. However, comparisons of the C8-oxylipin biosynthesis at different developmental stages are scarce, and the biosynthesis in basidiospores was completely neglected. In this study, we addressed this gap and were able to show that the biosynthesis of C8-oxylipins differs strongly between different developmental stages. The comparison of mycelium, primordia, young fruiting bodies, mature fruiting bodies, post sporulation fruiting bodies and basidiospores revealed that the occurrence of the two main C8-oxylipins octan-3-one and oct-1-en-3-ol distinguished in different stages. Whereas oct-1-en-3-ol levels peaked in the mycelium and decreased with ongoing maturation, octan-3-one levels increased during maturation. Furthermore, oct-2-en-1-ol, octan-1-ol, oct-2-enal, octan-3-ol, oct-1-en-3-one and octanal contributed to the C8-oxylipins but with drastically lower levels. Biotransformations with [U-¹³C]linoleic acid revealed that early developmental stages produced various [U-¹³C]oxylipins, whereas matured developmental stages like post sporulation fruiting bodies and basidiospores produced predominantly [U-¹³C]octan-3-one. Based on the distribution of certain C8-oxylipins and biotransformations with putative precursors at different developmental stages, two distinct biosynthetic cycles were deduced with oct-2-enal (aldehydic-cycle) and oct-1-en-3-one (ketonic-cycle) as precursors.

Keywords Lipoxygenase · 1-octen-3-ol · 3-octanone · Mushroom aroma · Linoleic acid

Introduction

Volatile compounds like oct-2-en-1-ol (**1**), octan-1-ol (**2**), oct-2-enal (**3**), octanal (**4**), octan-3-ol (**5**), oct-1-en-3-ol (**6**), oct-1-en-3-one (**7**) and octan-3-one (**8**) are known as the main C8-oxylipins from which octan-3-ol (**5**), oct-1-en-3-ol (**6**), oct-1-en-3-one (**7**) and octan-3-one (**8**) are the predominant C8-oxylipins contributing to the characteristic

mushroom aroma (Kleofas et al., 2014; Malheiro et al., 2013; Matsui et al., 2003; Tressl et al., 1982). Although these oxylipins are known for several decades, their biosynthesis is scarcely understood. It is widely accepted that these oxylipins are lipoxygenase-derived metabolites, which play an important role, e.g. in sporulation, sexual and asexual life cycle or act as infochemicals (Brodhun & Feussner 2011; Holighaus et al., 2014). The proposed steps of the C8-oxylipin pathway in mushrooms are the oxygenation of polyunsaturated fatty acids (PUFA) by lipoxygenases (LOX) with a subsequent cleavage by hydroperoxide lyases (HPL) (Combet et al., 2006). In higher fungi of the phyla Basidiomycota and Ascomycota, the C18-PUFA (9Z,12Z)-Octadeca-9,12-dienoic acid (subsequently stated with the trivial name linoleic acid) is the predominant fatty acid (Brodhun and Feussner, 2011). This indicates that the oxygenation of linoleic acid by LOX is the initial step in oxylipin biosynthesis. LOX targets a (1Z,4Z)-pentadiene motif in linoleic acid

Section editor: Marc Stadler.

✉ Martin Rühl
martin.ruehl@uni-giessen.de

¹ Institute of Food Chemistry and Food Biotechnology, Justus Liebig University Giessen, Giessen, Hesse, Germany

² Fraunhofer Institute for Molecular Biology and Applied Ecology IME Business Area Bioresources, Giessen, Hesse, Germany

and produces either 13-hydroperoxy-9,11-octadecadienoic acid (13-HPOD) or 9-hydroperoxy-10,12-octadecadienoic acid (9-HPOD), via radical rearrangements and the insertion of molecular oxygen. Until now, only three LOX-type enzymes from Basidiomycota have been characterised that mainly produce 13-HPOD (Karrer & Rühl 2019; Kuribayashi et al., 2002; Plagemann et al., 2013). Although homogenates of *Aspergillus* species converted linoleic acid into 8-hydroperoxy-9,12-octadecadienoic acid (8-HPOD) and 5*S*,8*R*-dihydroxy octadecadienoic acid (5,8-diHODE) as major products, 10*R*-hydroperoxy-8,12-octadecadienoic acid (10*R*-HPOD) and 10*R*-hydroxy-8,12-octadecadienoic acid (10*R*-HODE) have been detected as minor products. The characterisation of the precocious sexual inducer (psi) factor producing genes (*ppoA*, *ppoB* and *ppoC*) revealed that *ppoC* from *A. nidulans* encodes for a 10*R*-dioxygenase (10-DOX), which mainly produces 10-HPOD (Brodhun et al., 2010). Nonetheless, LOX/DOX that oxygenate linoleic acid to 10-HPOD in Basidiomycota yet have to be found. Several studies showed that homogenates of fruiting bodies from Basidiomycota produce a variety of C8-oxylipins and are able to convert linoleic acid (Assaf et al., 1995; Husson et al., 2001; Wurzenberger & Grosch 1982). Remarkably, the most detected oxylipins in fruiting bodies include high amounts of compounds 5–8 (Cruz et al., 1997; Li et al., 2016; Mau et al., 1997). The C8-oxylipins 1–4 are represented more unregularly with notably lower amounts in fruiting bodies from which either oct-2-en-1-ol (1) and octan-1-ol (2) or oct-2-enal (3) and octanal (4) are predominant (Cho et al. 2006, Li et al., 2016; Matsui et al., 2003; Mau et al., 1997).

Furthermore, the comparison of the volatile composition at different developmental stages or parts focused mainly on oct-1-en-3-ol (6) or, in case several C8-oxylipins have been analysed, was limited to fruiting bodies. However, when different developmental stages of fruiting bodies from fungi of the phylum Basidiomycota were observed, maturation was accompanied with vigorous variations in the occurrence of mainly compounds 5–8 while compounds 1–4 seem to undergo minor variations (Cho et al. 2006, Li et al., 2016; Matsui et al., 2003; Mau et al., 1997). Unfortunately, all studies lack a comparison of the C8-oxylipin composition at different stages of the fungal life cycle. So far, differences in the occurrence of C8-oxylipins were only shown for fruiting bodies, where different maturity stages of the basidiocarp were investigated. An exception is the recently published work on the volatilome of *Cyclocybe aegerita* (V. Brig.) Vizzini, where different stages during fructification have been analysed. Nevertheless, C8-oxylipin biosynthesis in basidiospores was completely neglected, and only oct-1-en-3-ol (6) and octan-3-one (8) have been detected (Orban et al., 2020). In this study, this gap is addressed, and the C8-oxylipin composition as well

as the C8-oxylipin-biosynthesis via biotransformations with [U-¹³C]labeled linoleic acid to C8-oxylipins in mycelium, primordia, immature fruiting bodies, mature fruiting bodies, basidiospores and fully mature fruiting bodies after sporulation within the mushroom *C. aegerita*, used as a model fungus (Frings et al., 2020), is investigated. Additionally, the fatty acid composition between different morphological stages is compared.

Materials and methods

Chemicals

All chemicals were commercially obtained and used without further treatment. [U-¹³C] linoleic acid (99% ¹³C, 97% pure) was purchased from Sigma-Aldrich (St. Louis, USA).

Fungal cultivation and harvesting

For mycelium propagation, 1.5% malt-extract-agar was used. High petri-dishes with 1.5% malt-extract were inoculated with an *C. aegerita* AAE-3 (Herzog et al., 2016) mycelium-overgrown circular agar slice (diameter 0.5 cm) and incubated at 24 °C in darkness until it reached the edge of the petri-dishes. The obtained mycelium was gently removed from the agar-plate and used subsequently for volatile measurements and biotransformations without storage or any other treatment. For fruiting, the overgrown petri-dishes were further cultivated at 24 °C with a 12 h dark/night shift at 95% relative air humidity (Rumed-Rubarth Apparate GmbH, Laatzen, Germany) until the desired developmental stage was obtained. Primordia, immature fruiting bodies with closed caps and post sporulation fruiting bodies were harvested with a scalpel, sliced and immediately used for further experiments. Basidiospores of *C. aegerita* were harvested by cultivation of substrate blocks with immature fruiting bodies (provided by druid-Austernpilze, Ottrau, Germany) at 24 °C in a 12 h dark/night shift at 85% relative air humidity in a climate chamber until sporulation. Dropped basidiospores were gently isolated from the fruiting bodies without damaging them and used for further measurements. Images of the different developmental stages were taken with a Samsung 32 MP camera. Microscopic images were taken using an Olympus microscope BX43 (Olympus Europa SE & CO. KG, Hamburg, Germany) with 20× and 100× magnification equipped with a SC50 (5.0 MP) camera.

Biotransformations and gas chromatography

For biotransformation, one of the following substrates [U-¹³C]linoleic acid, (*E*)-oct-2-en-1-ol (1), octan-1-ol (2), (*E*)-oct-2-enal (3), octanal (4), octan-3-ol (5), oct-1-en-3-ol

(6), oct-1-en-3-one (7) or octan-3-one (8) with a final concentration of 50 μM were incubated with either mycelium, primordia, immature fruiting bodies, mature fruiting bodies, post sporulation fruiting bodies or basidiospores in 50 mM phosphate buffer (pH 7.5) in a headspace-vial at room temperature. All experiments have been conducted in triplicates. For volatile composition measurements, the fungal parts were soaked in 50 mM phosphate buffer and immediately used for GC-analysis. The resulting products were extracted for 30 min at 30 °C by a solid phase microextraction (SPME) fibre (polydimethylsiloxane/divinylbenzene). After extraction, the volatiles were desorbed in the GC inlet at 250 °C. Analysis was carried out on a Agilent Technologies 7890A GC-system (Santa Clara, USA), equipped with a VFwax column (30 m \times 0.25 mm \times 0.25 μm film thickness, Santa Clara, USA) operated in splitless or 1/50 split mode under the following parameters: carrier gas, He with a constant flow of 1.2 mL \cdot min⁻¹. Oven temperature was at 40 °C (3 min), 5 °C \cdot min⁻¹ to 240 °C and hold for 7 min. The mass spectrometer operated in electron impact mode with an electron energy of 70 eV and scanned in a range of m/z 33–300.

C8-oxylipin identification and quantification

C8-oxylipins were identified by using authentic standards. Furthermore, the identities were confirmed by their characteristic fragmentation pattern based on standards and the National Institute of Standards and Technology (NIST) Chemistry WebBook. All oxylipins were measured in the headspace of commercial vials. To avoid contaminations and minimise known discriminations of headspace compositions by internal standards or other supplemented compounds, no internal standard was added.

Fatty acid analysis

Fatty acid extraction was carried out via homogenation of the samples with N₂(liq), followed by the addition of 3 mL *n*-hexane. The mixture was incubated for 20 min at room temperature. Cell debris were removed by centrifugation for 10 min at 4,063 g. Fatty acid containing organic phase was removed from the aqueous phase and concentrated to ~1 mL via a rotary evaporator. Next, 4 mL 0.5 M methanolic NaOH-solution was added to the concentrated extract, followed by incubation for 10 min at 80 °C. For methylation, 3.5 mL 20% methanolic boron trifluoride was added to the extract and incubated for another 5 min at 80 °C. After the mixture was cooled down, 5 mL saturated NaCl-solution was added. The organic phase was separated, dried over anhydrous Na₂SO₄ and analysed via GC–MS using a VFwax column (30 m \times 0.25 mm \times 0.25 μm film thickness, Santa Clara, USA) operating in splitless mode under the following parameters: carrier gas, He with a constant flow of 1.2 mL \cdot

min⁻¹. Oven temperature was at 40 °C (3 min), 3 °C \cdot min⁻¹ to 240 °C and hold for 12 min. The mass spectrometer operated in electron impact mode with an electron energy of 70 eV and scanned in a range of m/z 33–300. Fatty acids were identified by their characteristic fragmentation pattern based on authentic standards and the National Institute of Standards and Technology (NIST) Chemistry WebBook.

Data processing

The peak areas of the identified C8-oxylipins were used to determine the relative amount of the respective substance. Each relative peak area of a detected C8-oxylipin at a certain developmental stage was added up and considered 100%, meaning that the peak area of a certain C8-oxylipin correlates to the added up peak areas. This approach enables an appropriate overview of the C8-oxylipin composition. Additionally, means of the peak area of a certain C8-oxylipin were expressed as AU/g of fresh weight tissue to display the occurrence of each C8-oxylipin at different developmental stages to distinguish between the relative composition of C8-oxylipins and the actual levels. The processed data were used to generate the heatmaps using OriginPro (OriginLab Corporation, Northampton, MA, USA).

Results

Endogenous C8-oxylipin composition and biotransformation of [U-¹³C]linoleic acid

The composition of endogenous C8-oxylipins at different developmental stages were analysed by means of SPME-GC/MS peak areas. To verify which developmental stage produced the highest amount of a certain C8-oxylipin, the obtained peak areas were expressed as arbitrary units per gram of fresh weight tissue (AU/g ft) (Fig. 1). Measuring the volatilome at different developmental stages only allows detection of accumulated C8-oxylipins prior to harvesting. Since we were also interested in the overall enzymatic activity towards linoleic acid conversion at a certain developmental stage, additional biotransformation experiments with [U-¹³C]linoleic acid were carried out to provide informations on enzymatically produced [U-¹³C]C8-oxylipins and conceivable induction of the endogenous biosynthesis. In total, eight C8-oxylipins were identified, which eluted as a mixture of endogenous and [U-¹³C]-labeled compounds (Fig. 2).

The highest AU/g ft of oct-2-en-1-ol (1), octan-1-ol (2), oct-1-en-3-ol (6), oct-1-en-3-one (7) and octan-3-one (8) was detected in mycelial samples followed by a striking decrease at the primordial stage. With ongoing maturation, the levels of most C8-oxylipins recovered in immature fruiting bodies

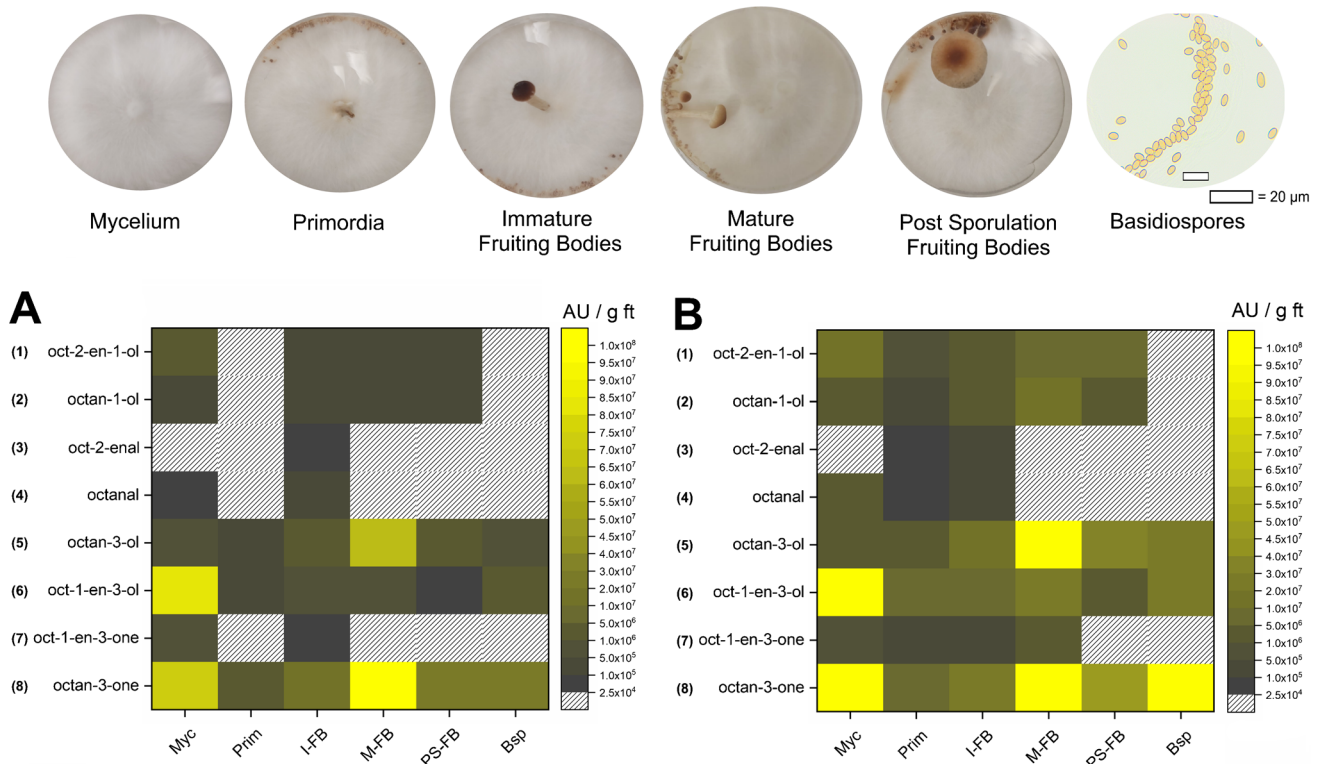


Fig. 1 Various developmental stages of *C. aegerita* that were used for SPME-GC/MS measurements and biotransformations with [^{13}C]linoleic acid. Endogenous C8-oxylipin occurrence is shown as arbitrary units per gram of fresh weight (AU/g ft) (A). C8-oxylipin occurrence after biotransformation of [^{13}C]linoleic acid is shown as arbitrary

units per gram of fresh weight (AU/g ft) (B). Myc=mycelium, Prim=Primordia, I-FB=immature fruiting bodies, M-FB=mature fruiting bodies, PS-FB=post sporulation fruiting bodies, Bsp=basidiospores (Fig. 1). Dashed boxes = not detected/low peak area

and decreased afterwards. An exception was octan-3-one (8), which steadily increased or remained at high levels after the primordial stage (Fig. 1A). C8-aldehydes were only detected at two stages being most present in immature fruiting bodies (Fig. 1A). Octan-3-ol (5) was detected throughout all developmental stages, starting with low levels in the mycelium and primordia, followed by an increased extent in immature and mature fruiting, and decreased thereafter. Addition of [^{13}C]linoleic acid resulted in a pattern comparable to non-treated fungal tissue for oct-2-en-1-ol (1), oct-1-en-3-ol (6), oct-1-en-3-one (7) and octan-3-one (8) (Fig. 1B). Interestingly, primordia were able to produce low levels of compounds 1–4 and oct-1-en-3-one (7) from [^{13}C]linoleic acid, although no endogenous production was detected (Fig. 1A). Surprisingly, mature and post sporulation fruiting bodies produced slightly more octan-1-ol (2) than mycelium after incubation, which is opposing to the naturally occurring levels (Fig. 1A, B). Somewhat comparable results were obtained for octanal (4) and octan-3-ol (5) production of non-treated and incubated fungal tissue. Although highest endogenous octanal levels were detected in immature fruiting bodies, after incubation with [^{13}C]linoleic acid mycelium produced higher levels of octanal than

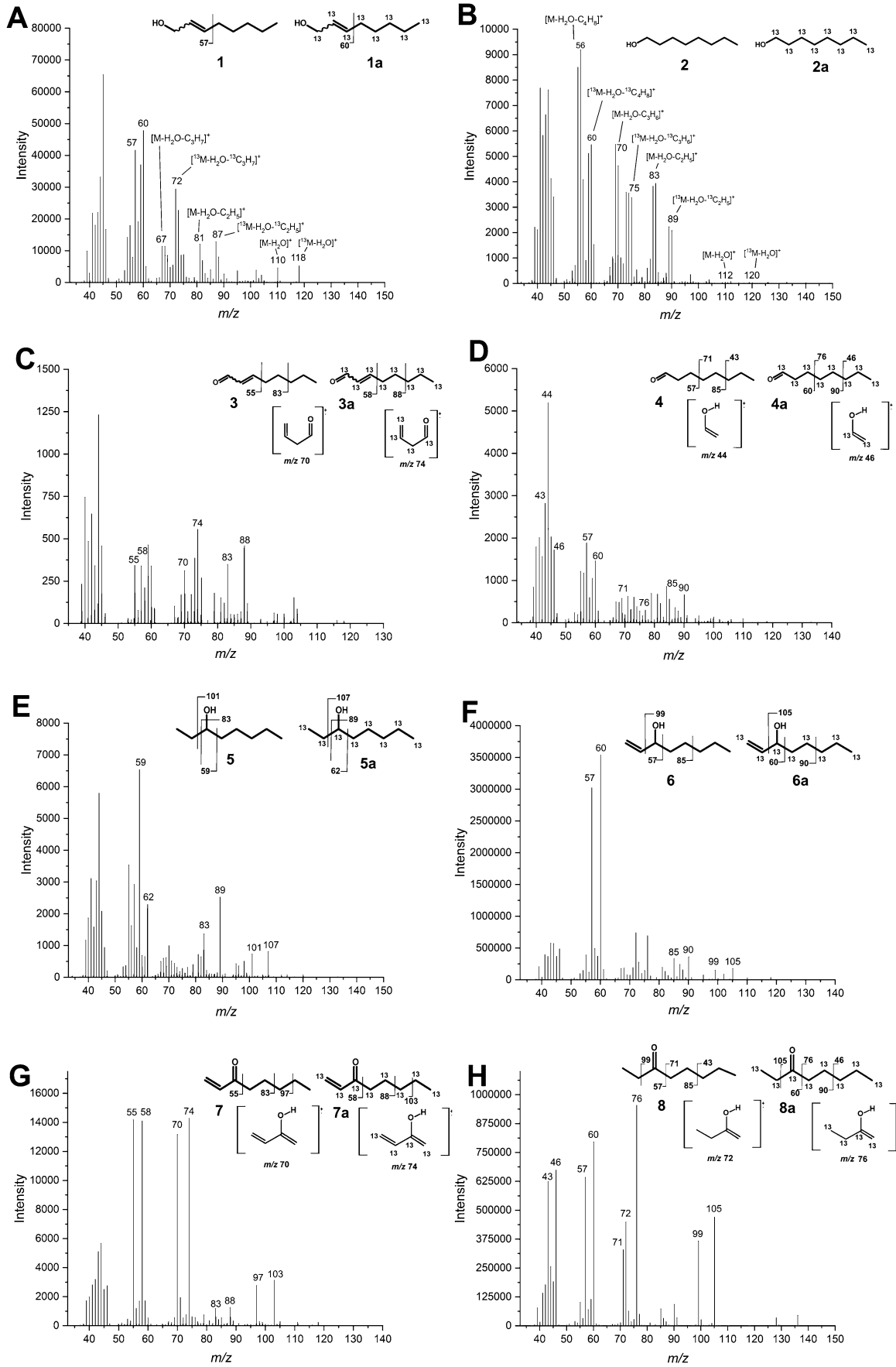
immature fruiting bodies (Fig. 1A, B). Levels of octan-3-ol (5) increased with ongoing maturity when [^{13}C]linoleic acid was added to the fungal tissue. This is also opposing the endogenous occurring levels (Fig. 1A, B).

Effects of putative precursors on oxylipin composition

Based on an emerged pattern of mutual occurring C8-oxylipins, especially between primordia and immature fruiting bodies, the hypothesis that certain C8-oxylipins derive from putative short chain precursors, oct-2-enal (3) or oct-1-en-3-one (7), has been evaluated via additional biotransformation experiments (Fig. 3).

Primordia showed a completely different C8-oxylipin pattern when oct-2-enal (3) or oct-1-en-3-one (7) was added.

Fig. 2 Mass spectra of the co-eluted endogenous and [^{13}C]labeled C8-oxylipins. Characteristic fragmentations pattern of **A** oct-2-en-1-ol (1), [^{13}C]oct-2-en-1-ol (1a). **B** octan-1-ol (2), [^{13}C]octan-1-ol (2a). **C** oct-2-enal (3), [^{13}C]oct-2-enal (3a). **D** octanal (4), [^{13}C]octanal (4a). **E** octan-3-ol (5), [^{13}C]octan-3-ol (5a). **F** oct-1-en-3-ol (6), [^{13}C]oct-1-en-3-ol (6a). **G** oct-1-en-3-one (7), [^{13}C]oct-1-en-3-one (7a). **H** octan-3-one (8), [^{13}C]octan-3-one (8a)



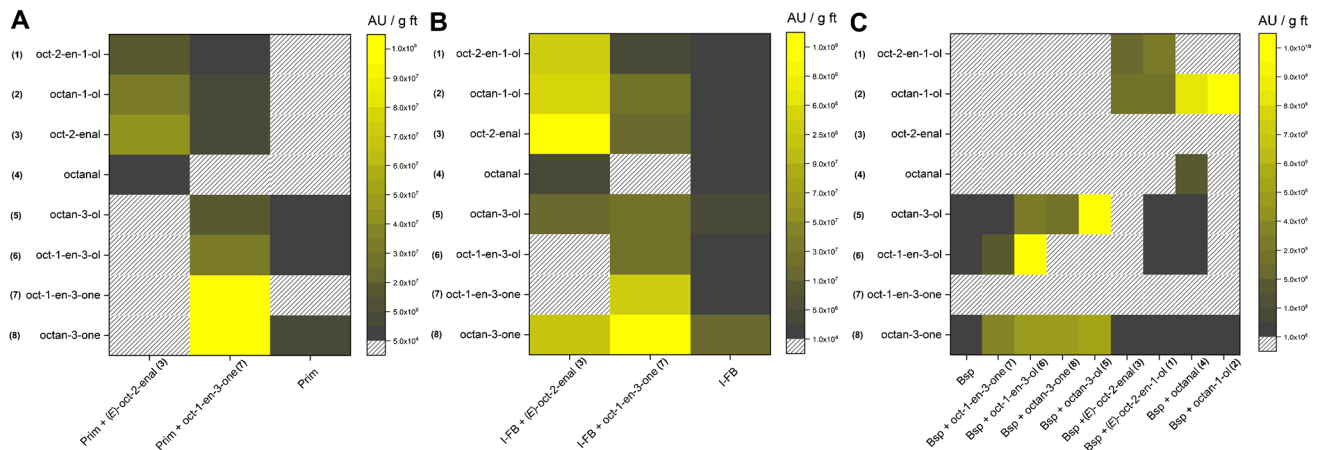


Fig. 3 Influence of different C8-oxylipins on their composition at different developmental stages. Means of SPME-GC/MS peak areas were expressed as arbitrary units per gram of fresh weight tissue

(AU/g ft). **A** Prim=primordia, **B** I-FB=immature fruiting bodies, **C** Bsp=basidiospores. Dashed boxes=not detected or low peak area ($<5 \cdot 10^4$ AU/g ft)

Addition of oct-1-en-3-one (7) led to strikingly increased levels of octan-3-ol (5), oct-1-en-3-ol (6) and octan-3-one (8), while addition of oct-2-enal (3) led to a drastic increase of oct-2-en-1-ol (1), octan-1-ol (2) and octanal (4), compared to the endogenously produced C8-oxylipin composition (Fig. 1, Fig. 3A). A similar pattern was observed in immature fruiting bodies with a strong increase of octan-3-ol (5), oct-1-en-3-ol (6) and octan-3-one (8) when oct-1-en-3-one (7) was added. However, an increase of oct-2-en-1-ol (1) and octan-1-ol (2) with oct-2-enal (3) as a substrate was detected (Fig. 3B). Due to the small number of endogenously produced C8-oxylipins, basidiospores showed the lowest endogenous background. Therefore, they were used for a more detailed investigation of the C8-oxylipin pathway using various substrates for additional biotransformation experiments. In basidiospores, a complete conversion of oct-1-en-3-one (7) to octan-3-one (8), oct-1-en-3-ol (6) and octan-3-ol (5) was observed (Fig. 3C), whereas oct-1-en-3-ol (6) was converted to octan-3-ol (5) and octan-3-one (8) but in drastically lower levels. A weak reduction of octan-3-one (8) resulted in a slight increase of octan-3-ol (5), while the reversed oxidation of octan-3-ol (5) to octan-3-one (8) was also detected (Fig. 3C). Just like oct-1-en-3-one (7), oct-2-enal (3) was completely transformed resulting in high octan-1-ol (2) and oct-2-en-1-ol (1) levels. Furthermore, basidiospores reduced octanal (4) to octan-1-ol (2) and the addition of oct-2-en-1-ol (1) led to increased octan-1-ol (2) levels, whereas octan-1-ol (2) was not converted (Fig. 3C).

Free fatty acid composition at different developmental stages

Due to the fact that fatty acids are the precursors of C8-oxylipins, the free fatty acid composition between mycelium, immature fruiting bodies, mature fruiting bodies and

basidiospores was investigated. The analysed fatty acids were grouped into saturated fatty acids (SFA), monounsaturated fatty acids (MUFA) and polyunsaturated fatty acids (PUFA) of which palmitic acid (hexadecanoic acid, 16:0) was the most prominent SFA and linoleic acid ((9Z,12Z)-Octadeca-9,12-dienoic acid, 18:2 (9Z, 12Z)) the most prominent PUFA. Regarding MUFA, oleic acid ((9Z)-Octadeca-9-enoic acid, 18:1 (9Z)) and *cis*-vaccenic acid ((11Z)-Octadec-11-enoic acid, 18:1 (11Z)) were similarly distinctive (Table 1).

In the mycelium and fruiting body samples, the fatty acid composition was alike (Table 1). However, the ratio of SFA and MUFA increased by ~15% with ongoing maturation. Simultaneously, the linoleic acid ratio decreased with

Table 1 Fatty acid composition in % at various developmental stages. SFA saturated fatty acids, MUFA monounsaturated fatty acids, PUFA polyunsaturated fatty acids. Myc mycelium, I-FB immature fruiting bodies, M-FB mature fruiting bodies, Bsp basidiospores

Fatty acid	Myc / %	I-FB / %	M-FB / %	Bsp / %
14:0	0.4 ± 0.0	0.2 ± 0.0	0.1 ± 0.0	0.6 ± 0.0
15:0	0.3 ± 0.1	1.2 ± 0.1	2.8 ± 0.1	0.4 ± 0.0
16:0	19.0 ± 0.7	20.0 ± 0.3	23.4 ± 0.2	34.8 ± 1.0
17:0	-	0.2 ± 0.1	0.2 ± 0.0	-
18:0	1.1 ± 0.1	2.4 ± 0.2	0.9 ± 0.1	2.5 ± 0.1
SFA*	21%	24%	27%	38%
16:1 (11Z)	-	0.3 ± 0.1	0.4 ± 0.0	-
18:1 (9Z)	1.4 ± 0.0	3.4 ± 0.3	3.5 ± 0.1	18.7 ± 0.6
18:1 (11Z)	1.3 ± 0.0	4.2 ± 0.3	7.2 ± 0.2	1.6 ± 0.0
MUFA*	3%	8%	11%	20%
18:2 (9Z, 12Z)	76.5 ± 0.6	68.2 ± 0.6	61.6 ± 0.2	41.4 ± 0.4
20:2 (11Z, 14Z)	-	0.1 ± 0.1	-	-
PUFA*	77%	68%	62%	41%

* = summated and rounded values of the corresponding fatty acids. Significance can be calculated from the data above

maturation. In basidiospores, the fatty acid composition was drastically different compared to the other analysed compartments. SFA, especially palmitic acid rose to ~35% while linoleic acid accounted for only ~41%. Furthermore, oleic acid soared to ~19% in basidiospores (Table 1).

Discussion

C8-oxylipin composition

Unlike prior studies in which oct-1-en-3-ol (**6**) was the predominant volatile in basidiomycetous mycelium or fruiting body homogenates (Akakabe et al., 2005, Cho et al. 2006, Cruz et al., 1997, Li et al., 2016, Matsui et al., 2003, Tressl et al., 1982), the most abundant C8-oxylipins in *C. aegerita* throughout all developmental stages was octan-3-one (**8**). This discrepancy is mainly caused due to the used extraction and homogenation method, which is often overlooked. This becomes clear in studies of Combet et al., (2009) and Rapior et al., (1998), who compared either homogenised, sliced and whole samples of fruiting bodies of *A. bisporus* or different extraction methods of fruiting bodies of *C. aegerita*, respectively. Disruption of fungal tissue could lead to the release of membrane bound fatty acids, interfering with endogenous formation and, thus, complicate the understanding of C8-oxylipin biosynthesis. Moreover, cellular compartments could also be harmed and, thus, might trigger the formation and release of C8-oxylipins (Combet et al., 2009). While homogenised samples and liquid extraction led to higher production of oct-1-en-3-ol (**6**), headspace measurements of whole or sliced samples showed higher octan-3-one (**8**) levels (Combet et al., 2009). Previous studies focused on disruption and liquid extraction methods and consequently found oct-1-en-3-ol (**6**) as the main C8-oxylipin in different fungal species. Nonetheless, the variety of different C8-oxylipins (up to eight) detected in these studies is widely in accordance with our findings (Akakabe et al., 2005, Cho et al. 2006, Cruz et al., 1997, Li et al., 2016, Matsui et al., 2003, Tressl et al., 1982).

Although octan-3-one is the predominant oxylipin in this study and not oct-1-en-3-ol (**6**), both were detected throughout all developmental stages emphasising their biological importance. Electroantennographic experiments showed that the fungivorous beetle *Bolitophagus reticulatus* is able to differentiate between the most common C8-oxylipins to assess host quality (Holighaus et al., 2014). Here, oct-1-en-3-ol (**6**) acts as repellent and octan-3-one (**8**) as attractant. Contradictory, the three wood-living generalist beetles *Malthodes fuscus*, *Anaspis marginicollis*, *Anaspis rufilabris* and the moth *Epinotia tedella* were attracted to oct-1-en-3-ol (**6**), whereas the

generalist predator on fungus-insects *Lordithon lunulatus* distinguished between oct-1-en-3-ol (**6**) and octan-3-one (**8**) and was attracted by a mixture of both C8-oxylipins (Fäldt et al. 1998). Besides interspecies communication, C8-oxylipins might also operate as intra-species signals as shown in *Penicillium paneum* where oct-1-en-3-ol (**6**) functions as a self-inhibitor signal in spore germination (Schulz-Bohm et al., 2017). These studies reveal that C8-oxylipins have different functions and, consequently, their occurrence depends on the developmental stage of the fungus. To investigate the enzymatic potential of each developmental stage towards the production of different C8-oxylipins, [U-¹³C]linoleic acid has been added to different fungal tissues. The resulting [U-¹³C]C8-oxylipins co-eluted with the endogenous C8-oxylipins and, therefore, the detected mass spectra were a mixture of non-labeled α -cleavage fragmentations, McLafferty ions and their corresponding fragmentations with a ¹³C-mass shift (Fig. 2A–H).

Influence of linoleic acid on C8-oxylipin composition

In general, major differences in the production of [U-¹³C] C8-oxylipins were detected that indicates varying enzymatic activities at certain developmental stages (Fig. 1B). Especially the developmental process of fruiting bodies shows drastic morphology dependent C8-oxylipin production (Fig. 1). This is highlighted by the cluster-like occurrence of certain C8-oxylipins, noticeable particularly for compounds **5–8** in late developmental stages (Fig. 1B) and compounds **1–4** in early developmental stages (Fig. 1B). Since post sporulation fruiting bodies and basidiospores showed low oct-1-en-3-one (**7**) but increasing octan-3-one (**8**) production, accompanied with fairly consistent levels of octan-3-ol (**5**) and oct-1-en-3-ol (**6**), we propose the existence of a biocatalytic cycle with oct-1-en-3-one (**7**) as precursor defined as ketonic-cycle (oct-1-en-3-one-cycle) (Fig. 1, Fig. 4). In contrast, compounds **1–4** were predominantly detected in early developmental stages with decreasing contribution in more mature developmental stages. Therefore, we propose a second biocatalytic cycle with oct-2-enal (**3**) as precursor that is defined as aldehydic-cycle (oct-2-enal-cycle) (Fig. 1, Fig. 4).

In primordia, only three C8-oxylipins (octan-3-ol (**5**), oct-1-en-3-ol (**6**) and octan-3-one (**8**)) occurred endogenously, although primordia were able to produce all eight C8-oxylipins when [U-¹³C]linoleic acid was added (Fig. 1A, B). Interestingly, with the addition of [U-¹³C]linoleic acid to primordia, all C8-oxylipins were detected as non-labeled and [U-¹³C]compounds that indicates the induction of endogenous C8-oxylipin biosynthesis. In contrast, all eight C8-oxylipins emerged endogenously in immature fruiting bodies. Therefore, an upregulation of aldehydic- and

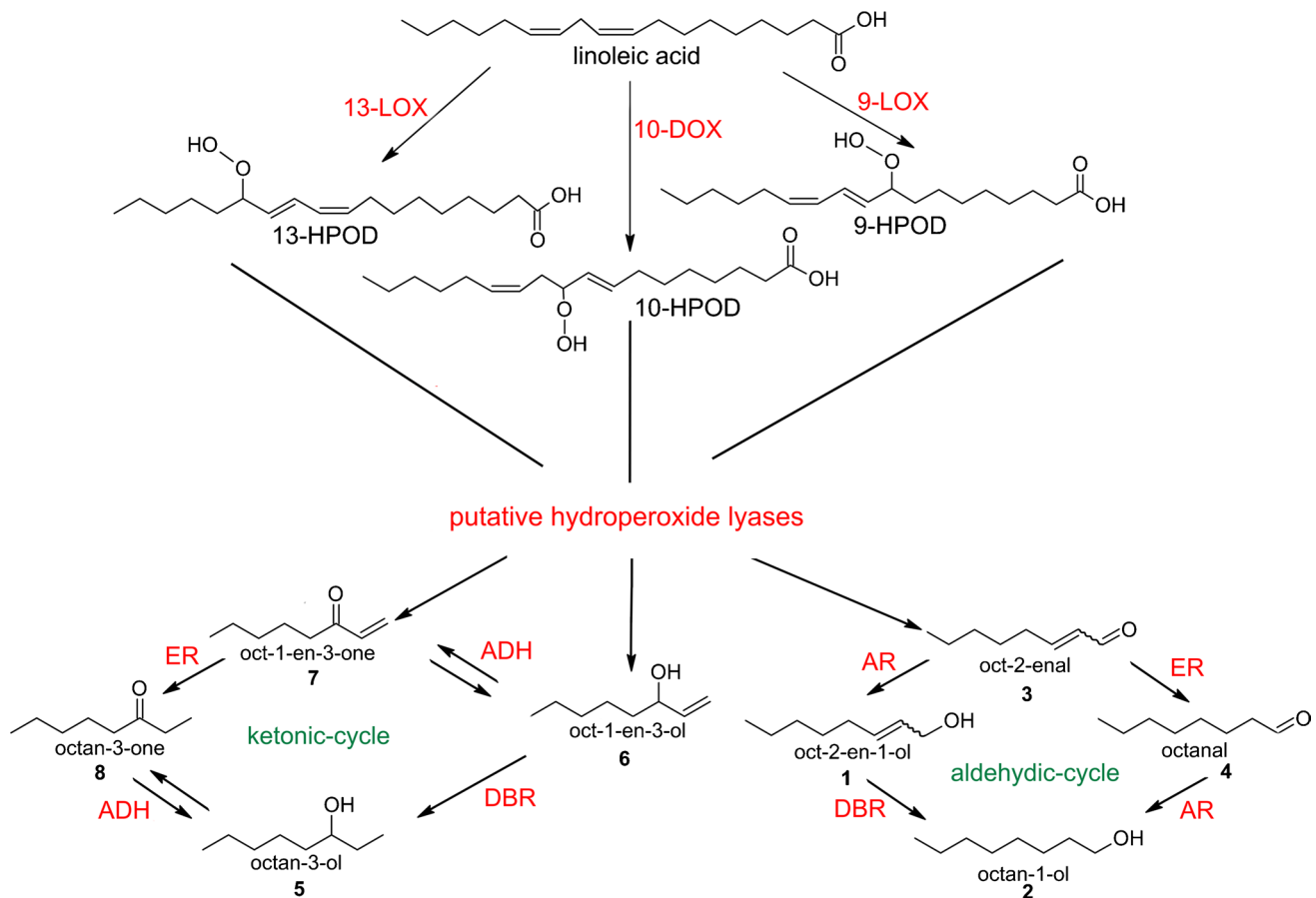


Fig. 4 Hypothetical C8-oxylipin pathway in Basidiomycota. The oxygenation of linoleic acid by lipoxygenases/dioxygenases (LOX, DOX) is considered as the initial step. Subsequently, the hydroperoxy-fatty acids (HPOD) are cleaved by putative hydroperoxide lyases (HPL) through an unknown mechanism which could lead to two distinct

biocatalytic cycles with oct-1-en-3-one (7) and oct-2-enal (3) as precursors. Further modifications via ene-reductases (ER), double bond reductases (DBR), aldo-keto reductases (AR) and alcohol dehydrogenases (ADH) could lead to the variety of known C8-oxylipins

ketonic-cycle related genes in the transition from primordia to immature fruiting bodies seems conceivable. By comparing the AU/g ft of each C8-oxylipin in these two developmental stages, it is clearly noticeable that immature fruiting bodies produced more C8-oxylipins of both cycles compared to primordia, which is consistent with a conceivable upregulation of the aldehydic- and ketonic-cycle between these two stages (Fig. 3A, B). Furthermore with ongoing maturity, a downregulation of the aldehydic and an upregulation of the ketonic-cycle seems reasonable (Fig. 1). This is elucidated by the comparison of the C8-oxylipin composition and biosynthesis in immature fruiting bodies, mature fruiting bodies, post sporulation fruiting bodies and basidiospores, where the total number of different C8-oxylipins declined from eight in immature fruiting bodies, to five in mature and post sporulation fruiting bodies, and three in basidiospores (Fig. 1). The vanishing C8-oxylipins with maturation are all related to the aldehydic-cycle, while the ketonic-cycle related C8-oxylipins remain in high amounts. This

strengthens the hypothesis of two distinct biosynthetic pathways. Similar observations were made by Li et al., (2016), who showed that egg-shaped, bell-shaped and mature fruiting bodies of *Tricholoma matsutake* produced predominantly octan-3-one (8) and oct-1-en-3-ol (6). With ongoing maturation of *T. matsutake* increasing levels of octan-3-one and decreasing oct-1-en-3-ol (6) levels have been detected. On the other hand, octan-1-ol (2), octanal (4) and oct-2-en-1-ol (1) were either not detected or in low levels that decreased with ongoing maturity. This is in accordance with our hypothesis that a ketonic cycle (e.g. octan-3-one (8)) is getting more prominent during maturation, whereas the aldehydic-cycle (e.g. octan-1-ol (2)) is decreasing concurrently. Furthermore in *T. matsutake*, oct-2-enal was present in higher proportions in immature fruiting stages (egg- and bell-shaped fruiting bodies) followed by a strong decrease with maturation, which underlines the downregulation of the aldehydic-cycle in mature developed stages and is fairly in accordance with our hypothesis. Mau et al., (1997)

compared the octan-3-ol (5), oct-1-en-3-ol (6), octan-1-ol (2) and oct-2-en-1-ol (1) levels in liquid extracts from aging fruiting bodies of *V. volvacea*. Amounts of ketonic-cycle related C8-oxylipins, particularly oct-1-en-3-ol (6) increased with maturity. This indicates a higher activity of the ketonic-cycle in more developed fruiting bodies. In contrast, aldehydic-cycle related C8-oxylipins were detected overall in lower amounts, which did not undergo any significant change in their composition. Moreover, Cho et al. (2006) analysed different maturity grades of fruiting bodies from *T. matsutake* that showed an increase in the overall level of ketonic- and aldehydic-cycle related C8-oxylipins. Yet, higher relative peak areas of the ketonic-cycle related C8-oxylipins were identified in all developmental stages conceivably induced by a higher biocatalytic activity of the ketonic-cycle. Nevertheless, it has to be mentioned that liquid extracts from *T. matsutake* and not the headspace was analysed. Studies by Kleofas et al., (2015) and Tressl et al., (1982) demonstrated that liquid extracts of fruiting bodies of *Calocybe gambosa* and *Agaricus campestris* contained strikingly more ketonic-cycle related C8-oxylipins compared to the aldehydic-cycle, which supports our hypothesis of an increased respectively high activity of the ketonic-cycle in mature developmental stages.

It is noteworthy that the total amount and number of C8-oxylipins decline with maturation (Fig. 1). Although fatty acids are involved in many biological functions, the differences in the fatty acid composition, especially the steady decline of linoleic acid contribution at more mature developmental stages and the decrease of C8-oxylipins is noticeable (Table 1). Furthermore, we were able to demonstrate that the fatty acid composition of basidiospores consists of significantly higher ratios of SFA and MUFA, which could be explained by their differing role in morphological and physiological stages (Table 1).

Biotransformations of precursors from the ketonic- and aldehydic-cycle

As already mentioned, an upregulation of the aldehydic- and ketonic-cycle in the transition from primordia to immature fruiting bodies is hypothesised. Therefore, these two developmental stages were chosen for biotransformation experiments with the precursors oct-1-en-3-one (7) and oct-2-enal (3). As presumed, a specific and strong cluster-like increase of C8-oxylipins from the ketonic-cycle was detected in immature fruiting bodies when oct-1-en-3-one (7) was used as a substrate. Additionally, oct-1-en-3-one (7) also seemed to induce endogenous C8-oxylipin production explained by the slight increase of octan-1-ol (2), oct-2-en-1-ol (1) and oct-2-enal (3) (Fig. 3B). An opposing effect was observed when oct-2-enal (3) was added to immature fruiting bodies. The drastic cluster-like increase of aldehydic-cycle related

C8-oxylipins was accompanied with a minimal increase of octan-3-ol (5) and octan-3-one (8), while oct-1-en-3-ol (6) and oct-1-en-3-one (7) decreased (Fig. 3B). A comparable impact was observed for primordia. Addition of oct-1-en-3-one (7) led to a strong increase of ketonic-cycle related C8-oxylipins and a slight increase of aldehydic-cycle related C8-oxylipins 1–3 (Fig. 3A). In contrast, adding oct-2-enal to primordia, aldehydic-cycle related C8-oxylipins raised vigorously with a distinct reduction of ketonic-cycle related C8-oxylipins (Fig. 3A). Based on these observations, oct-1-en-3-one (7) and its derived compounds could have an inducing effect on the ketonic- and aldehydic-cycle. An opposing inhibitory effect on the ketonic-cycle seems to be caused by oct-2-enal-derived compounds.

Biotransformations in Basidiospores

As related to primordia and immature fruiting bodies, addition of oct-1-en-3-one (7) to basidiospores led to a strong increase of the ketonic-cycle related oxylipins octan-3-one (8), oct-1-en-3-ol (6) and octan-3-ol (5). Furthermore, addition oct-1-en-3-ol (6) to basidiospores resulted in a slight increase of octan-3-one (8) and octan-3-ol (5) suggesting an oxidation of the alcohol with a following reduction of the double-bond leading to octan-3-one (8). The oxidation of octan-3-ol (5) was also observed when added to basidiospores, indicating an alcohol dehydrogenase (ADH) equilibrium system between octan-3-ol (5), oct-1-en-3-ol (6) and the corresponding ketones. A comparable equilibrium system was not observed for the aldehydic-cycle in basidiospores. Adding oct-2-en-1-ol (1) or octan-1-ol (2) to basidiospores did not lead to an oxidation to the aldehydes octanal (4) or oct-2-enal (3). However, oct-2-enal (3) and octanal (4) were completely or strongly reduced to oct-2-en-1-ol (1) and/or octan-1-ol (2) (Fig. 3C). The addition of oct-2-enal (3) and octan-1-ol (2), likewise in primordia and immature fruiting bodies (Fig. 3A, B), seems to inhibit the ketonic-cycle, which is reflected by the decrease of oct-1-en-3-ol (6) and octan-3-ol (5) levels (Fig. 3C).

Independent ketonic- and aldehydic cycle

The aldehydic- and ketonic-cycle seems to consist mainly of ene-reductases (ER), keto-/aldehyde-reductases (KR, AR) and alcohol dehydrogenases (ADH), which all play an important role after the oxidation of linoleic acid and the subsequent, putative cleavage of 13-, 10-, 9-HPOD to shortened C8-oxylipins (Fig. 4). A recently published study by Orban et al., (2021) investigating the transcriptome of different fruiting stages in *C. aegerita* supports our hypothesis of distinct pathways within the C8-oxylipin biosynthesis. By combining transcriptome and volatilome data, different sets of putative LOX, DOX, ER and ADH genes potentially

involved in oct-1-en-3-ol (**6**) and octan-3-one (**8**) biosynthesis could be identified. Darriet et al., (2002) were able to show the reduction of oct-1-en-3-one (**7**) and oct-1,5-dien-3-one in *S. cerevisiae* cells. Chen and Wu (1983) pointed out a reduction of oct-1-en-3-one (**7**) to oct-1-en-3-ol (**6**) and octan-3-one (**8**) in *A. bisporus*. Furthermore, Wanner and Tressl (1998) were able to identify two enone-reductases from *S. cerevisiae* with a reduction activity towards oct-1-en-3-one (**7**). The hypothesis of ERs reducing C8-oxylipin related alkenals and alkenones are reinforced by our recently characterised ene-reductase CaeEnR1 from *C. aegerita*. On the one hand, we were able to show that oct-1-en-3-one (**7**) and oct-2-enal (**3**) were reduced to octan-3-one and octanal. On the other hand, a reduction of oct-1-en-3-ol (**6**) or oct-2-en-1-ol (**1**) was not observed, suggesting a different set of enzymes involved in the transformation of C8-oxylipin related alcohols (Fig. 4) (Karrer et al., 2021a, b). Nevertheless, the role of the putative intermediates 13-, 10- and 9-HPOD has to be clarified in further experiments. Yet, only a coherence of 10-HPOD and oct-1-en-3-ol (**6**) was indicated by Wurzenberger and Grosch (1984b), who showed that a crude extract of *A. bisporus* was able to cleave 10-HPOD to oct-1-en-3-ol (**6**), while 9-, 12- and 13-HPOD were not converted to any C8-oxylipin. Furthermore, Assaf et al., (1995) detected an accumulation of 13-HPOD, accompanied with an increase of oct-1-en-3-ol (**6**) after adding linoleic acid to a homogenate of *Pleurotus pulmonarius*. Nevertheless, the addition of 13-HPOD as a precursor did not lead to an increase of oct-1-en-3-ol (**6**). Although, Joh et al. (2012) proposed a cleavage of 13-HPOD to oct-1-en-3-one (**7**) with subsequent reductions or a direct cleavage of 10-HPOD to oct-1-en-3-ol (**6**) in *P. ostreatus*. This would imply two biosynthetic pathways including the involvement of a DOX producing 10-HPOD and a LOX converting linoleic acid to 13-HPOD. However, no coherence between 9-HPOD and certain C8-oxylipins exists, although it is well known that fungi of the phylum Basidiomycota harbour various LOX in their genomes. Additionally, it was shown that gene expression levels highly depend on the developmental stages (Orban et al., 2021; Tasaki et al., 2019). Few of the known LOX genes from *P. ostreatus*, *P. sapidus*, *P. dryinus*, *P. sajor-caju* and *C. aegerita* have been cloned, heterologously expressed and tested for their specific activity towards linoleic acid (Karrer & Rühl 2019; Karrer et al., 2021a, b; Kuribayashi et al., 2002; Leonhardt et al., 2013; Plagemann et al., 2013). However, among these LOX, only three were comprehensively characterised which predominantly produce 13-HPOD and rarely minor amounts of 9-HPOD from linoleic acid (Karrer & Rühl 2019; Kuribayashi et al., 2002; Plagemann et al., 2013), whereas 10-HPOD has not been detected as a LOX product. Only DOX from Ascomycota are known to produce 10-HPOD from linoleic acid (Brodhun et al., 2010). Taken together previous findings and results

from our biotransformation experiments, the existence of two independent ketonic- and aldehydic-cycles, branching after HPOD-cleavage, seems reasonable (Fig. 4).

Conclusion

Although further research in C8-oxylipin biosynthesis is required, we were able to show that two morphology dependent and distinct biocatalytic cycles seem reasonable by combining metabolomic analysis. The aldehydic-cycle appears to be more active in early developmental stages, whereas the ketonic-cycle is active throughout all developmental stages, peaking at the stage of sporulation. The existence of distinct pathways was underlined with biotransformation experiments using the putative precursor of the aldehydic-cycle oct-2-enal (**3**) and the precursor of the ketonic-cycle oct-1-en-3-one (**7**). With the addition of each precursor, a drastic increase of the corresponding aldehydic- or ketonic-cycle related C8-oxylipins was detected, which supports our hypothesis. Nonetheless, genes encoding for putative LOX, DOX as well as the modifying enzymes of shortened oxylipins have to be the focus of further studies.

Acknowledgements We would like to thank druid-Austernpilze for supplying the *C. aegerita* substrate blocks with immature fruiting bodies and Florian Hennicke for the monokaryotic *C. aegerita* strains. We thank two anonymous reviewers whose comments helped to improve and clarify the manuscript.

Author contribution The work was conceived by DK and MR. Experiments were performed by DK, AA, NH and VW. The manuscript was written through contributions of all authors.

Funding Open Access funding enabled and organized by Projekt DEAL. Part of the work was financially supported by the Deutsche Forschungsgemeinschaft (project: RU2137/1) and by the excellence initiative LOEWE within the project “AROMaplus” financed by the Hessian Ministry of Science and Art.

Data availability All datasets are presented in the main manuscript and in the supporting file.

Code availability Not applicable.

Declarations

Ethics approval Not applicable.

Conflict of interest The authors declare no competing interests.

Open Access This article is licensed under a Creative Commons Attribution 4.0 International License, which permits use, sharing, adaptation, distribution and reproduction in any medium or format, as long as you give appropriate credit to the original author(s) and the source, provide a link to the Creative Commons licence, and indicate if changes were made. The images or other third party material in this article are

included in the article's Creative Commons licence, unless indicated otherwise in a credit line to the material. If material is not included in the article's Creative Commons licence and your intended use is not permitted by statutory regulation or exceeds the permitted use, you will need to obtain permission directly from the copyright holder. To view a copy of this licence, visit <http://creativecommons.org/licenses/by/4.0/>.

References

- Akakabe Y, Matsui K, Kajiwara T (2005) Stereochemical correlation between 10-hydroperoxyoctadecadienoic acid and 1-octen-3-ol in *Lentinula edodes* and *Tricholoma matsutake* mushrooms. *Biosci Biotech Bioch* 69:1539–1544. <https://doi.org/10.1271/bbb.69.1539>
- Assaf S, Yizhak H, Carlos GD (1995) Biosynthesis of 13-hydroperoxylinoleate, 10-oxo-8-decenoic acid and 1-octen-3-ol from linoleic acid by a mycelial-pellet homogenate of *Pleurotus pulmonarius*. *J Agric Food Chem* 43:2173–2178. <https://doi.org/10.1021/jf00056a040>
- Brodhun F, Schneider S, Göbel C, Hornung E, Feussner I (2010) PpoC from *Aspergillus nidulans* is a fusion protein with only one active haem. *Biochem J* 425:553–565. <https://doi.org/10.1042/BJ20091096>
- Brodhun F, Feussner I (2011) Oxylipins in fungi. *The. FEBS J* 278:1047–1063. <https://doi.org/10.1111/j.1742-4658.2011.08027.x>
- Chen CC, Wu CM (1984) Studies on the enzymic reduction of 1-octen-3-one in mushroom (*Agaricus bisporus*). *J Agric Food Chem* 32:1342–1344. <https://doi.org/10.1021/jf00126a030>
- Cho IH, Choi H-K, Kim Y-S (2006) Difference in the Volatile Composition of Pine-Mushrooms (Sing.) According to Their Grades. *J Agric Food Chem* 54(13):4820–4825
- Combet E, Henderson J, Eastwood DC, Burton KS (2009) Influence of sporophore developmental, damage, storage, and tissue specificity on the enzymic formation of volatiles in mushrooms (*Agaricus bisporus*). *J Agric Food Chem* 57:3709–3717. <https://doi.org/10.1021/jf8036209>
- Combet E, Eastwood DC, Burton KS, Henderson J (2006) Eight-carbon volatiles in mushrooms and fungi: properties, analysis, and biosynthesis. *Mycoscience* 47:317–326. <https://doi.org/10.1007/S10267-006-0318-4>
- Cruz C, Noel-Suberville C, Montury M (1997) Fatty acid content and some flavor compounds release in two strains of *Agaricus bisporus*, according to three stages of development. *J Agric Food Chem* 45:64–67. <https://doi.org/10.1021/jf960300t>
- Darriet P, Pons M, Henry R, Dumont O, Findeling V, Cartolaro P (2002) Impact odorants contributing to the fungus type aroma from grape berries contaminated by powdery mildew (*Uncinula necator*); incidence of enzymatic activities of the yeast *Saccharomyces cerevisiae*. *J Agric Food Chem* 50:3277–3282. <https://doi.org/10.1021/jf011527d>
- Fäldt J, Jonsell M, Nordlander G, Borg-Karlson AK (1999) Volatiles of bracket fungi *Fomitopsis pinicola* and *Fomes fomentarius* and their functions as insect attractants. *J Chem Ecol* 25:567–590. <https://doi.org/10.1023/A:1020958005023>
- Frings RA, Maciá-Vicente JG, Buße S, Čmoková A, Kellner H, Hofrichter M, Hennicke F (2020) Multilocus phylogeny- and fruiting feature-assisted delimitation of European *Cycloclabe aegerita* from a new Asian species complex and related species. *Mycol Prog* 19:1001–1016. <https://doi.org/10.1007/s11557-020-01599-z>
- Gupta DK, Rühl M, Mishra B, Kleofas V, Hofrichter M, Herzog R, Pecyna JM, Sharma R, Kellner H, Hennicke F, Thines M (2018) The genome sequence of the commercially cultivated mushroom *Agrocybe aegerita* reveals a conserved repertoire of fruiting-related genes and a versatile suite of biopolymer-degrading enzymes. *BMC Genomics* 19:48. <https://doi.org/10.1186/s12864-017-4430-y>
- Herzog R, Solovyeva I, Rühl M, Thines M, Hennicke F (2016) Dikaryotic fruiting body development in a single dikaryon of *Agrocybe aegerita* and the spectrum of monokaryotic fruiting types in its monokaryotic progeny. *Mycol Prog* 15:947–957. <https://doi.org/10.1007/s11557-016-1221-9>
- Husson F, Bompas D, Kermasha S, Belin JM (2001) Biogenesis of 1-octen-3-ol by lipoxygenase and hydroperoxide lyase activities of *Agaricus bisporus*. *Process Biochem* 37:177–182. [https://doi.org/10.1016/S0032-9592\(01\)00201-1](https://doi.org/10.1016/S0032-9592(01)00201-1)
- Holighaus G, Weißbecker B, von Fragstein M, Schütz S (2014) Ubiquitous eight-carbon volatiles of fungi are infochemicals for a specialist fungivore. *Chemoecology* 24:57–66. <https://doi.org/10.1007/s00049-014-0151-8>
- Joh T, Kudo T, Tasaki Y, Hara T (2012) Mushroom flavor compounds and the biosynthesis mechanism (in Japanese). *Aroma Res* 13:26–30.
- Karrer D, Rühl M (2019) A new lipoxygenase from the agaric fungus *Agrocybe aegerita*: biochemical characterization and kinetic properties. *PLoS ONE* 14:e0218625. <https://doi.org/10.1371/journal.pone.0218625>
- Karrer D, Gand M, Rühl M (2021a) Engineering a lipoxygenase from *Cycloclabe aegerita* towards long chain polyunsaturated fatty acids. *AMB Expr* 11:37. <https://doi.org/10.1186/s13568-021-01195-8>
- Karrer D, Gand M, Rühl M (2021b) Expanding the biocatalytic toolbox with a new type of ene/yne-reductase from *Cycloclabe aegerita*. *ChemCatChem* 13:2191–2199. <https://doi.org/10.1002/cctc.202002011>
- Kleofas V, Sommer L, Fraatz MA, Zorn H, Rühl M (2014) Fruiting body production and aroma profile analysis of *Agrocybe aegerita* cultivated on different substrates. *Nat Prod Res* 06:233–240. <https://doi.org/10.4236/nr.2014.56022>
- Kleofas V, Popa F, Niedenthal E, Rühl M, Kost G, Zorn H (2015) Analysis of the volatiles of *Calocybe gambosa*. *Mycol Progress* 14:93. <https://doi.org/10.1007/s11557-015-1117-0>
- Kuribayashi T, Kaise H, Uno C, Hara T, Hayakawa T, Joh T (2002) Purification and characterization of lipoxygenase from *Pleurotus ostreatus*. *J Agric Food Chem* 50:1247–1253. <https://doi.org/10.1021/jf0112217>
- Leonhardt RH, Plagemann I, Linke D, Zelena K, Berger RG (2013) Orthologous lipoxygenase of *Pleurotus* spp. – a comparison of substrate specificity and sequence homology. *J Mol Catal B Enzym* 97:189–195. <https://doi.org/10.1016/j.molcatb.2013.08.014>
- Li Q, Li Z, Li W, Li X, Huang W, Yang W, Zheng L (2016) Chemical compositions and volatile compounds of *Tricholoma matsutake* from different Geographical Areas at Different Stages of Maturity. *Food Sci Biotechnol* 25:71–77. <https://doi.org/10.1007/s10068-016-0010-1>
- Malheiro R, de Pinho PG, Soare S, da Silva Ferreira AC, Baptista P (2013) Volatile biomarkers for wild mushrooms species discrimination. *Food Res Inter* 54:186–194. <https://doi.org/10.1016/j.foodres.2013.06.010>
- Matsui K, Sasahara S, Akakabe Y, Kajiwara T (2003) Linoleic Acid 10-hydroperoxide as an intermediate during formation of 1-Octen-3-ol from linoleic acid in *Lentinus decedetes*. *Biosci Biotech Bioch* 67:2280–2282. <https://doi.org/10.1271/bbb.67.2280>
- Mau JL, Chyau CC, Li JY, Tseng YH (1997) Flavor compounds in straw mushrooms *Volvariella volvacea* harvested at different stages of maturity. *J Agric Food Chem* 45:4726–4729. <https://doi.org/10.1021/jf9703314>

- Orban A, Hennicke F, Rühl M (2020) Volatilomes of *Cyclocybe aegerita* during different stages of monokaryotic and dikaryotic fruiting. *Biol Chem* 401:995–1004. <https://doi.org/10.1515/hsz-2019-0392>
- Orban A, Weber A, Herzog R, Hennicke F, Rühl M (2021) Transcriptome of different fruiting stages in the cultivated mushroom *Cyclocybe aegerita* suggests a complex regulation of fruiting and reveals enzymes putatively involved in fungal oxylipin biosynthesis. *BMC Genomics* 22:324. <https://doi.org/10.1186/s12864-021-07648-5>
- Plagemann I, Zelena K, Arendt P, Ringel PD, Krings U, Berger RG (2013) LOXPsa1, the first recombinant lipoxygenase from a basidiomycete fungus. *J Mol Catal b: Enzym* 87:99–104. <https://doi.org/10.1016/j.molcatb.2012.11.004>
- Rapier S, Breheret S, Talou T, Pelissier Y, Milhau M, Bessiere JM (1998) Volatile components of fresh *Agrocybe aegerita* and *Tricholoma sulfureum*. *Cryptogam Mycol* 19:15–23
- Schulz-Bohm K, Martin-Sanchez L, Garbeva P (2017) Microbial Volatiles: small molecules with an important role in intra- and inter-kingdom interactions. *Front Microbiol* 8:2484. <https://doi.org/10.3389/fmicb.2017.02484>
- Tasaki Y, Kobayashi D, Sato R, Hayashi S, Joh T (2019) Variations in 1-octen-3-ol and lipoxygenase gene expression in the oyster mushroom *Pleurotus ostreatus* according to fruiting body developmental, tissue specificity, maturity, and postharvest storage. *Mycoscience* 60:170–176. <https://doi.org/10.1016/j.myc.2019.02.005>
- Tressl R, Bahri D, Engel KH (1982) Formation of eight-carbon and ten-carbon components in mushrooms (*Agaricus campestris*). *J Agric Food Chem* 30:89–93. <https://doi.org/10.1021/jf00109a019>
- Wanner P, Tressl R (1998) Purification and characterization of two enone reductases from *Saccharomyces cerevisiae*. *Eur J Biochem* 255:271–278. <https://doi.org/10.1046/j.1432-1327.1998.2550271.x>
- Wu S, Zorn H, Krings U, Berger RG (2005) Characteristic volatiles from young and aged fruiting bodies of Wild *Polyporus sulfureus* (Bull.:Fr.) Fr. *J Agric Food Chem* 53:4524–4528. <https://doi.org/10.1021/jf0478511>
- Wurzenberger M, Grosch W (1982) The enzymic oxidative breakdown of linoleic acid in mushrooms (*Psalliota bispora*). *Z Lebensm Unter Forsch* 175:186–190. <https://doi.org/10.1007/BF01139769>
- Wurzenberger M, Grosch W (1984a) Stereochemistry of the cleavage of the 10-hydroperoxide isomer of linoleic acid to 1-octen-3-ol by a hydroperoxide lyase from mushrooms (*Psalliota bispora*). *Biochim Biophys Acta* 795:63–165. [https://doi.org/10.1016/0005-2760\(84\)90117-6](https://doi.org/10.1016/0005-2760(84)90117-6)
- Wurzenberger M, Grosch W (1984b) The formation of 1-octen-3-ol from the 10-hydroperoxide isomer of linoleic acid by a hydroperoxide lyase in mushrooms (*Psalliota bispora*). *Biochim Biophys Acta* 794:25–30. [https://doi.org/10.1016/0005-2760\(84\)90293-5](https://doi.org/10.1016/0005-2760(84)90293-5)

Publisher's note Springer Nature remains neutral with regard to jurisdictional claims in published maps and institutional affiliations.